

Department of Internal Medicine I

Medical University of Vienna

Institute of Cancer Research

(Head: Prof. Dr. Maria Sibilio)

**The role of FGFR4 activity on proliferation,
differentiation and downstream signaling in glioma**

Masterthesis submitted for the fulfillment of the requirements for the
degree of

Master of Science M.Sc.

Submitted by

Carola Nadine Jaunecker, B.Sc.

Vienna, Dec,2019

Supervision

External supervisor (Medical University of Vienna)

Univ. Prof. Mag. Dr. Walter Berger

Daniela Lötsch- Gojo, PhD

Internal Supervisor (University for Veterinary Medicine Vienna)

Dr.rer.nat. Sabine Macho- Maschler

Independent evaluator (University for Veterinary Medicine Vienna)

Dr. Florian Grebien

Danksagung

Zunächst möchte ich mich bei all den Menschen bedanken, die maßgeblich zur Durchführung dieser Arbeit beigetragen haben:

Zunächst bei **Univ. Prof. Dr. Mag. Walter Berger**, der mir diese Arbeit erst ermöglicht hat und mir besonders in der Endphase stets mit seinem unendlichen Wissen zur Seite gestanden hat. Außerdem bei meiner internen Betreuerin **Dr. rer.nat. Sabine Macho – Maschler** für den letzten Feinschliff und ihre Unterstützung beim Einreichen der Arbeit.

Des Weiteren bedanke ich mich bei **Daniela Lötsch-Gojo, Mirjana Stojanovic, Dominik Kirchhofer, Christine Pirker** und **Carina Dinhof** sowie der gesamten Berger und Heffeter Gruppe für ihre Tipps und Ratschläge sowie die familiäre Aufnahme und die angenehme Arbeitsatmosphäre, die es mir leicht gemacht hat, jeden Tag mit Freude zur Arbeit zu kommen.

Mein größter Dank gilt jedoch meiner Betreuerin **Lisa Gabler**, für ihre freundschaftliche Beratung, die kompetente Einschulung und die unzähligen Entwurfskorrekturen, die schließlich zur Fertigstellung dieser Arbeit führten. Für all die unglaublich spannenden Dinge, die ich in diesem Jahr lernen durfte, die sicher über die Kompetenzen einer durchschnittlichen Masterarbeit hinaus gehen. Außerdem für ihre enthusiastische Art, mit der sie mich durch das ganze Jahr und selbst durch die letzte nervenaufreibende Phase motivieren konnte.

Außerdem möchte ich mich noch bei einigen Menschen bedanken, ohne die nichts davon möglich gewesen wäre: Bei meinen Eltern, **Jeanine** und **Peter**, sowie meinem Stiefvater **Helmut**, die mich in meiner Neugierde und in meinem Wissensdurst stets bestärkten und mich immer vor neue Herausforderungen stellten. Abgesehen davon gilt mein herzlichster Dank meinen Großeltern, **Hilde** und **Hans**, für alles was sie für mich getan haben. So vieles, nicht zuletzt diese Arbeit, wäre ohne eure Unterstützung nicht möglich gewesen. Außerdem bedanke ich mich bei meinem Onkel **Hannes**, meiner Tante **Ulli** und meiner ganzen Familie, insbesondere meiner Cousine **Isabella**, die in jeder Phase meines Lebens unerschütterlich an meiner Seite standen und mir Rückhalt gaben. Außerdem bei meiner gesamten restlichen Familie, **Doris, Eyal und Franzi**, sowie bei meinen Freunden, **Steffi, Toni** und **Pati**, die mich immer wieder motiviert haben und mich, wenn nötig, immer auf andere Gedanken bringen konnten.

Table of contents

1	Introduction.....	1
1.1	Cancer incidence and mortality worldwide	1
1.2	Etiology of cancer	2
1.3	Hallmarks of cancer	2
1.3.1	Sustained growth signaling.....	3
1.3.2	Resisting cell death.....	3
1.3.3	Enabling replicative immortality	4
1.3.4	Inducing angiogenesis	4
1.3.5	Activating invasion and metastasis	5
1.4	WHO classification of tumors of the central nervous system (CNS)	6
1.5	Glioblastoma multiforme (GBM).....	8
1.5.1	IDH status.....	9
1.5.2	O(6)-methylguanine DNA methyltransferase (MGMT)	9
1.5.3	GBM therapy	10
1.5.4	Gliosarcoma	12
1.6	Receptor Tyrosine Kinases (RTK)	12
1.7	Fibroblast growth factor receptors and their ligands.....	14
1.7.1	Fibroblast growth factors (FGFs)	14
1.7.2	Fibroblast growth factor receptors (FGFRs).....	15
1.7.3	Splicing variants of FGFRs	16
1.7.4	FGFR signaling.....	18
1.8	Fibroblast growth factor receptor 4 (FGFR4).....	21
1.8.1	Differences between FGFR4 and other FGFRs	21
1.8.2	Gene organization of FGFR4.....	22

1.8.3	Physiological role of FGFR4	22
1.8.4	FGFR4 in cancer	24
1.8.5	FGFR 4 Gly/Arg polymorphism and its role in cancer	24
1.9	Epithelial to mesenchymal transition (EMT)	26
1.9.1	Role of FGFR4 in epithelial to mesenchymal transition.....	27
2	Aim of the study	30
3	Material and Methods	31
3.1	Cell culture	31
3.2	Retroviral vectors with FGFR4 variants.....	33
3.3	Calcium phosphate transfection of Hek293 cells for retrovirus production	35
3.4	Retroviral transduction of glioma cell lines	36
3.5	Cell proliferation and migration assays	36
3.5.1	Cytotoxicity assay (MTT)	36
3.5.2	ATP assay	37
3.5.3	Colony formation assay (Clonogenic assay)	39
3.5.4	Sphere formation assay and re-differentiation assay	41
3.5.5	Migration assay	41
3.5.6	Invasion assay.....	42
3.5.7	Wound healing assay	42
3.5.8	Confocal laser scanning microscopy.....	43
3.6	Protein isolation and analysis methods	44
3.6.1	Total protein isolation.....	44
3.6.2	Membrane protein enriched fraction	45
3.6.3	Cytosolic and Nuclear extracts	47
3.6.4	Protein determination.....	47
3.6.5	Sodium dodecyl sulfate polyacrylamide gel electrophoresis (SDS-PAGE)	47

3.6.6	Western blot	48
3.6.7	Antibody incubation	51
3.7	Polymerase Chain reaction (PCR)	52
3.7.1	RNA isolation with Trizol.....	53
3.7.2	Reverse transcription of RNA to cDNA	54
3.7.3	Quantitative real time PCR (qPCR).....	54
3.7.4	Restriction fragment length polymorphism PCR (RFLP PCR).....	57
3.8	Knock-down of FGFR4 expression via RNAi.....	61
3.9	Fluorescence-activated cell sorting (FACS)	62
3.10	In vivo tumor formation in severe combined immunodeficiency (SCID) mice	63
3.11	Statistical analysis	63
4	Results	64
4.1	Endogenous expression of FGFR4 in GBM and GS cell lines.....	64
4.2	Determination of the endogenous <i>FGFR4 388Gly / 388Arg</i> status.....	65
4.3	Generation of FGFR4 over-expressing cellular models.....	66
4.4	Localization of FGFR4 in ectopically over-expressing cell lines	68
4.5	FGFR4 expression levels in genetically modified cell lines	71
4.6	Klotho beta (<i>KLB</i>) is co-regulated with FGFR4 expression in BTL1376	75
4.7	Functionality of FGFR4 kinase-dead variant and impact on downstream signaling	77
4.8	Effects of FGFR4 inactivation on two-dimensional growth	79
4.8.1	Clone formation capacity	79
4.8.2	Impact of stimulation and inhibition of FGFR on clone formation capacity.....	80
4.9	Effects of FGFR4 inactivation on three-dimensional growth.....	81
4.9.1	Sphere formation and re-differentiation upon inactivation of FGFR4 in BTL1376	82
4.9.2	Sphere formation and re-differentiation upon inactivation of FGFR4 in SIWA M1	83

4.9.3	Sphere formation with stimulation of FGFR4 via FGF23 in SIWA M1	84
4.10	<i>In vivo</i> aggressiveness of FGFR4-inactivated SIWA-M1	85
4.11	Sensitivity of FGFR4 modified cell models towards receptor inhibition.....	86
4.12	Inhibition of FGFR4 downstream signaling by Ponatinib	91
4.13	Investigation of migration and invasion capacity of FGFR4 modified glioma cells ..	92
4.14	Analysis of epithelial and mesenchymal cell markers upon FGFR4 modulation ...	94
5	Discussion	99
6	Conclusion.....	113
7	Abstract	114
8	Zusammenfassung	115
9	Appendix.....	116
10	Abbreviations	117
11	Bibliography	122
12	List of Tables.....	138
13	List of Figures.....	139

1 Introduction

1.1 Cancer incidence and mortality worldwide

According to the estimations of the International Agency for research on cancer 18.1 billion people have been diagnosed with cancer across 20 world regions in 2018. Causing 9.6 billion deaths cancer is still among the most threatening illnesses nowadays (“New Global Cancer Data: GLOBOCAN 2018 | UICC” n.d.), (Bray et al. 2018). The most prevalent type of cancer is lung cancer (11.6%), followed by female breast cancer (11.6%), male prostate cancer (7.1%) and colorectal cancer (6.1%) (Bray et al. 2018). Clearly, there are gender specific differences in cancer incidence and mortality. While lung cancer followed by liver and stomach cancer are the most common cancer types among males, in women breast cancer followed by colorectal and lung cancer are most prevalent. Concerning mortality lung and colorectal cancer are the most prevalent forms of cancer accounting for 18.4 and 9.2% of all cancer deaths, respectively (**Figure 1**).

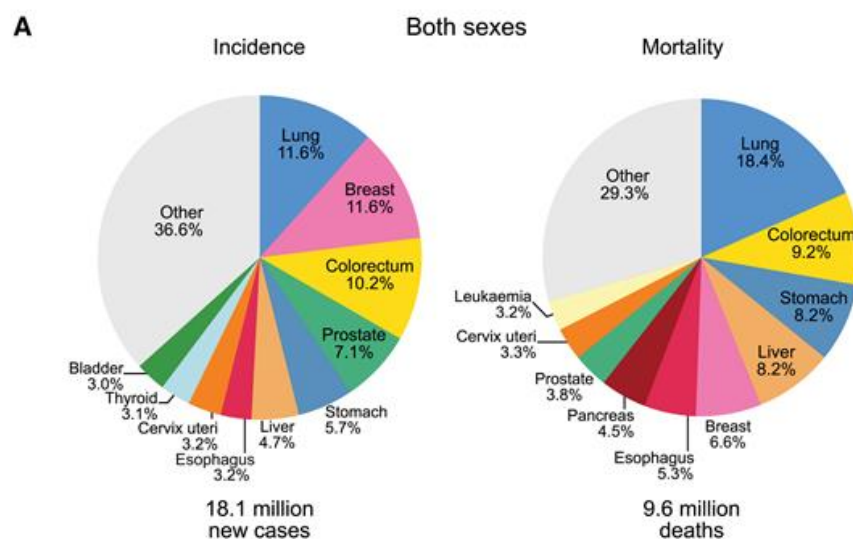


Figure 1 Cancer incidence and mortality rates worldwide adapted from Bray et al. 2018

1.2 Etiology of cancer

In general, neoplasms can be divided into two major subgroups. Benign tumors such as adenomas or fibromas (WebMd n.d.) and malignant tumors, casually referred to as cancer. Contrarily to malignant cancers, benign tumors are characterized by non-invasive, encapsulated growth pattern and low cellular replication rate. However, also benign tumors can be harmful as soon as they displace important cellular compartments of organs of the body. In opposition to benign tumors, cancer is defined by its highly aggressive growth behavior as well as invasion into surrounding tissues and metastasis (Rachna, Saunders, WebMd).

There are different theories existing which discuss the causative risk factors leading to cancer. Depending on the tumor entity, tumor genesis can be either caused by an inherited genetic predisposition or by life style-associated environmental factors (Robbins, Loh, and Matthay 2012; Trichopoulou, Lagiou, and Trichopoulos 2003; SOUTHAM 1963; Heston 1965; Tomasetti, Li, and Vogelstein 2017).

In both cases, cancer arises due to a single or multiple mutations in somatic cells or germ cells, leading to aberrant gene expression resulting in disturbed cellular homeostasis. Mutations which are capable to maintain the deregulated cell proliferation and do not depend on other mutations are called “driver” mutations. On the one hand, proto-oncogenes, genes involved in positive cell cycle regulation, are affected by driver mutations, which in turn are propagated to so-called oncogenes. On the other hand, mutations can also occur in tumor suppressor genes, which are normally involved in DNA damage protection, cell cycle control or inducing apoptosis, often resulting in reduced apoptotic capacity (Lodish et al. 2000; Stratton, Campbell, and Futreal 2009; Roy, Walsh, and Chan 2014). Taken together, the interplay between activating mutations in proto-oncogenes and inactivating mutations in tumor suppressor genes consequently leads to sustained proliferation signaling, evasion of environmental inhibitory signals as well as avoidance of apoptosis.

1.3 Hallmarks of cancer

Despite diversity and complexity within and between different tumors being rather high, the hallmarks of cancer proposed in 2000 (Douglas Hanahan and Weinberg 2000) identified six cellular mechanisms which need to be altered during the multi-step process of tumor

initiation, promotion, progression and metastasis. These hallmarks include sustained growth signaling, insensitivity to inhibitory signals, evasion of apoptosis, induction of angiogenesis and metastasis. Furthermore, many cellular mechanisms underlying those hallmarks have been elucidated (**Figure 2**)

1.3.1 Sustained growth signaling

While non-malignant cells are dependent on extracellular growth factors in order to enter cell cycle, cancer cells have evolved some mechanisms to become independent from such growth stimulants. Three common ways of achieving autonomy are known so far. The first one is established by autocrine signaling loops, where cancer cells produce growth factors like for example platelet derived growth factor (PDGF) and tumor growth factor α (TGF α) in glioblastomas and sarcomas, respectively. The second mechanism in cancer cells to maintain growth signaling is mediated via overexpression of growth factor receptors on the cell surface. Hence, cells are hyper-responsive to extracellular growth factors or even undergo ligand-independent signaling. The third and most complex way for achieving continuous proliferation are alterations of downstream signaling cascades regardless of receptor activation. The MAPK but also the PI3K/Akt signaling pathway is often affected by such mutations in cancer cells. (Douglas Hanahan and Weinberg 2000)

1.3.2 Resisting cell death

Programmed cell death, or apoptosis, is a mechanism which has evolved to protect the body from the risk of developing cancer if a cell is under physiologic stress or experiences irreversible damage. Apoptosis can be executed following two different signaling cascades: the extrinsic program by activation of death receptors like for example the Fas ligand/Fas receptor pathway and the intrinsic program where the apoptotic signaling cascade is initiated by mitochondrial signals (Movassagh and Foo 2008). Either way leads to activation of effector caspases, which degrade the cell compartments until they are engulfed by neighboring cells or by specialized phagocytic cells. To maintain homeostasis within the cell, pro- and anti-apoptotic signals must be well-balanced. Cancer cells have developed mechanisms to interfere with the mentioned pathways in order to prevent cell death despite DNA damage or

cell stress. One of the most common cancer mutations affects the DNA damage sensor and tumor suppressor gene *TP53* (encoding for p53 protein). Under physiological conditions, p53 is responsible for repairing DNA breaks and induces apoptosis if damage is irreversible. Loss of function mutations within this gene as well as complete p53 loss have been reported among a huge variety of different tumor entities (Fulda 2010; D Hanahan and Weinberg 2000; Douglas Hanahan and Weinberg 2011, Petitjean et al. 2007). Apart from that, overexpression of antiapoptotic protein members of the Bcl-2 family, are often up regulated in cancer cells (D Hanahan and Weinberg 2000; Douglas Hanahan and Weinberg 2011; Dole et al. 1994). On the contrary, pro-apoptotic Bcl2 family members like Bax or Bak are frequently lost in malignant cell types (Levine, Sinha, and Kroemer 2008). Furthermore, anti- apoptotic signals can be transmitted via the PI3K/Akt pathway, which is often aberrantly regulated in cancer cells (Douglas Hanahan and Weinberg 2000).

1.3.3 *Enabling replicative immortality*

Furthermore, limitless replicative potential is achieved by re-activation of telomerase, circumventing the continuous loss of chromosomal ends during each replication cycle. There are different mechanisms known including activating point mutations in the gene promoter of the catalytic subunit of telomerase, the *telomerase reverse transcriptase (TERT)* gene, and alternative lengthening of telomeres (ALT). Enabling replicative immortality is an essential hallmark for all malignant tumors (Low and Tergaonkar 2013; Douglas Hanahan and Weinberg 2000; Douglas Hanahan and Weinberg 2011).

1.3.4 *Inducing angiogenesis*

In order to sustain the tumor mass and provide it with oxygen and nutrients, neo-angiogenesis via predominantly vessel sprouting is induced if the tumor exceeds a certain volume. Tumor cells undergo this angiogenic switch by e.g. secretion of vascular endothelial growth factors (VEGF). These pro-angiogenic factors are released and activated for example by metalloproteases (MMP9) which are mainly sequestered by infiltrating stroma cells into the extracellular matrix (ECM) (Kessenbrock, Plaks, and Werb 2010). Additionally, fibroblast growth factors (FGF1/FGF2) are involved in sustaining angiogenesis (Douglas Hanahan and Weinberg 2000; Douglas Hanahan and Weinberg 2011; Cross and Claesson-Welsh 2001).

1.3.5 Activating invasion and metastasis

During cancer progression, cells alter their shapes and consequently get anchorage independent from other cells as well as from the extracellular matrix (ECM). This process is associated with downregulation of E-cadherin and reactivation of genes which are involved in cell migration during embryogenesis and inflammation. These molecular and morphological changes can further lead to local invasion and intravasation of tumor cells into either lymphatic or blood vessels, hence initiating metastasis. (Hanahan and Weinberg 2011, Talmadge and Fidler 2010).

Despite these genetic alterations may be sufficient for tumor formation, the microenvironment of the tumor and the interaction with other cells of the body has gained huge interest during the last decade also as a therapeutic target. Subsequently, the hallmarks of cancer were extended by four more capabilities which are acquired by tumor cells in order to interact with the microenvironment and enhance genomic instability (Douglas Hanahan and Weinberg 2011). Especially the crosstalk between tumor and the immune system has become more important in the recent years. Since cancer generally has evolved various mechanisms to suppress the immune response against the mutated, malignant cells, reactivation of the immune system to target tumor cells for example by the application of check-point inhibitors has been proven to be a successful therapy opportunity (Dougan and Dranoff 2009).

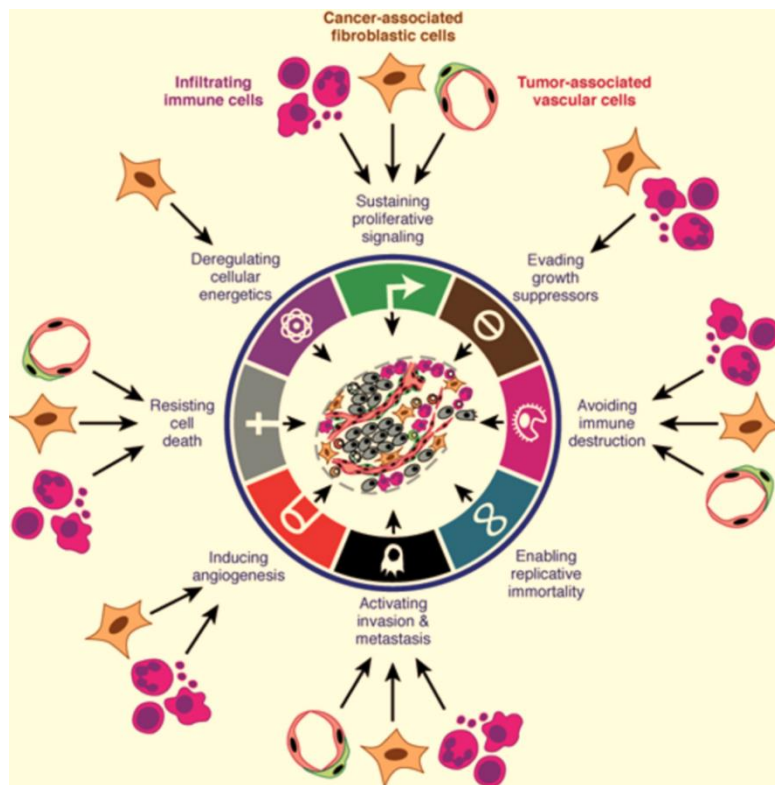


Figure 2. The hallmarks of cancer
(DeVita, Lawrence, and Rosenberg n.d.)

1.4 WHO classification of tumors of the central nervous system (CNS)

In 2016, the world health organization (WHO) published a revised version of CNS tumor classification guidelines. Therein, the rather complex and diverse group of tumors affecting brain and spinal cord region are classified by means of their structures, their aggressiveness and their more and more also genetic phenotypes. In total, the classification includes 17 groups of CNS tumors each divided in different subgroups of tumor entities (**Figure 3**). While earlier classifications were based on histological features and similarities within the different tumors, the revised version from 2016 for the first time includes the genetic and molecular background of CNS tumors which was only mentioned as supplementary information in earlier days. Thereby, differences within tumor entities were further classified and give a more comprehensive picture predicting tumor aggressiveness and therapy success (Louis et al. 2016).

WHO classification of tumours of the central nervous system

Diffuse astrocytic and oligodendroglial tumours		Neuronal and mixed neuronal-glial tumours		Melanotic schwannoma	9560/1	Osteochondroma	9210/0
Diffuse astrocytoma, IDH-mutant	9400/3	Dysembryoplastic neuroepithelial tumour	9413/0	Neurofibroma	9540/0	Osteosarcoma	9180/3
Gemistocytic astrocytoma, IDH-mutant	9411/3	Gangliocytoma	9492/0	Atypical neurofibroma	9540/0		
Diffuse astrocytoma, IDH-wildtype	9400/3	Ganglioglioma	9505/1	Plexiform neurofibroma	9550/0	Melanocytic tumours	
Diffuse astrocytoma, NOS	9400/3	Anaplastic ganglioglioma	9505/3	Perineurioma	9571/0	Meningeal melanocytosis	8728/0
Anaplastic astrocytoma, IDH-mutant	9401/3	Dysplastic cerebellar gangliocytoma (Lhermitte-Duclos disease)	9493/0	Hybrid nerve sheath tumours	9540/3	Meningeal melanocytoma	8728/1
Anaplastic astrocytoma, IDH-wildtype	9401/3	Desmoplastic infantile astrocytoma and ganglioglioma	9412/1	Malignant peripheral nerve sheath tumour	9540/3	Meningeal melanoma	8723/3
Anaplastic astrocytoma, NOS	9401/3	Papillary glioneuronal tumour	9509/1	Epithelioid MPNST	9540/3	Meningeal melanomatosis	8728/3
Glioblastoma, IDH-wildtype	9440/3	Rosette-forming glioneuronal tumour	9509/1			Lymphomas	
Giant cell glioblastoma	9441/3	Diffuse leptomeningeal glioneuronal tumour	9506/1	Meningiomas		Diffuse large B-cell lymphoma of the CNS	9680/3
Gliosarcoma	9442/3	Central neurocytoma	9506/1	Meningothelial meningioma	9530/0	Immunodeficiency-associated CNS lymphomas	
Epithelioid glioblastoma	9440/3	Extraventricular neurocytoma	9506/1	Fibrous meningioma	9532/0	AIDS-related diffuse large B-cell lymphoma	
Glioblastoma, IDH-mutant	9445/3*	Cerebellar liponeurocytoma	9506/1	Transitional meningioma	9537/0	EBV-positive diffuse large B-cell lymphoma, NOS	
Glioblastoma, NOS	9440/3	Paraganglioma	8693/1	Psammomatous meningioma	9533/0	Lymphomatoid granulomatosis	9766/1
Diffuse midline glioma, H3 K27M-mutant	9385/3*	Tumours of the pineal region		Angiomatous meningioma	9534/0	Intravascular large B-cell lymphoma	9712/3
Oligodendroglioma, IDH-mutant and 1p/19q-codeleted	9450/3	Pineocytoma	9361/1	Microcystic meningioma	9530/0	Low-grade B-cell lymphomas of the CNS	
Oligodendroglioma, NOS	9450/3	Pineal parenchymal tumour of intermediate differentiation	9362/3	Secretory meningioma	9530/0	T-cell and NK/T-cell lymphomas of the CNS	
Anaplastic oligodendroglioma, IDH-mutant and 1p/19q-codeleted	9451/3	Pineoblastoma	9362/3	Chordoid meningioma	9538/1	Anaplastic large cell lymphoma, ALK-positive	9714/3
Anaplastic oligodendroglioma, NOS	9451/3	Papillary tumour of the pineal region	9395/3	Clear cell meningioma	9538/1	Anaplastic large cell lymphoma, ALK-negative	9702/3
Other astrocytic tumours		Embryonal tumours		Atypical meningioma	9538/1	MALT lymphoma of the dura	9698/3
Pilocytic astrocytoma	9421/1	Medulloblastomas, genetically defined	9475/3*	Papillary meningioma	9538/3	Histiocytic tumours	
Piloxyoid astrocytoma	9425/3	Medulloblastoma, WNT-activated	9476/3*	Rhabdoid meningioma	9538/3	Langerhans cell histiocytosis	9751/3
Subependymal giant cell astrocytoma	9364/1	Medulloblastoma, SHH-activated and TP53-mutant	9476/3*	Anaplastic (malignant) meningioma	9530/3	Erdheim-Chester disease	9750/1
Pleomorphic xanthoastrocytoma	9424/3	Medulloblastoma, SHH-activated and TP53-wildtype	9471/3			Rosai-Dorfman disease	
Anaplastic pleomorphic xanthoastrocytoma	9424/3	Medulloblastoma, non-WNT/non-SHH	9477/3*	Mesenchymal, non-meningothelial tumours		Juvenile xanthogranuloma	9755/3
Ependymal tumours		Medulloblastoma, histologically defined	9470/3	Solitary fibrous tumour / haemangiopericytoma**		Germ cell tumours	
Subependymoma	9383/1	Medulloblastoma, classic	9471/3	Grade 1	8815/0	Germioma	9064/3
Myxopapillary ependymoma	9394/1	Medulloblastoma, desmoplastic/nodular	9471/3	Grade 2	8815/1	Embryonal carcinoma	9070/3
Ependymoma	9391/3	Medulloblastoma with extensive nodularity	9471/3	Grade 3	8815/3	Yolk sac tumour	9071/3
Papillary ependymoma	9393/3	Medulloblastoma, large cell / anaplastic	9474/3	Haemangioblastoma	9120/0	Choriocarcinoma	9100/3
Clear cell ependymoma	9391/3	Medulloblastoma, NOS	9470/3	Epithelioid haemangiopericytoma	9133/3	Teratoma	9090/1
Tanyocytic ependymoma	9396/3*	Embryonal tumour with multilayered rosettes, C19MC-altered	9478/3*	Angiosarcoma	9120/3	Mature teratoma	9080/0
Ependymoma, RELA fusion-positive	9396/3*	Embryonal tumour with multilayered rosettes, NOS	9478/3	Kaposi sarcoma / PNET	9140/3	Immature teratoma	9080/3
Anaplastic ependymoma	9392/3	Medulloblastoma, NOS	9501/3	Ewing sarcoma	9364/3	Teratoma with malignant transformation	9084/3
Other gliomas		CNS neuroblastoma	9500/3	Lipoma	8850/0	Mixed germ cell tumour	9085/3
Choroid glioma of the third ventricle	9444/1	CNS ganglioglioma	9490/3	Angiolipoma	8861/0	Tumours of the sellar region	
Angiocentric glioma	9431/1	CNS embryonal tumour, NOS	9473/3	Hibernoma	8860/0	Craniopharyngioma	9350/1
Astroblastoma	9430/3	Atypical teratoid/rhabdoid tumour	9508/3	Liposarcoma	8850/3	Adamantinomatous craniopharyngioma	9351/1
Choroid plexus tumours		CNS embryonal tumour with rhabdoid features	9508/3	Desmoid-type fibromatosis	8821/1	Papillary craniopharyngioma	9352/1
Choroid plexus papilloma	9390/0	Tumours of the cranial and paraspinal nerves		Inflammatory myofibroblastic tumour	8825/0	Granular cell tumour of the sellar region	9662/0
Atypical choroid plexus papilloma	9390/1	Schwannoma	9560/0	Benign fibrous histiocytoma	8830/0	Pituitary	9432/1
Choroid plexus carcinoma	9390/3	Cellular schwannoma	9560/0	Fibrosarcoma	8810/3	Spindle cell oncocytoma	8290/0
		Plexiform schwannoma	9560/0	Undifferentiated pleomorphic sarcoma / malignant fibrous histiocytoma	8802/3	Metastatic tumours	
				Leiomyoma	8890/0		
				Leiomyosarcoma	8890/3		
				Rhabdomyoma	8900/0		
				Rhabdomyosarcoma	8900/3		
				Chondroma	9220/0		
				Chondrosarcoma	9220/3		
				Osteoma	9180/0		

Figure 3. WHO classification of tumors of the central nervous system 2016 (Smith 2017)

The WHO grading is based on histological features and criteria in order to characterize the tumor entity. Besides parameters like age, radiological features and tumor location, the genetic background has become increasingly important, since some genetic changes, like mutational status of *isocitrate dehydrogenase 1/2 (IDH 1/2)* were found to be very powerful prognostic and even predictive factors in brain tumors (Louis et al. 2016).

Grade I lesions are referred to as tumors with low proliferative potential. Accordingly, surgical resection often is sufficient to cure the disease. Examples for this tumor grading are meningioma, schwannoma and ganglioglioma.

Grade II lesions are also characterized by a low proliferative activity but in contrast to grade I lesions are infiltrative and often recur after resection. Some grade II tumors tend to progress to a more malignant form of tumor, for example grade II diffuse astrocytoma tends to transform to or anaplastic astrocytoma.

Grade III tumors are characterized by clear histological signs of malignancy including nuclear atypia and sometimes brisk mitotic activity. Grade II tumors with anaplastic features are then

characterized as grade III neoplasia. Therefore, anaplastic astrocytoma (*IDH* mutant), also anaplastic ependymoma and anaplastic ganglioglioma are assigned to grade III tumors.

Grade IV designation is applied to the most malignant form of CNS tumors. They are characterized by high mitotic activity and invasiveness. Due to the fast growth, the tumor area is often insufficiently nourished, thereby the tumor center is prone to undergo necrosis. Characteristically, glioblastoma and some embryonal neoplasms are found in this category (Louis et al. 2016).

1.5 Glioblastoma multiforme (GBM)

Within the diverse group of CNS tumors, gliomas account for 80 % of all malignant brain tumors (Goodenberger and Jenkins 2012). Gliomas can be further specified into low grade glioma (LGG), which refers to WHO grade I and II and high-grade gliomas (HGG) characterized by grade III and IV.

Accounting for 14.7% of all primary brain tumors, glioblastoma multiforme (GBM) is the most prevalent form of malignant brain tumors in adults (Ostrom et al. 2018). GBM belongs to the group of high-grade glioma with predominantly astrocytic differentiation. Showing features like nuclear atypia, cellular polymorphism as well as diffuse growth pattern, it is assigned to WHO grade IV tumors (**Figure 4**). These kinds of neoplasms can either arise *de novo* from glial cells, called primary GBM, or develop from a lower grade precursor lesion which is then characterized as secondary GBM (Ohgaki and Kleihues 2013). Primary and secondary GBMs also differ in their genetic profile, for example by their *IDH1/2* status, which was found to be a very powerful prognostic and predictive marker in GBM. Although a variety of genetic and environmental factors have been studied as potential reason for this tumor, the actual etiology remains widely unknown.

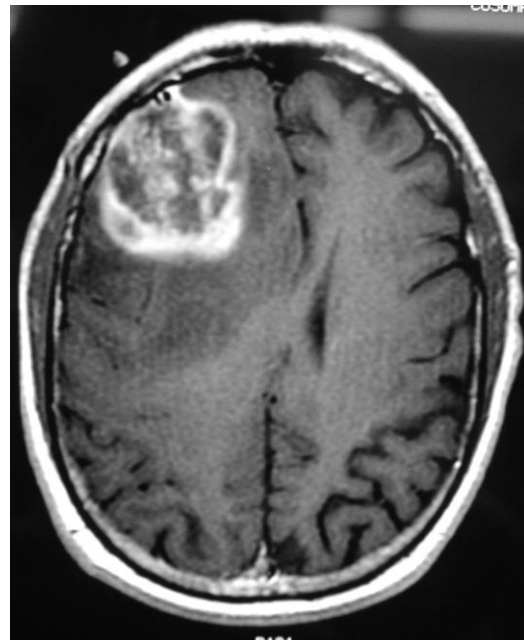


Figure 4. MRI of glioblastoma multiforme (GBM)
(Uddin n.d.)

GBM is most commonly centered in the temporal lobe (31% of cases) and parietal lobe (23% of cases) and generally infiltrates the adjacent cortex and the contralateral hemisphere (Louis, David N. et al. 2016). Despite its rapid infiltrative growth, metastasis through the cerebrospinal fluid is rather seldom and although GBM can promote invasion by remodeling the extracellular matrix, intravasation is very rare (Louis, David N. et al. 2016).

1.5.1 *IDH status*

Besides primary and secondary lesions, GBMs can be further classified by the genetic mutation status of *IDH 1/2*. Accordingly, *IDH wild-type (IDH wt)* and *IDH mutated (IDH mut)* GBM show many differences regarding their localization, histological features and their therapy response. Therefore, the *IDH* status has become of major interest as a predictive molecular marker for many different CNS tumors. In general, *IDH wt* tumors usually arise *de novo*, whereas *IDH* mutated tumors normally progress from a lower grade precursor lesion. *IDH* is an enzyme involved in the Tricarboxylic acid (TCA) cycle, decarboxylating isocitrate to α -ketoglutarate and thereby reducing NAD^+ to NADH. Therefore, the *IDH* status can affect glucose sensing. Since low levels of NADH simulate low glucose levels, mutations in the *IDH1/2 gene* can lead to increased nutrient uptake and decreased differentiation of the tumor cells (Miranda et al. 2017). Furthermore, *IDH* mutations are usually correlated with impaired protection against oxidative stress, increased DNA and histone methylation due to inhibition of demethylases (Raineri and Mellor 2018) and *TP53* mutations, consequently impairing DNA repair (Ichimura et al. 2009). Therefore, *IDH* mutated GBM show improved response to alkylating drugs like temozolomide, the typical chemotherapy for treating GBM (Reitman and Yan 2010, Houillier et al. 2010, SongTao et al. 2012a, Cohen et al. 2013, Li et al. 2016). Accordingly, *IDH* mutated GBM are often characterized by a better overall survival (Louis, David N. et al. 2016).

1.5.2 *O(6)-methylguanine DNA methyltransferase (MGMT)*

Another genetic marker predicting clinical outcome is the methylation status of the *O⁶-methylguanine DNA methyltransferase (MGMT)* promoter in the tumor cells. This enzyme is under physiological conditions involved in DNA repair after alkylation. Expression of *MGMT* is often repressed through promoter hypermethylation in tumor cells, which consequently leads

to impaired DNA repair, enhanced mutation rate and higher sensitivity towards alkylating drugs like temozolomide (H. Li et al. 2016, SongTao et al. 2012).

1.5.3 GBM therapy

GBM belongs to the most aggressive tumors in the CNS. With a median survival of approximately 12 months and a 5-year survival rate of only 3-5%, prognosis is rather poor (Holland 2000, Krex et al. 2007) and new targeted therapy methods are urgently needed. But due to the heterogeneity within GBM, complete eradication of all tumor cell populations is difficult and, even often successfully removed, most tumors recur. Another drawback in treating GBM and other CNS tumors is that drug delivery into the brain parenchyma is very complex and inefficient because of the blood brain barrier, which protects the brain from toxic substances but also complicates delivery of most drugs to the tumor site (Miranda et al. 2017).

Gold standard therapy

Up to now, most patients diagnosed with GBM receive a gold standard therapy consisting of surgical maximal tumor resection with concomitant radiotherapy coupled with temozolomide (TMZ) followed by adjuvant chemotherapy (Stupp et al. 2005). TMZ is an alkylating drug causing G2/M phase arrest and apoptosis due to DNA damage via methylation of O⁶ and N⁷ positions of guanine bases (Miranda et al. 2017, Hirose et al. 2001, Mhaidat et al. 2007). This kind of DNA damage is normally repaired by the protein O⁶-methylguanine-DNA methyltransferase (MGMT). Therefore, patients with a methylated, hence, silenced *MGMT* promoter benefit better from therapy with TMZ (1.5.2) (SongTao et al. 2012, Miranda et al. 2017).

Immunotherapy

Recently, this golden standard scheme has been started to be supported by attempts to activate the own immune system to fight against the cancer. Nevertheless, due to the blood brain barrier the brain had always been believed to be an immune-privileged organ. Hence, it was believed that the immune cells present in the CNS were not capable to interact with the systemic immune system of the body (McGranahan et al. 2019). Furthermore, due to a low mutational burden GBM is a very immune-suppressive, frequently immunologically quiet tumor (McGranahan et al. 2019). However, infiltrating lymphocytes, especially T-cells, were found in

GBM patients with disrupted blood brain barrier function, suggesting an active immune response against the tumor even in GBM. The tumor counteracts with various mechanisms to circumvent the immune response, for instance downregulation of major histocompatibility complex (MHC I and II) expression (A. Wu et al. 2003), upregulation of the immune-checkpoint molecules cytotoxic T-Lymphocyte associated protein 4 (CTLA-4) and programmed cell death protein-1 (PD-1) and recruitment of regulatory T cells (Rivest 2009; Thomas, Ernstoff, and Fadul 2012; Ransohoff and Engelhardt 2012; Reardon et al. 2014).

Up to now, many attempts have been made to activate an immune response targeting the tumor in GBM patients. For instance using checkpoint inhibitors like blocking CTLA-4 or PD-1 has revolutionized treatment of other cancers like lung cancer and melanoma (Dine et al. 2017; Johnson, Rieth, and Horn 2014; Garrett and Collins 2011). A clinical study using nivolumab, a PD-1 inhibitor (NCT02550249), did not show survival benefit combined with severe adverse side effects. Nevertheless, combination with other immune stimulatory drugs might be feasible (Schalper et al. 2019; McGranahan et al. 2019), and checkpoint inhibitor treatment in the neoadjuvant setting has recently been suggested to improve GBM patient survival (Cloughesy et al. 2019; Arrieta, Iwamoto, and Lukas 2019).

Targeted therapy with RTKIs

As cancer cells are driven by sustained proliferation, mostly based on autocrine growth factor signaling (Sporn and Roberts 1985), receptor tyrosine kinases (RTKs) have become a key therapeutic target in order to disrupt this vicious cycle. So far, RTK inhibitors targeting e.g. VEGFR (AZD2171 (Batchelor et al. 2007) or SU1498 (Popescu et al. 2015)) and PDGFR (AG1433) (Popescu et al. 2015) have been investigated in recurrent GBM. Although inhibition of VEGF signaling is capable to restore vascular organization, it did not show survival effects (Batchelor et al. 2007). Furthermore, drugs targeting epidermal growth factor receptors (EGFR), which are often amplified in GBM, have been tested. Accordingly, EGFR inhibitors like gefitinib and erlotinib were most effective in patients harboring EGFR variant III (EGFRvIII) mutations. However, loss of the tumor suppressor gene PTEN might contribute to resistance against EGFR inhibitors (Mellinghoff et al. 2005). However, none of these compounds has been approved for clinical use so far.

Since none of these targeted therapies showed clear benefits regarding clinical outcome, new targeted therapies are urgently needed. The presented study focuses on fibroblast growth factor receptors (FGFR), which were found to be amplified in a variety of cancers including

GBM. Prolonged survival by administration of an FGFR inhibitor could be achieved in mouse GBM xenograft models harboring a *FGFR3-TACC* (transforming acidic coiled coil) in frame fusion (Singh et al. 2012). Reduced tumor growth and prolonged survival was achieved by administration of FGFR inhibitors like PD173074 or AZD4547 suggesting that FGFR inhibition might be a promising approach also in gliomas harboring this kind of mutation (Singh et al. 2012).

1.5.4 Gliosarcoma

Gliosarcoma (GS) belongs to *IDH*- wildtype GBM and account for approximately 2% of all GBM. Since GS are characterized by a biphasic histological pattern consisting of more glial as well as mesenchymal cells, systemic metastases and penetration of the skull are more frequent than in other GBM and exhibit dismal prognosis (Louis, David N. et al. 2016). GS can arise as a primary tumor originating from neoplastic glial cells or occur during the post-treatment phase of GBM (Louis, David N. et al. 2016).

1.6 Receptor Tyrosine Kinases (RTK)

Receptor tyrosine kinases (RTKs) are membrane-bound growth factor receptors consisting of an extracellular ligand binding domain, a transmembrane domain and an intracellular signaling domain. Intracellular signaling is most commonly initiated as soon as a ligand binds to the extracellular domain, causing dimerization of the receptor and autophosphorylation of the intracellular kinase domains, leading to activation of intracellular signal transduction (Schlessinger and Ullrich 1992, Lemmon and Schlessinger 2010). Since RTKs drive cellular processes like proliferation, differentiation, migration and survival, their activation needs to be tightly regulated. (Spangle and Roberts 2017). Hyperactivation or upregulation of RTKs is a frequent event in human cancers leading to sustained proliferation and prolonged survival as already mentioned in chapter 1.3. (Schlessinger und Ullrich 1992, Gschwind et al. 2004, Arora und Scholar 2005, Casaletto und McClatchey 2012).

In addition, various mutations, amplifications and deregulations of RTK- coding genes have been identified in GBM. Upregulation of epidermal growth factor receptor (EGFR), platelet derived growth factor and receptor (PDGF/PDGFR), vascular endothelial growth factor receptor (VEGFR) and MET were found in at least 50% of GBMs (Snuderl et al. 2011).

In the past years, various RTK mutations have been identified in human cancers and first receptor tyrosine kinase inhibitors (RTKIs) have been implemented in the clinics routine. Correspondingly, targeted anticancer therapy using either monoclonal antibodies against the extracellular, ligand binding domain of the respective RTK or inhibition of downstream signaling by small molecule kinase inhibitors have been developed (Zwick, Bange, and Ullrich 2002). Generally, RTKIs interact with their target by binding into the ATP binding pocket of the intracellular kinase domain and thus inhibiting downstream signaling (**Figure 5**) (Mohammadi et al. 1997).

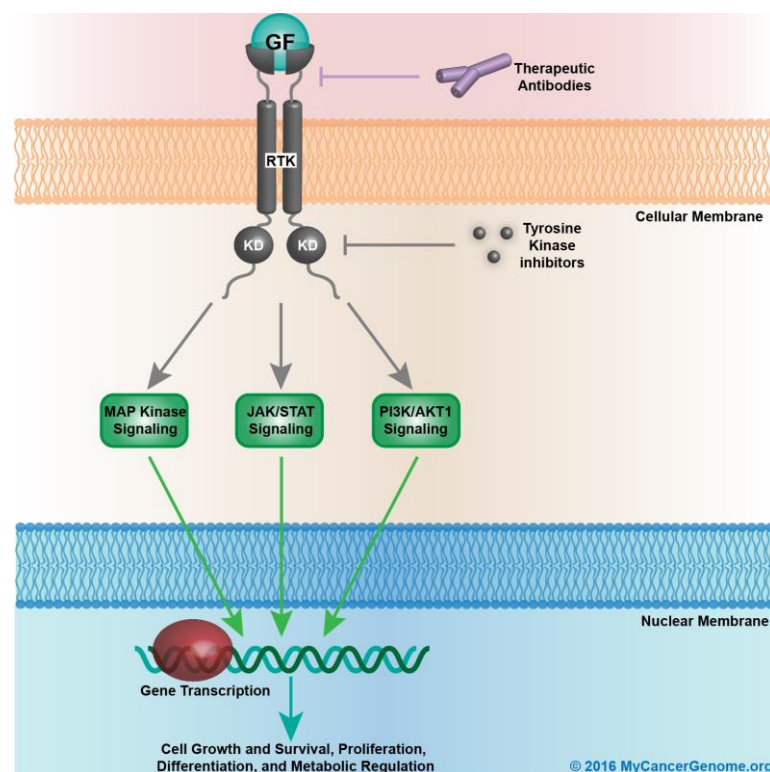


Figure 5. Receptor tyrosine kinases signaling pathways and therapeutic intervention methods.

Receptor tyrosine kinases act on many cellular processes such as proliferation, differentiation, survival and migration by activation of various signaling pathways such as MAPK-, STAT- and PI3K/Akt pathway (My Cancer Genome n.d.)

1.7 Fibroblast growth factor receptors and their ligands

Another class of receptor tyrosine kinases are fibroblast growth factor receptors (FGFRs), which are usually activated by binding of their corresponding ligands, namely the 22 fibroblast growth factors (FGFs). During embryogenesis and wound healing, FGFRs are major players in cell homeostasis, angiogenesis, cell migration and differentiation (Presta et al. 2005; Eswarakumar, Lax, and Schlessinger 2005).

1.7.1 Fibroblast growth factors (FGFs)

FGF subfamily	FGF	Cofactor	Receptor specificity
FGF1 subfamily	FGF1 FGF2	+ Heparin or Heparan sulfate	[All FGFRs [FGFR 1c, 3c > 2c, 1b, 4Δ
FGF4 subfamily	FGF4 FGF5 FGF6		[FGFR 1c, 2c > 3c, 4Δ
FGF7 subfamily	FGF3 FGF7 FGF10 FGF22		[FGFR 2b > 1b
FGF8 subfamily	FGF8 FGF17 FGF18		[FGFR 3c > 4Δ > 2c > 1c >> 3b
FGF9 subfamily	FGF9 FGF16 FGF20		[FGFR 3c > 2c > 1c, 3b >> 4Δ
FGF15/19 subfamily	FGF15/19	+βKlotho	[FGFR 1c, 2c, 3c, 4Δ [FGFR 1c, 3c
	FGF21 FGF23	+αKlotho	

Figure 6. Subfamilies of fibroblast growth factors, their cofactors and receptors
(Ornitz and Itoh 2015)

Up to now, 22 fibroblast growth factors are known which can be divided into seven subgroups based on evolutionary changes and their affinity to different FGFRs (**Figure 6**) (Ornitz and Itoh 2001; Baird and Böhlen 1991; Yun et al. 2010).

Canonical (secreted) FGFs are the largest group of FGFs, represented by the subfamilies 1, 4, 7 and 8 and bind to FGFRs in a heparin/heparan sulfate- dependent manner. Heparin or

heparan sulfate proteoglycane (HSP) protect FGFs from thermal denaturation and stabilize the interaction with the receptor. Canonical FGFs are secreted by translocation through the membrane induced by an N-terminal signal peptide (Ornitz and Itoh 2015).

Endocrine FGFs (FGF15/19 family) primarily function as endocrine factors with very low affinity to heparin/heparan sulfate facilitating the release through the extracellular membrane. Still, these FGFs regulate intracellular pathways in a FGFR dependent manner but, instead of heparin, they use members of the klotho family as cofactors. FGF15 is the murine ortholog of human FGF19. Only FGF19 and FGF23 are known to predominantly activate FGFR4 (Itoh, Ohta, and Konishi 2015; X. Wu and Li 2009; A.-L. Wu et al. 2011; Raja et al. 2019; X. Wu et al. 2010; Grabner et al. 2017; Wyatt and Drüeke 2016).

Intracellular FGFs are represented by the FGF11 subfamily also known as iFGFs. They are not secreted and do not interact with signaling FGFRs. Instead they bind to the C-terminal end of voltage gated sodium channels (Na_v), together with MAPK scaffolding protein IB12 and microtubules (Ornitz and Itoh 2015).

1.7.2 Fibroblast growth factor receptors (FGFRs)

FGFR are classical RTKs that belong to the immunoglobulin (Ig) superfamily and therefore consist of an extracellular ligand-binding domain, a transmembrane domain and an intracellular kinase domain (Ahmad, Iwata, and Leung 2012). Furthermore they contain an acidic box located between two Ig loops in the extracellular domain which contributes to receptor auto-inhibition together with Ig I loop (Kalinina et al. 2012) (compare **Figure 10**). Up to now, five different FGFR genes have been identified, FGFR 1-5 (Sleeman et al. 2001). Contrary to the other members of the FGFR family, the existence of FGFR5 is critically discussed in literature. FGFR5 has been assumed to be a decoy receptor inhibiting activation of other FGFRs, as it has been postulated that FGFR5 lacks the intracellular signaling domain (Zhou et al. 2016). However, newest data suggest that FGFR5 might play a role in Erk 1/2 signaling (Zhou et al. 2016). Depending on the type of FGFR and on the regarding splice variant each receptor has its own ligand binding spectrum (**Figure 6**) (Zhou et al. 2016).

1.7.3 Splicing variants of FGFRs

Specificity of fibroblast growth factor binding to their receptors is mainly determined by their affinity to the immunoglobulin domains of the extracellular part of the receptor. In order to allow an enhanced variability of binding affinities to the four different FGFRs, different splice variants of predominantly FGFR 1, 2 and 3 exist (Holzmann et al. 2012) (**Figure 7**).

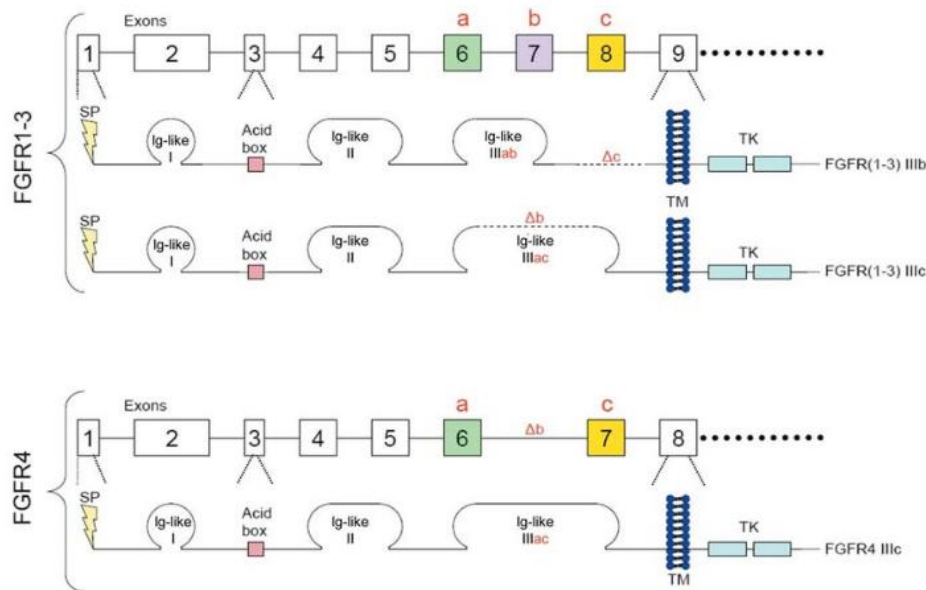


Figure 7. Splice variants of FGFRs
(Holzmann et al. 2012)

The extracellular domains of FGFRs consist of three immunoglobulin loops of which the third determines the ligand specificity. The IgIII loops of FGFR 1-3 are encoded by exon 7-9. Alternative splicing either includes exon 6 and 7 leading to the FGFR-IIIb variant, or skips exon 7 resulting in the IIIc variant. Regarding the binding spectra of the different splice variants, ligand specificity is much more restricted in the FGFR-IIIb variant compared to the FGFR-IIIc variant (Holzmann et al. 2012). As this domain is responsible for ligand-binding, mutations in either of these exons can have distinct outcomes. While loss of the FGFR1-IIIc variant is embryonic lethal, deletion of FGFR1-IIIb does not cause a phenotype (Holzmann et al. 2012). Presence of different splice variants highly varies regarding to their tissue distribution.

In general, FGFR-IIIb variants are more prevalent in epithelial tissue while the FGFR-IIIc variants are characteristic for mesenchymal tissue (**Figure 8**) (Holzmann et al. 2012).

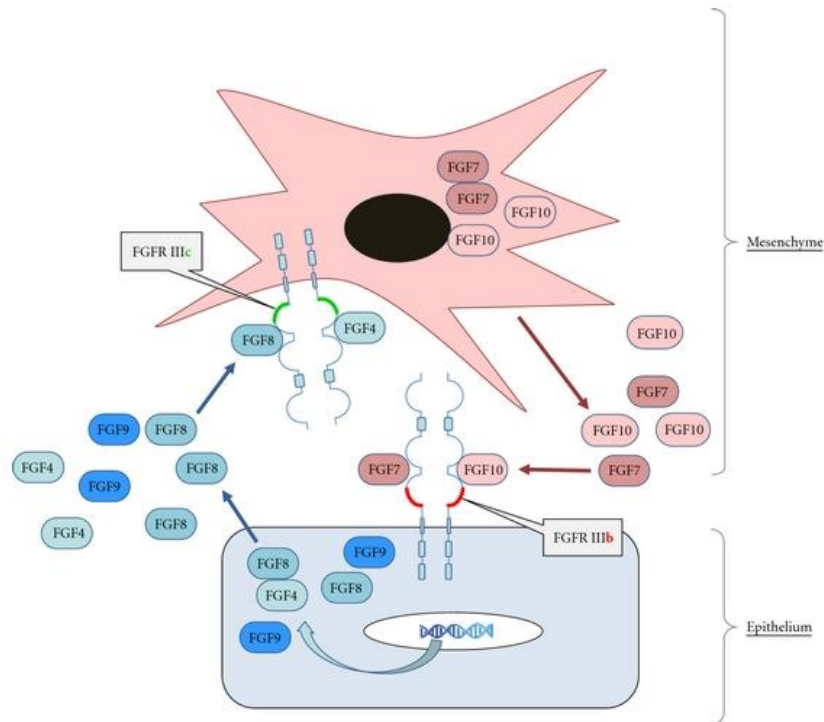


Figure 8. Tissue distribution of different FGFR splice variants
(Holzmann et al. 2012)

During cancer progression, alternative splicing can cause hyperactivation of FGFR signaling. For example, a transformation from FGFR2-IIIb to FGFR2-IIIc variant is a marker for tumor progression and invasiveness in bladder and prostate cancer. Furthermore, prevalent presence of FGFR1-IIIc variant has been associated with highly aggressive non small cell lung cancers and glioblastomas. (Holzmann et al. 2012)

FGFR4 differs in many ways from other FGFRs as described later in 1.8.1. Interestingly, due to loss of exon 7 there are no different splice variants of FGFR4 resulting in a very specific ligand binding spectrum, since only the FGFR4-IIIc variant is present (Heinzle et al. 2014; Holzmann et al. 2012).

1.7.4 FGFR signaling

Canonical signaling via receptor dimerization

FGFRs contribute to many different cellular processes including proliferation, cell migration, differentiation and survival e.g. by activating Ras/MAPK signaling, PI3K/Akt and STAT pathways (Regad 2015). Under healthy conditions, expression of FGFRs and FGFR signaling is tightly controlled in a tissue- and time-dependent manner. Since FGFR-signaling hits multiple hallmarks of cancer, overexpression, constitutive dimerization and aberrant signaling of FGFRs is very common in myeloproliferative syndromes, lymphomas, prostate, breast cancer and other malignant diseases (Corn et al. 2013, Eswarakumar et al. 2005) (**Figure 9**).

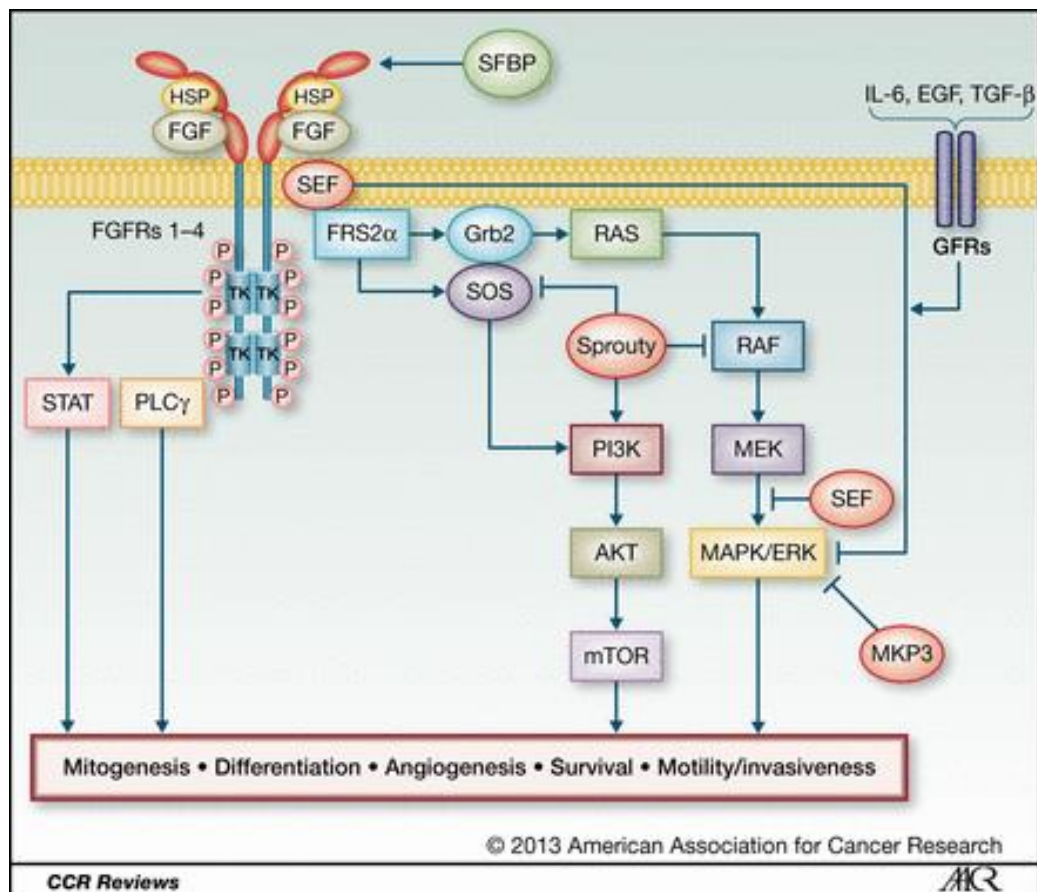


Figure 9. FGFR signaling
(Corn et al. 2013)

FGFR signaling is induced by binding of FGFs to the extracellular immunoglobulin domain in a heparin or klotho protein dependent manner, thereby inducing receptor dimerization and conformational changes in the FGFR structure. Close proximity of the two monomers subsequently enables the transphosphorylation of tyrosine residues in the kinase domains on the C termini (**Figure 10**). Recent studies postulated that activation of FGFR via phosphorylation happens in three sequential steps leading to full activation of FGFR downstream signaling (Ahmad, Iwata, and Leung 2012). Phosphorylated tyrosine residues serve as docking site for adaptor proteins like FGFR substrate 2 α (FRS2 α) or the SH2 domain of phospholipase C γ (PLC γ) (Ahmad, Iwata, and Leung 2012). Activation of various signaling pathways like PI3K/Akt pathway, MAPK pathway and Stat signaling is induced via these adapter proteins, thereby driving cells into growth and proliferation, as well as prolonged survival and migration (**Figure 9**) (Ahmad, Iwata, and Leung 2012). Although kinase domains are relatively well conserved, FGFR4 differs most from FGFR1 (Powers, McLeskey, and Wellenstein 2000).

Furthermore, kinase-independent functions of RTKs have been investigated among other receptors. A study focusing on epidermal growth factor receptor (EGFR) showed that kinase inactive members of the ErbB family are capable of activating MAPK signaling and DNA synthesis (Deb et al. 2001). To study downstream signaling upon kinase inactivation, a mutation affecting the ATP-binding site of the kinase domain (K721M) was used, resulting in complete downregulation of MAPK signaling. Nevertheless, the study proved that the co-expression of the K721M variant together with ErbB2 could stimulate MAPK signaling. Taking together, this data suggest that kinase activation is not required for all EGFR functions (Deb et al. 2001). Based on these findings, kinase-independent signaling might also be postulated for other, related RTK signaling pathways.

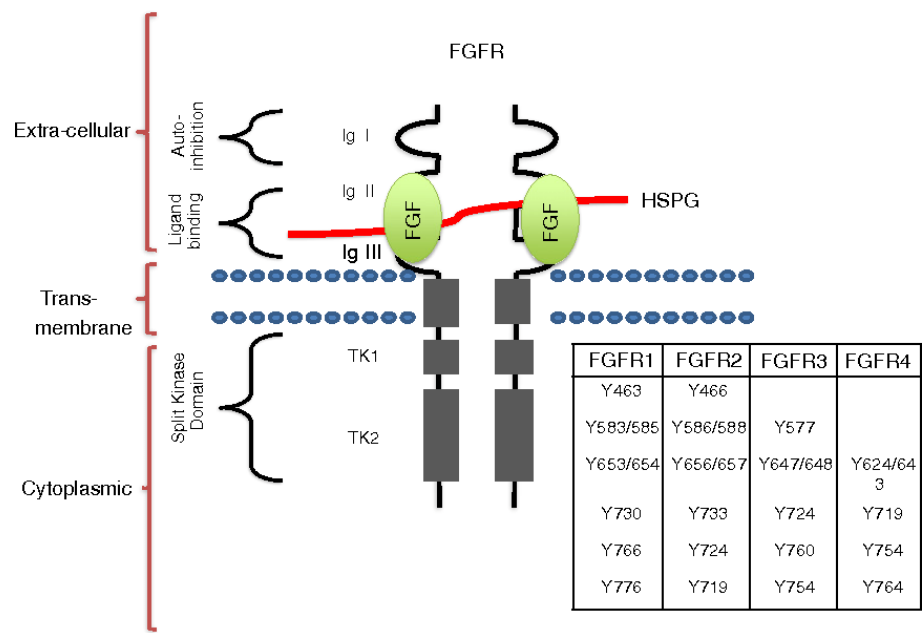


Figure 10. Structure of FGFR
(Ahmad, Iwata, and Leung 2012)

Noncanonical FGFR signaling involving N-CAM and N-cadherin

While canonical FGFR signaling normally acts via binding of FGFs followed by receptor dimerization and phosphorylation of adaptor proteins FRS2 α and PLC γ , noncanonical signaling involves FGFR interactions with neural cell adhesion molecule (N-CAM), cadherins, neurofascin and cell adhesion molecule L1 (**Figure 11**). Notably, extracellular interactions between FGFR and cell adhesion molecules lead to induction of intracellular signaling cascades and thereby promote processes like neurite outgrowth (Kirschbaum et al. 2009; Saffell et al. 1997).

Furthermore, interaction between FGFR and cell adhesion molecules has been proposed to influence cell attachment to the extracellular matrix and thus tumor cell migration and metastasis. Dependency of cell matrix attachment on the interaction between FGFR and N-CAM provided an explanation for observed metastasis upon N-CAM deletion (Heinzle et al. 2014). Furthermore, N-cadherin, which is normally expressed on mesenchymal cells also interacts with FGFR in various ways. It is involved in promoting tumor invasion and metastasis as well as altering FGFR signaling by inhibition of ligand induced internalization of FGFR. Furthermore, FGFR4 over-expressing tumor cells showed increased invasiveness due to loss

of membranous N-cadherin, which could be reconstituted by administration of FGFR kinase inhibitors, indicating kinase dependency of this effect (Heinzle et al. 2014).

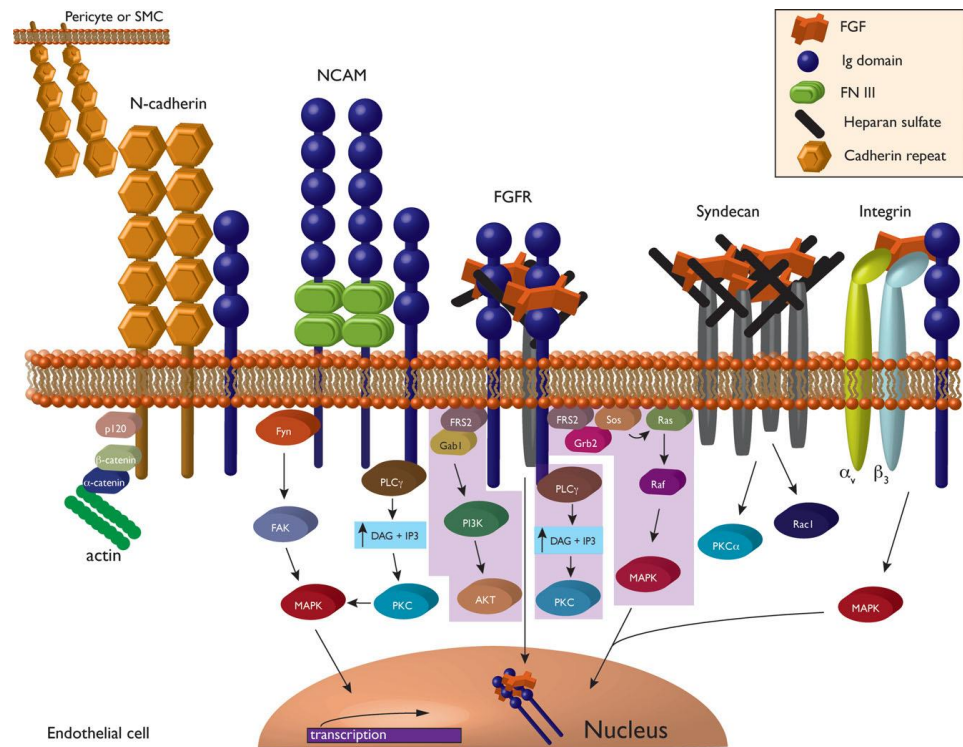


Figure 11. Non- canonical FGFR signaling
(Murakami, Effenbein, and Simons 2008)

1.8 Fibroblast growth factor receptor 4 (FGFR4)

1.8.1 Differences between FGFR4 and other FGFRs

Although FGFR4 is structurally similar to other FGFRs, it differs in various aspects from those family members. First of all, the IgIII domain of FGFR4 is not alternatively spliced, therefore FGFR4-IIIb variant does not exist as in other FGFR isoforms. As exon 7 is lost in the case of FGFR4, only the FGFR4-IIIc variant exists resulting in a distinct and narrower ligand-binding spectrum. In addition to FGF1 and FGF2, FGFR4 provides binding niches for members of FGF4-, FGF8- and the hormonal FGF19 subfamilies (Heinzle et al. 2014). Furthermore, based on homology, the kinase domain of FGFR4 differs clearly from the kinase domain of FGFR1

and of other family members (Powers, McLeskey, and Wellenstein 2000). All of these differences may allow for a more specific targeting and thus inhibition of FGFR4 might not cause as grave adverse side effects as known from other FGFR inhibitors (Heinzle et al. 2014). Nevertheless, FGFR4 might be a suitable target for cancer therapy since its overexpression has been found in a plethora of cancer types including colorectal, prostate, breast and ovarian cancers as well as in rhabdomyosarcomas, lung cancer and glioblastoma (Heinzle et al. 2014). The fact that FGFR4 deletion- contrary to other FGFRs- does not cause an embryonic lethal phenotypes suggests that specific inhibition of FGFR4 in cancer might be better tolerable (Heinzle et al. 2014). Furthermore, differences in IC50 values of RTKIs suggest differences in the kinase domain of FGFR4 and other FGFR allowing a more specific targeting in cancer therapy (Heinzle et al. 2014).

1.8.2 Gene organization of *FGFR4*

The human *FGFR4* gene is located on the long arm of chromosome 5 (5q 35.1) and spans more than 11 kb. Furthermore, it consists of 18 exons encoding for a highly conserved protein structure of 762-802 amino acids depending on the transcript variant (Kostrzewa and Müller 1998).

The promoter region of the *FGFR4* gene reaches from position -198 to -9 and contains more than 1 transcription start point (TSP), a feature limiting gene transcription of many proto-oncogenes, but no TATA or CCAAT elements. The latter is a common feature among many housekeeping genes, oncogenes and growth factors. The *FGFR4* promoter region harbors many binding motifs for transcription factors like specify protein 1 (Sp1), activating protein 2 (AP2) and GC factor (GCF) upstream of the TSPs (Heinzle et al. 2014).

1.8.3 Physiological role of *FGFR4*

Embryonic development and organogenesis

While FGFR4 expression in adults is mainly restricted to specific organs like liver, gall bladder and parts of the urinary tract (THE HUMAN PROTEIN ATLAS, n.d.), it plays an important role during developmental processes. Interestingly, *FGFR4* expression during embryonic development differs from that of the other FGFRs. *In situ* hybridization data in mouse embryos show that *FGFR4* expression is tightly regulated in time and tissue distribution. While *FGFR4*

expression in adult mice is mainly located in liver, kidney and lung, in embryos it was predominantly found in tissues of mesodermal origin as well as the developing lung and gut (Korhonen, Partanen, and Alitalo 2002). Especially the mesenchymal tissue and especially the one differentiating into muscle tissue show high FGFR4 expression. Furthermore, transcripts for *FGFR4* are also found in the metanephros. In conclusion, these data show that FGFR4 might be important for the development of skeletal muscle and organs from endodermal origin (Zhao und Hoffman 2004, Zhao et al. 2006, Buckingham und Montarras 2008, Heinzle et al. 2014, Peláez-García et al. 2013).

Muscle tissue

Since FGFR4 acts in differentiation and wound healing, it also plays an important role during regeneration and differentiation of muscle fibers. FGFR4 was found to be strongly expressed in differentiating myoblasts and newly formed myotubes (P. Zhao and Hoffman 2004). With FGFR1-IIIc and FGFR4 being the main players in myogenic stem cell migration and muscle cell differentiation, respectively, FGFR4 deficiency results in muscle degeneration, however does not affect myogenesis. Contrary, upregulation or hyperactivation of FGFR4 in muscle tissue can promote rhabdomyosarcomas (Taylor et al. 2009; Marics et al. 2002). Although FGFR4 is expressed in muscle fibroblasts during regeneration, it is not present in mature skeletal muscle indicating that FGFR4 might only be important during muscle cell differentiation (Taylor et al. 2009).

Glucose metabolism and bile acid synthesis

Recently, evidence was accumulating that FGFR4 is also related to metabolic syndromes. Based on studies showing that FGFR4 deletion in mice resulted in obesity, insulin resistance and glucose intolerance despite normal diet, FGFR4 deregulation has been demonstrated to contribute to metabolic syndrome phenotypes. This assumption was supported by the fact, that restoration of FGFR4 expression could restore normal plasma lipid levels (Huang et al. 2007, Ge et al. 2014).

Another important function of FGFR4 in metabolism is the role of the FGF19- FGFR4 axis in the regulation of bile acid (BA) synthesis. The impact of FGFR4 on BA synthesis was shown in mice lacking FGFR4, resulting in an elevated BA synthesis and elevated secretion of bile acids (Heinzle et al. 2014; Hagel et al. 2015; Shah et al. 2002; Zaid et al. 2013; Liu et al. 2013). Especially FGF19, a growth factor mainly signaling via FGFR4, seems to play a major role in

bile acid metabolism and hepatocyte proliferation (Peláez-García et al. 2013). FGF19 or the mouse orthologue FGF15 were identified to inhibit bile acid synthesis by repression of CYP7A1 (cholesterol 7 α -hydroxylase), the first and rate-limiting step in bile acid synthesis (Inagaki et al. 2005; A.-L. Wu et al. 2011; X. Wu and Li 2009).

1.8.4 *FGFR4 in cancer*

Since FGFR4 signaling acts in cellular processes like proliferation, differentiation and migration, its deregulation, constitutive receptor dimerization or overexpression hits multiple hallmarks of cancer. FGFR4 overexpression has been observed in rhabdomyosarcoma, hepatocellular and pancreatic cancer, adenocarcinoma, GBM and many other cancers (Heinzle et al. 2014).

Furthermore, upregulation of FGFR4 and thus hyper-activation by ligands like FGF19 increased aggressiveness in colorectal cancer and hepatocellular carcinoma. Inhibition via downregulation of FGFR4 using shRNA proved dependency of these mechanisms on FGFR4 downstream signaling (Peláez-García et al. 2013). Apart from that, FGFR4 overexpression was found in many grade III astrocytomas enhancing tumor aggressiveness and affecting patient survival. Based on their aggressive phenotype, astrocytomas harboring FGFR4 overexpression were assigned to grade III astrocytomas and showed similar clinical outcome as glioblastoma patients (Yamada et al. 2002).

1.8.5 *FGFR 4 Gly/Arg polymorphism and its role in cancer*

Among all alterations affecting the *FGFR4* gene, one single nucleotide polymorphism (SNP) in exon 9, resulting in amino acid change from glycine to arginine at position 388 in the transmembrane domain (**Figure 12**), has been reported to have major influence on tumor progression and invasiveness (da Costa Andrade et al. 2007; Taylor et al. 2009; Bange et al. 2002), (Nami Sugiyama et al. 2010). (**Figure 12**). It was postulated that this alteration affects tumor aggressiveness by stabilizing the FGFR4 in the membrane and prolonging signaling and activation of the receptor (Wang et al. 2008). Consequently, FGFR4 downstream signaling is constitutively active and mediates many cancer-promoting functions like proliferation, survival and migration (Bange et al. 2002; Taylor et al. 2009). Especially in colorectal and prostate

cancer, the FGFR4-Arg variant has been connected with increased cell motility and tumor invasiveness (Peláez-García et al. 2013; Wang et al. 2008).

Conversely, for head and neck cancer, the FGFR4-Gly variant was associated with higher cancer risk (Wimmer et al. 2019; Ansell et al. 2009) while interestingly, the FGFR4-Arg variant seems to enhance therapy success by sensitizing cells towards chemotherapeutics like cisplatin (Ansell et al. 2009). However, although cancer incidence seems to be higher in FGFR4-Gly variant, other studies have shown that if malignancy occurs, patients are facing faster progression and worse prognosis as if their tumors carry the FGFR4-Arg variant (da Costa Andrade et al. 2007).

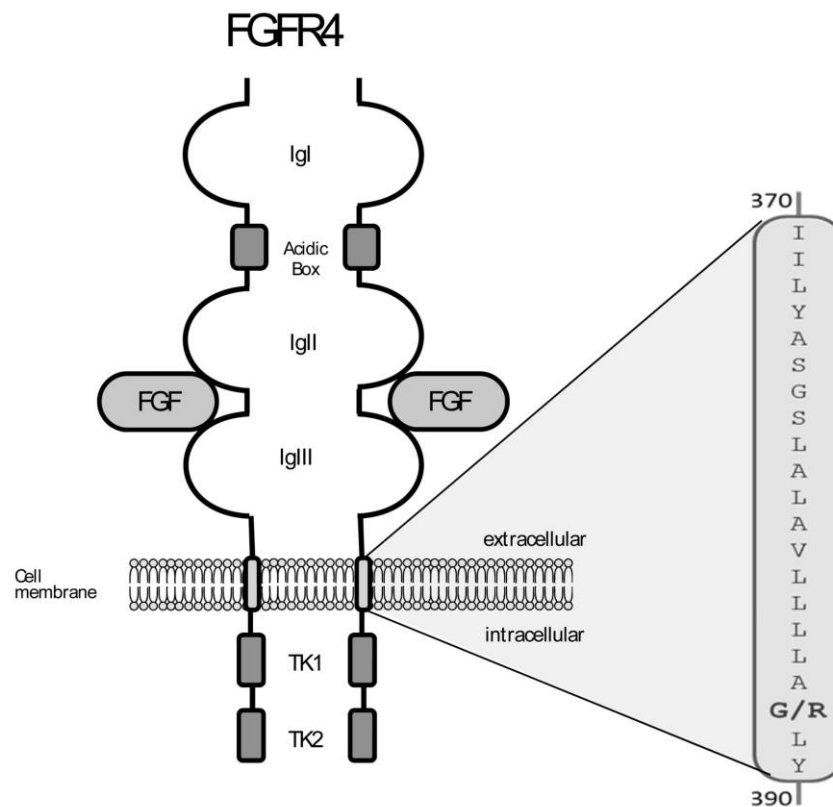


Figure 12. FGFR4- Position of single nucleotide polymorphism (SNP) in transmembrane domain
(Heinzle et al. 2014)

1.9 Epithelial to mesenchymal transition (EMT)

Epithelial tissues are under physiological conditions composed of one or more organized layers of cells connected by tight cell junctions. Nevertheless, during development and a variety of pathological conditions this cell layer can be affected in numerous ways. Probably the most remarkable one is a state of high plasticity whereby cells lose their epithelial markers and change to a mesenchymal phenotype known as epithelial to mesenchymal transition (EMT) (**Figure 13**). This process is mainly characterized by loss of epithelial markers, such as E-cadherin or CD31 and gain of mesenchymal markers such as N-cadherin, Vimentin or snail. Consequently, cells undergoing EMT acquire new migratory and invasive properties enabling them to invade into surrounding tissues (Kalluri and Weinberg 2009).

Recent studies have shown that the process of EMT plays a role in a huge variety of diseases such as renal fibrosis and cancer (Sporn and Roberts 1985; Barriere et al. 2015). Physiologically EMT is applied during embryogenesis and wound healing, however reactivation of these processes can lead to tumorigenesis, tumor invasion and metastasis (Giannelli et al. 2016; Craene and Berx 2013; Kalluri and Weinberg 2009; Kovacic et al. 2012; Kim et al. 2017; Zeisberg et al. 2007; Stenmark, Frid, and Perros 2016). The acquisition of mesenchymal markers and a more migratory phenotype was also investigated in endothelial cells, referred to as endothelial to mesenchymal transition (EndEMT), which is physiologically needed for heart development. Nevertheless, pathological activation of EndEMT is a crucial factor in building up the tumor microenvironment, as EndEMT derived cells are believed to function as fibroblasts in the tumor, thereby contributing to tissue remodeling and fibrosis. Accounting for approximately 40% of all migratory cancer associated fibroblasts (CAFs), EndEMT plays an important role during cancer progression and angiogenesis (Potenta, Zeisberg, and Kalluri 2008).

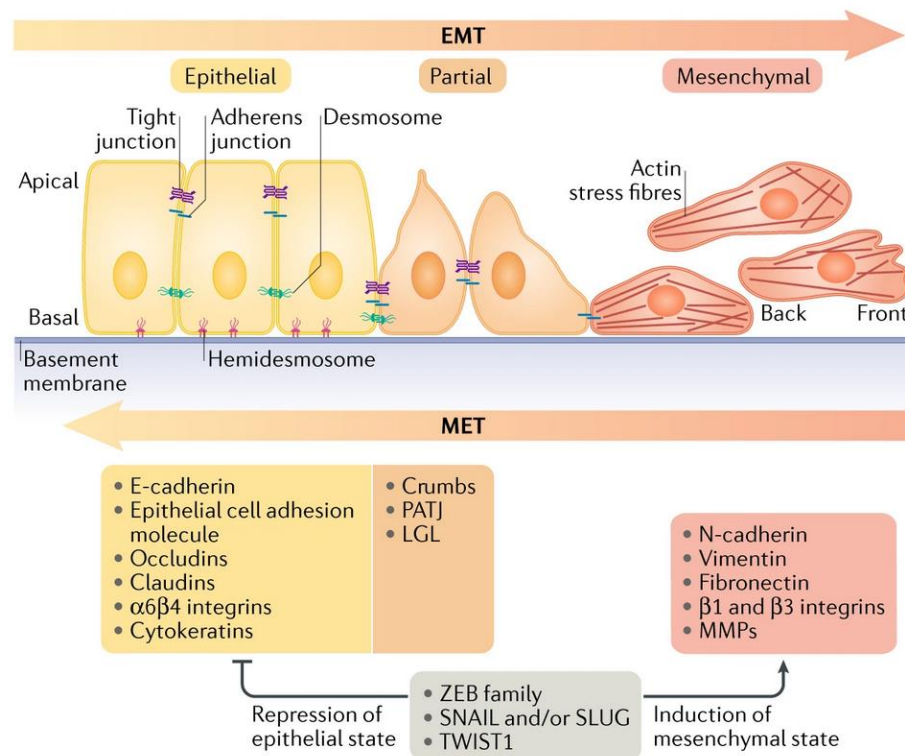


Figure 13. Epithelial to mesenchymal transition (EMT)
(Dongre and Weinberg 2019)

1.9.1 Role of FGFR4 in epithelial to mesenchymal transition

Since FGFR4 is involved in cell migration and differentiation, aberrant activation of FGFR4 during cancer progression can enhance EMT and thus tumor invasion and metastasis. FGFR4 has been associated with enhanced tumor progression and invasiveness in many different forms of cancer (Liu et al. 2013, Peláez-García et al. 2013, Shi et al. 2015a, (Gauglhofer et al. 2014). A study performed in colorectal cancer cells showed that knock-down of FGFR4 resulted in impaired migratory and invasive capacity and could decrease expression of mesenchymal markers like *TWIST1*, *SNAIL* or *ZEB1* while restoring E-cadherin expression on the membrane (Peláez-García et al. 2013).

Downregulation of E-cadherin and consequently loss of attachment to neighboring cells is mainly mediated by helix-loop-helix transcription factors like snail. Furthermore, glycogen synthase kinase 3 (GSK3 β) plays a role in the process of EMT, as active GSK3 β signaling is proposed to be important for maintaining the epithelial architecture (Lan, Qi, and Du 2014). During EMT GSK3 β can be phosphorylated and thus inactivated by Akt which is part of the

PI3K pathway and, thus, one of the main downstream signaling cascades of FGFR4 (Lan, Qi, and Du 2014). As GSK3 β facilitates proteasomal degradation of snail, inactivation of GSK3 β via Akt signaling or via inhibition of GSK3 β could promote EMT via upregulation of snail (Lan, Qi, and Du 2014). A study in hepatocellular carcinoma proposed that FGF19, a ligand with high affinity for FGFR4, could promote EMT via β -catenin signaling. Since GSK3 β is phosphorylated and thus inactivated by Akt signaling it leads to accumulation of active β -catenin which can then be transported to the nucleus. In the nucleus β catenin drives expression of many mesenchymal markers like Twist or Snail and can thereby repress E-cadherin expression. Knock-down of FGF19 proved dependency of the FGF19-FGFR4 axis since knock-down resulted in impaired phosphorylation of GSK3 β and thus β -catenin mediated EMT signaling. (**Figure 14**) (H. Zhao et al. 2016).

#

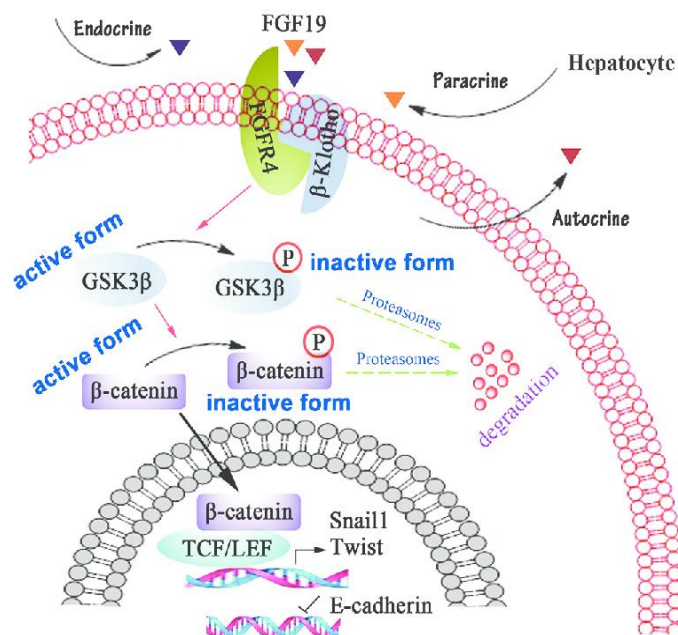


Figure 14. FGF19 modulates EMT via FGFR4- GSK3 β signaling
(H. Zhao et al. 2016)

Another way how FGFR4 has been associated with EMT is by interaction with Matrix-Metalloproteases (MMPs) and thus altering the composition of the extracellular matrix facilitating migration and invasion (N. Sugiyama et al. 2010). Especially the FGFR4-Arg variant could lead to MT1-MMP stabilization and its protection from lysosomal degradation (Nami Sugiyama et al. 2010). In turn, increased levels of MT1-MMP enhanced auto-phosphorylation of FGFR4-Arg variant. In contrast, the FGFR4-Gly variant downregulated MT1-MMP expression and overexpression of MT1-MMP induced degradation of FGFR4-Gly (Nami Sugiyama et al. 2010).

In summary FGFRs, and also FGFR4 signaling, are involved in many cellular processes driving tumor formation and progression as well as in EMT and, hence, promote tumor cell migration and metastasis (**Figure 15**).

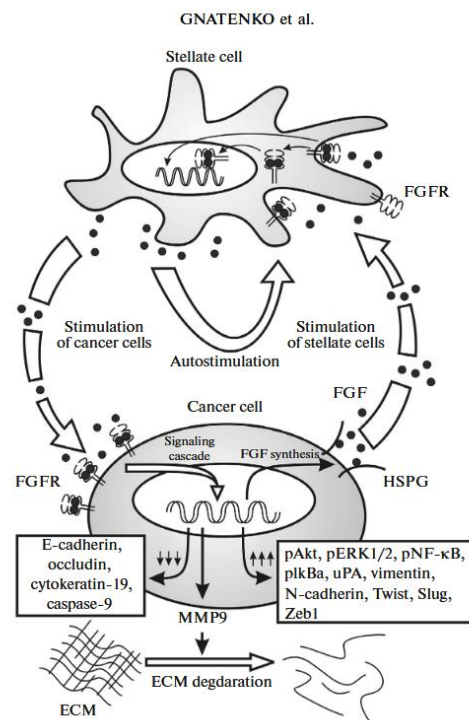


Figure 15. Role of FGFR4 signaling during epithelial to mesenchymal transition
(Gnatenko, Kopantsev, and Sverdlov 2017)

2 Aim of the study

Glioblastoma multiforme (GBM) and its subform gliosarcoma (GS) represent the most common and the most malignant types of tumors affecting the central nervous system. Among many different mutations driving tumor onset and progression in this very diverse tumor entity, a subgroup of GBM patients harbors a distinct overexpression of receptor tyrosine kinase FGFR4. As FGFR4 has been associated with tumor aggressiveness and poor overall survival in a variety of other tumors, the aim of this study was to dissect the role of FGFR4 in glioma. While other fibroblast growth factor receptors and their function in ontogenesis have been studied intensively, comparatively less is known about the oncogenic role of FGFR4. Especially since FGFR4 drives many cellular processes like proliferation, differentiation and migration, it might be a promising target in cancer therapy.

The aim of this study was to dissect the role of FGFR4 in glioma cell aggressiveness by inducing a dominant-negative mutation in the kinase domain via expression plasmids which were stably integrated into glioma cells by retroviral transduction or lipofection. This point mutation affects the intracellular signaling domain, leading to diminished activation of FGFR downstream signaling via PI3K/Akt, MAPK and Stat3 signal transduction. Furthermore, we aimed to point out the impact of the *G388R* SNP in the transmembrane domain of the receptor, which has already been associated with enhanced tumor cell aggressiveness in other tumor types. Our main interest was to shed light on the differences between cell clones expressing the genetically modified FGFR4 variants and the vector- control cell lines regarding cell proliferation, differentiation and migratory potential in the selected glioblastoma and gliosarcoma cell models.

3 Material and Methods

3.1 Cell culture

The glioblastoma multiforme (GBM) and gliosarcoma (GS) cell lines used in this study are indicated in **Table 1**. Cells were grown in cell culture flasks under humidified conditions with 5% CO₂ and 37 °C (normal cell culture conditions) in their respective medium (**Table 1**) supplemented with 10% fetal bovine serum (FBS). For passaging, the flasks were washed with trypsin/EDTA in order to remove remaining medium and then incubated in trypsin until cells detached. These detached cells were flushed with medium and split 1:2 up to 1:6 depending on the respective cells' proliferation rate. As BTL1376 is growing partially as floating spheres, cells were centrifuged prior trypsinization. The GBM cell line SIWA M1 originated from a prior mouse experiment where patient derived GBM cells were injected into SCID mice and then re-isolated from the developed tumor. To avoid contamination, cell lines were cultured in two independent batches that were handled separately. No antibiotics in the growth media were used among this study.

Table 1 Used cell lines in this study

Cell line	Medium	Tumor entity
SIWA M1	RPMI10	Glioblastoma multiforme mouse
SIWA M1 GFP	RPMI10	Glioblastoma multiforme mouse
SIWA M1 FGFR4-KD-GFP	RPMI10	Glioblastoma multiforme mouse
SIWA M1 FGFR4-Gly-GFP	RPMI10	Glioblastoma multiforme mouse
SIWA M1 FGFR4-Arg-GFP	RPMI10	Glioblastoma multiforme mouse
BTL1376	RPMI10	Gliosarcoma (human)
BTL1376 GFP	RPMI10	Gliosarcoma
BTL1376 FGFR4-KD-GFP	RPMI10	Gliosarcoma
BTL1376 FGFR4-Gly-GFP	RPMI10	Gliosarcoma

* RPMI-1640 medium supplemented with 10% FBS

For seeding, trypsinized cells were centrifuged for 5 minutes with 270 g and the pellet was resuspended in growth medium. Cell suspension was mixed in 1:2 ratio with trypan blue and pipetted into Neubauer counting chambers. The chosen cell concentration was highly variable depending on the aim of the respective assay (**Table 2**).

Table 2 Used cell concentrations

Method	SIWA M1	BTL1376
MTT	4*10 ⁴ /ml	4*10 ⁴ c/ml
Colony formation assay	2*10 ³ /ml	4*10 ³ /ml
Sphere formation assay	2*10 ³ /ml	4*10 ³ /ml
Retroviral transduction	0.5*10 ⁵ /ml	1*10 ⁵ /ml
Migration assay	2*10 ⁵ /ml	2*10 ⁵ /ml
Invasion assay	2*10 ⁵ /ml	2*10 ⁵ /ml
Wound healing assay	2*10 ⁵ -3*10 ⁵ /ml	
Stimulation assay (Protein isolation)	2,5*10 ⁵ /ml	
Confocal laser scanning microscopy	1*10 ⁴ /ml	2*10 ⁴ /ml
siRNA knock-down (FGFR4)-protein isolation	1.5*10 ⁵ /ml	
siRNA knock-down (FGFR4)-RNA isolation	2*10 ⁵ /ml	
<i>In vivo</i> tumor formation in SCID mice	1*10 ⁶ c/100 µl	1*10 ⁶ c/100 µl

For long-term storage, cells were frozen in liquid nitrogen. Therefore, cell suspension was centrifuged for 5 minutes with 270 g at room temperature and the cell pellet was carefully resuspended in the adequate medium containing 7.5 % DMSO avoiding bursting of the cells. Subsequently, the aliquots were first stored at -80 °C in a reservoir filled with isopropanol,

allowing gradually cooling and freezing of the cells before they were transferred into liquid nitrogen for long term storage.

3.2 Retroviral vectors with FGFR4 variants

The four FGFR4 variants show changes in only one base. Two of the FGFR4 variants are SNP variants (G388R) with either a glycine or an arginine at codon 388 or a point mutation in the kinase domain (K504M) of the FGFR4 resulting in receptor-inactivation and thus even in a dominant negative FGFR4. The fourth variant harbors a gain of function point mutation (K645E) leading to receptor hyper-activation. The K504M and K645E mutated FGFR4 vector were generated by site-directed mutagenesis and was kindly provided by Prof. D.J. Donoghue and Prof. J. Khan, respectively. The vector containing the loss of function mutation is exemplarily depicted below (**Figure 17**)

The four genetically modified FGFR4 variants had been cloned using In-fusion cloning (Takarabio, Kusatsu, Japan) into a pQCXIP (Addgene, Watertown, Massachusetts, USA) retroviral backbone. Thereby, *FGFR4* gene was fused to the CMV promoter as well as to the green fluorescent protein (GFP) reporter in such a way that the start and stop codon of the target gene was removed. Therefore, the CMV-*FGFR4*-GFP is in one reading frame. Characteristically, this plasmid harbors a cytomegalovirus (CMV) promoter leading to strong ubiquitous expression of the altered *FGFR4* gene. In addition, pQCXIP harbors an ampicillin bacterial resistance cassette as well as a puromycin (**Figure 16**) selectable marker allowing selection for cells with a stably integrated *FGFR4* variant in their genomes.

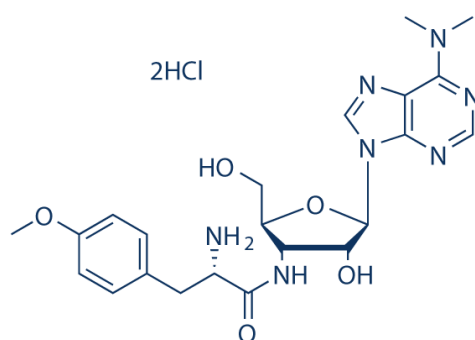


Figure 16. Puromycin

Puromycin used concentration [1µg/ml] in 0.9% sodium chloride (NaCl)
Selleckchem (Houston, Texas, USA)

Four such retroviral vectors have been used, all encoding a different FGFR4- GFP fusion gene. In detail, the FGFR4 vectors included one SNP variants (FGFR4-Gly or FGFR4-Arg), a dominant negative point mutation in the FGFR4 kinase domain K504M (**Figure 17**) or a gain of function point mutation (K645E). All retroviral plasmids contain a CMV promoter. Furthermore, the vectors carry a puromycin resistance cassette. A pQCXIP vector encoding for GFP under a CMV promoter served as control.

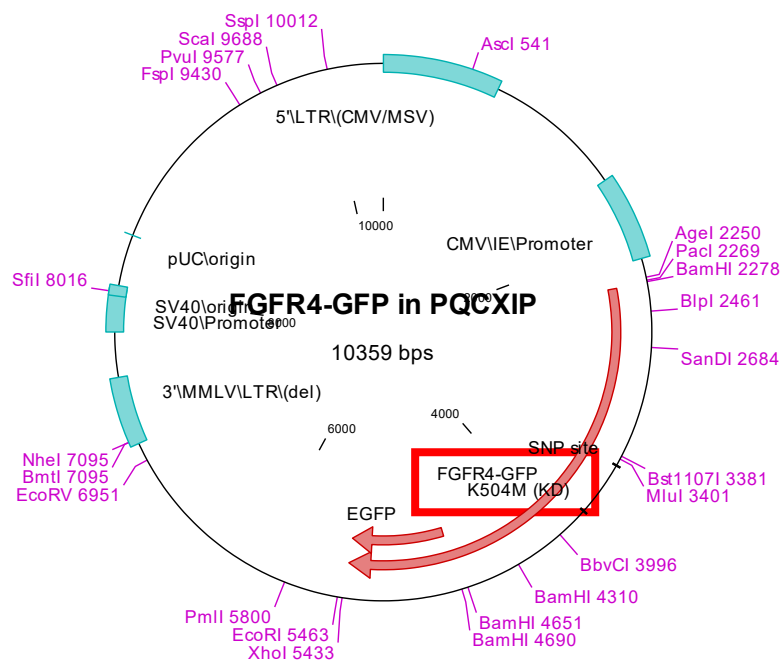


Figure 17 Vector map of FGFR4-KD-GFP variant: The FGFR4 gene contains a dominant negative mutation at position 504 where a lysine has been substituted by a methionine affecting the phosphorylation and hence leading to loss of function of FGFR4 signaling.

3.3 Calcium phosphate transfection of Hek293 cells for retrovirus production

For production of retroviral particles, fast proliferating Hek293 cells were transfected using CaCl_2 . Precisely, plasmids containing the respective FGFR4 variant and two helper plasmids encoding for enzymatic and scaffold retroviral proteins (for gag-pol-env) were transfected.

Workflow:

Hek293 cells were seeded in T25 flasks ($1.5 \cdot 10^6$ c/flask). After 24 h when cells were ~80 % confluent, the CaCl_2 mixture was prepared containing 5 μg DNA of the FGFR4 variant plasmid, 240 μM CaCl_2 and the two helper plasmids A169 (gag-pol) and A168 (env). To start the transfection reaction, air was bubbled into the 2*HBS (**Table 3**) using a glass pipette while the plasmid- CaCl_2 mix was added dropwise. Afterwards the solution was incubated for 12 minutes at room temperature before it was applied dropwise to the medium of Hek293 cells. Upon 5 h incubation, transfection medium was replaced by DMEM growth medium supplemented with 10%FBS. After 72 h, the supernatant containing the retroviral particles was filtrated (0.45 μm pores) from cell fragments and pure virus aliquots were stored at -80°C . All virus work was performed in a virus laboratory with L2 permission.

Table 3 2*HBS buffer

2*HBS buffer
50 mM HEPES
10 mM $\text{KCl}^{\text{£}}$
12 mM Dextrose
280 mM $\text{NaCl}^{\text{¥}}$
1.5 mM $\text{Na}_2\text{HPO}_4^{\text{ª}}$
=> pH to 7.05

[£] potassium chloride

[¥] sodium chloride

^ª Disodium hydrogen phosphate

3.4 Retroviral transduction of glioma cell lines

For retroviral transduction of glioma cell lines, cells were seeded in 6-well plates. The next day, growth medium was removed and replaced by 1 ml retroviral stock solution of the desired FGFR4 variant. Since the FGFR4 variants are fused to GFP as a reporter, transduction efficiency could be visualized on the Nikon Eclipse fluorescence microscope (Nikon Eclipse Ti-S). Depending on the transduction efficiency and the cells' performance, the retroviral stock solution was incubated between 16 and 30 h, then the wells were washed with normal growth medium and incubated for one or two days for recovery. Cells were observed under the microscope each day. Puromycin [1 µg/ml] was used to select for FGFR4-GFP integrated cells. Eventually, FGFR4-over-expressing cells were frozen in liquid nitrogen for long-term storage. All virus work was performed in a virus laboratory with L2 permission.

3.5 Cell proliferation and migration assays

3.5.1 Cytotoxicity assay (MTT)

Different methods, procedures and assay kits can be used to determine the cell viability towards cytotoxic drugs, which are known as cytotoxicity assays or cell viability assays. Such as, the widely used MTT assay makes use of a colorimetric detectable conversion of the slightly colored tetrazolium salts into strongly orange colored formazan (3-(4, 5-Dimethylthiazol-2-yl)-2, 5-diphenyltetrazolium bromide) (MTT). The MTT assay is based on the metabolic activity of viable cells and the activity of the enzyme NAD(P)H-dependent oxidoreductase (**Figure 18**). The assay can be used to determine the cell sensitivity towards a certain treatment and to calculate the half maximal inhibitory concentration (IC₅₀) of cytotoxic drugs. The intensity of the color corresponds directly to the reductive potential of this enzyme and hence to the metabolic activity, therefore, the viability of the cells.

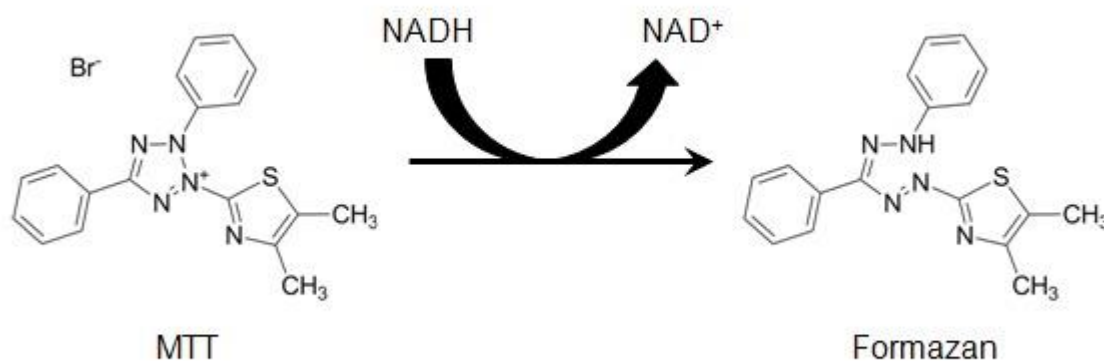


Figure 18. Formazan formation by NADH dependent oxidoreductase
(Structures of MTT and colored formazan product. " 2016)

Workflow:

On day one, cells are counted and seeded in appropriate cell numbers (**Table 2**) in 100 µl per well in a 96-well plate in their respective growth medium. The next day, cells are treated with increasing concentrations of drugs (**Table 4**) and kept under normal cell culture conditions. 72 h after treatment, cell viability is measured with EZ4U kit (Biomedica, Vienna, Austria) and cells are incubated at 37°C until the color changes. The metabolic activity of the cells is measured spectrophotometrically by measuring the absorbance at 450 nm with 620 nm as a reference on the Infinite M200 PRO microplate reader (Tecan, Männedorf, Switzerland). For cell vitality assays cells were treated with inhibitory drugs in triplicates, resulting in three different values per drug concentration.

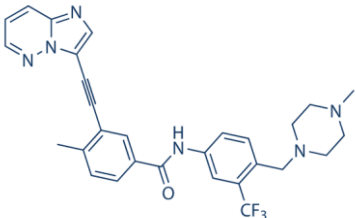
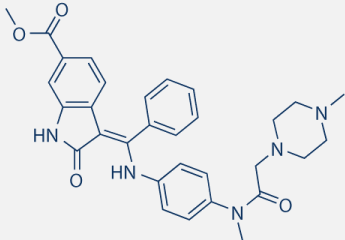
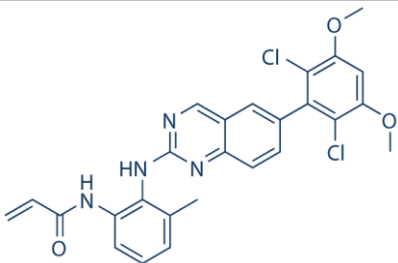
3.5.2 ATP assay

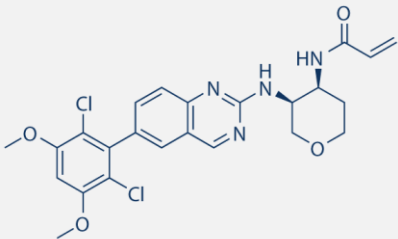
Another method to determine the cell viability is measuring the ATP level using the CellTiter-Glo Luminescent Cell Viability assay (Promega, Fitchburg, Madison, USA). We used this method for analyzing the drugs' cytotoxic potential in the semi-adherent GS cell line BTL1376.

Workflow:

The seeding and drugging of the cells was performed like described in section 3.5.1. After 72 h 80 µl of the medium was removed carefully and 100 µl of the solution (according to the protocol) were added. After cells have been lyzed, 100 µl of the mix was transferred into a white 96-well cell culture microplate (Greiner Bio, Kremsmünster, Austria). Subsequently luminescence was measured at the Infinite M200 PRO microplate reader (Tecan).

Table 4 Used drugs

Drug	Target	Chemical structure	Solvent	Company
Ponatinib	Receptor Tyrosine kinases		DMSO ^Δ	Selleckchem/ LC Labs (Woburn, Massachusetts, USA)
Nintedanib	Receptor tyrosine kinases		DMSO ^Δ	Selleckchem
Blu9931	FGFR4		DMSO ^Δ	Selleckchem

Blu554	FGFR4		DMSO ^Δ	Selleckchem
---------------	-------	--	-------------------	-------------

^Δ Dimethylsulfoxide

3.5.3 Colony formation assay (Clonogenic assay)

Colony formation assay is a commonly used method to investigate the proliferation behavior of cells and their ability to form clones out of a single cell. Optionally, agents interacting with the proliferation capacity of the cells including anti-proliferative drugs or pro-proliferative growth factors can be added.

Workflow:

Cells were seeded in duplicates or triplicates in very low density (**Table 2**) in a 24-well plate and kept overnight under normal cell culture conditions for recovery. Optionally, drugs or growth stimulants were added. After seven days, the medium was aspirated and the plate was dried overnight to avoid washing away of cells during the staining procedure. The next day, wells were washed with phosphate buffered saline (PBS) (**Table 5**) and cells were fixed with ice-cold 100% methanol at 4 °C for at least 20 minutes. Remaining methanol was washed away with PBS and subsequently fixed cells were stained using crystal violet (**Table 6**). Finally, wells were rinsed with tap water until background stain was completely removed. Photographs were taken using the Nikon D7200 camera. For quantification of the clone formation capacity, the crystal violet was dissolved by 2 % sodium dodecyl sulfate (SDS) overnight. The elution was transferred into a 96-well plate in triplets and absorbance was measured at the Infinite M200 PRO microplate reader (Tecan) with 560 nm.

Alternatively, pictures were analyzed using the Particle Analyzer of the Image J software. Therefore, pictures taken with the Nikon were converted into a binary format and subsequently analyzed with the Particle Analyzer software. Since area covered by cells was converted to black and background signal stayed white Integrated Density or part of the area covered by

cells was measured. A similar approach was also performed using an algorithm designed for R studio.

Another evaluation method uses the Typhoon scanner, which computes the area of each well which is covered with cells. Thus, it measures the fluorescence of crystal violet at 633 nm. Therefore, an empty well was included to subtract the background staining of the well.

Table 5. 10 PBS solution*

10*PBS		
Na₂HPO₄ * 2H₂O	9.5 g	Merck, Darmstadt, Germany
NaH₂PO₄ x H₂O	3.2 g	Merck
NaCl	4.4 g	VWR, Radnor, Pennsylvania, USA
ddH₂O bring to 1L		
Diluted with ddH₂O to create 1* working solution		

Table 6. Crystal violet solution

Crystal violet		
Stock solution	100 mg	(Sigma-Aldrich, St. Louis, Missouri, USA)
	1 ml Ethanol	VWR
Working solution	1:1000 in PBS	

3.5.4 Sphere formation assay and re-differentiation assay

To investigate 'stemness' of glioma cells, thus the ability of the cells to form neuro-spheres, cells were seeded in low cell concentrations (**Table 2**) in duplicates or triplicates in ultra-low attachment 24-well plates in serum-free NB+ medium (**Table 7**) and pictures were taken every day for evaluation. Optionally, growth factors can be added to see whether stimulation could enhance sphere formation. Cells that are able to form spheres, therefore de-differentiate, under the described culturing conditions are sought to possess stem cell-like features.

To investigate the capacity of cells to re-differentiate after sphere formation, spheres were spun down with 500 g for 8 minutes and the medium was replaced by their normal growth medium in 24-well plates. After re-differentiation, cells were fixed and stained like described above (3.5.3). Results were evaluated and quantified as described in 3.5.3 as well.

Table 7 NB+ Medium recipe

NB+ Medium	Company
500ml Neurobasal medium	Life technologies, Carlsbad, California, USA
1% B27 (50x)	life technologies
1% N ₂ supplement A (100x)	life technologies
2 µM L-Glutamine	
20 ng/ml Epidermal growth factor (EGF)	Sigma Aldrich
20 ng/ml basic fibroblast growth factor (bFGF)	Preprotech, Rocky hill, New Jersey, USA

3.5.5 Migration assay

As one characteristic hallmark of cancer cells is to invade and migrate through other tissues, our FGFR4 altered cancer cell models were also tested for their migratory potential *in vitro*. To investigate migratory capacity of the used cancer cell models, transwell migration assays were performed. This assay is based on the potential of the cells to migrate from a transwell insert into the lower well through a fine meshed net with pores of 8 µm. Cells are thereby attracted by nutrients exclusively present in bottom well. Cancer cells with high migratory potential are suspected to be highly aggressive and metastatic.

Workflow:

For migration assay, transparent polyethylene terephthalate (PET) membrane inserts (Szabo Scandic, Vienna, Austria) with a pore size of 8 µm were placed into each well of a 24-well plate. Glioma cells were seeded in duplicates in appropriate cell numbers (**Table 2**) in 400 µl serum-free medium into each transwell while the bottom well was filled with 800 µl growth medium supplemented with 10 % FBS. After 72 h, the transwells were taken out and non-migratory cells from the upper part of the net were washed away. Cells on the bottom part of the filter were fixed with methanol and stained with crystal violet. The cells in the lower plate were incubated for another 5-6 days to allow cells to settle and form clones before they were fixed and stained as well. The evaluation and quantification of the assay was continued as described in (3.5.3)

3.5.6 Invasion assay

Another characteristic feature of aggressive cancer cells is invasion into blood vessels (intravasation) and other tissues. To investigate the capacity of glioma cells to invade through a tense barrier, the transwells used in the migration assay were additionally coated with matrigel (BD Biosciences, San Jose, California, USA).

Workflow:

For the invasion assay, PET membrane inserts were coated with matrigel, which was thawed and stored at 4 °C. As matrigel is liquid at 4 °C and starts polymerizing at room temperature, cooled tips and tubes had to be used for coating the transwells. The matrigel was diluted 1:5 from a 5 mg/ml stock with cold serum-free medium before 70 µl were added to each transwell. Afterwards, the plate was incubated at 37 °C allowing the matrigel to polymerize. The next day before the cells were seeded, the excessive matrigel was washed away with serum-free medium so that only pores remained sealed. The experiment was continued as described in (3.5.5)

3.5.7 Wound healing assay

Another method to test the migratory potential of cells is the wound healing assay or scratch assay. In this experiment, cells are seeded densely as a confluent monolayer and then a

scratch is made with a microliter pipette tip. Cells are followed using live cell microscopy until the gap is closed.

Workflow:

Cells were seeded in high density (**Table 2**) in an 8-well glass chamber slide (ibidi, Gräfeling, Germany and Fitchburg, Wisconsin, USA) or 24 well plates and incubated overnight for recovery. The next day or after two days when cells were completely confluent, scratches were made using a p10 micropipette tip and cells were washed with growth medium. Live cell microscopy started immediately. During the analysis, photos were taken in a meaningful time interval varying between 15-45 minutes depending on the proliferative and migratory potential of the respective cell model for a total observation time of up to four days. The quantification was performed using T scratch software (CSE lab, Zurich, Switzerland).

3.5.8 Confocal laser scanning microscopy

For high resolution images and localization of the FGFR4 molecules within the cell, confocal laser scanning microscopy (CLSM) was used. In CLSM, a laser beam which is focused through a pinhole scans the focal plane of the sample. After exposure to the laser, the electrons are in an excited state whose reversal leads to fluorescence. The emitted light is then directed through another pinhole, in which out- of focus light is filtered. CLSM provides high contrast, high resolution images and avoids background signal by filtering out of focus light (**Figure 19**).

Workflow:

For the CLSM, cells were seeded in appropriate cell number (**Table 2**) in 300µl in each well of chamber slides with removable silicon chambers (ibidi). Afterwards cells were kept under normal cell culture conditions for resettlement. The next day, medium was sucked up and wells were washed carefully with PBS. Subsequently cells were fixed with 4 % paraformaldehyde (PFA) for 20 minutes at room temperature. After a second washing step with PBS, cells were stained with 1.4 µg/ml 4', 6-Diamidin-2-phenylindol (DAPI) and 5 µg/ml wheat germ agglutinin (WGA) in PBS and incubated for 10 minutes at room temperature. DAPI is used as a nuclear stain while WGA is used to stain membranes. Finally, wells were washed with PBS and covered with Vectashield (Vector Laboratories, Burlingame, California, USA). Pictures were taken at Zeiss LSM 700 Confocal laser scanning microscope (Zeiss, Oberkochen, Germany) and evaluated using Image J software.

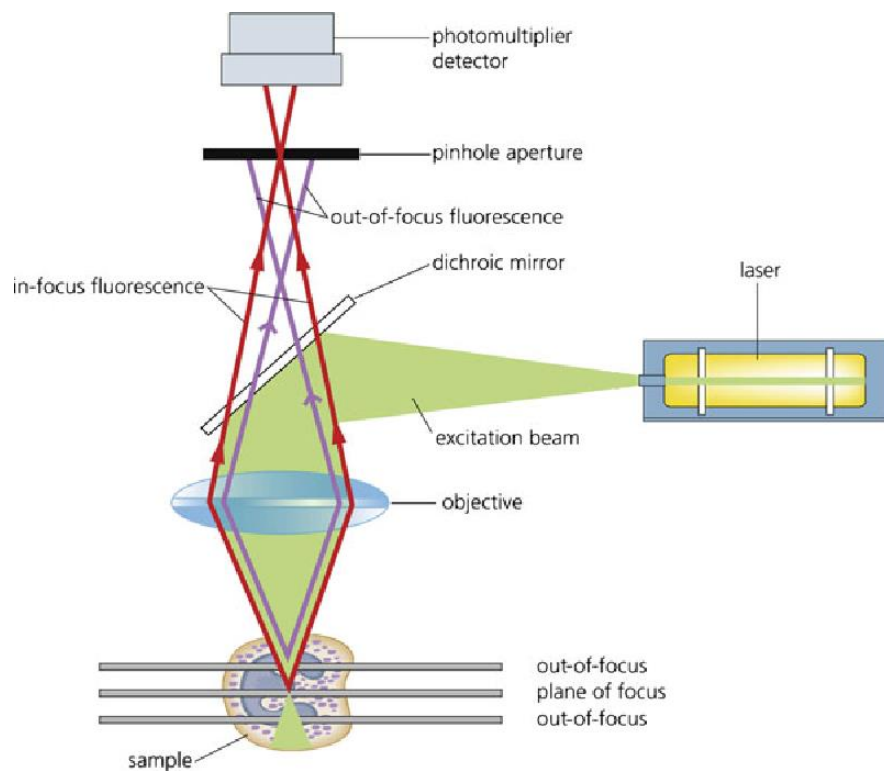


Figure 19. Confocal laser scanning microscopy.
(Hardham 2012)

3.6 Protein isolation and analysis methods

To investigate protein expression and activation levels of our cell models, proteins were isolated and further analyzed by Western blotting.

3.6.1 Total protein isolation

Cells were seeded in 6-well plates or T25 cell culture flasks and incubated overnight under normal cell culture conditions for recovery. For stimulation experiments, cells were starved by replacing the media by serum-free medium the day after seeding. After 24h of starvation, FGFs were added stimulating the FGFR-downstream signaling. Cells were stimulated with either 100 ng/ml FGF2, FGF19 or FGF23 for 15 minutes. Cells were scratched into PBS, collected in 15 ml Falcon tubes and centrifuged at 271 g at 4 °C for 8 minutes. After centrifugation, the cells were lysed in 30-50 μ l lysis buffer (**Table 8**) containing protease and phosphatase

inhibitors for 1 h on ice. Better lysis could be obtained by pipetting the lysates up and down every ten minutes during the incubation period. Afterwards, samples were sonicated for 8 minutes in an ultrasound bath to achieve complete lysis of the cell pellet. Finally, samples were centrifuged at 20,000 g at 4 °C for 15 minutes. The supernatant containing protein lysates was collected and stored at -80 °C. From the protein lysates 2.5µl were isolated for protein concentration determination (3.6.4).

Table 8 *Lysis buffer recipe*

Lysis buffer		
Lysis buffer	50 mM Tris/HCl (pH 7.6)	VWR
	300 mM NaCl	VWR
	0.5% Triton X-100	Sigma – Aldrich, St. Louis, Missouri, USA
cOmplete (Protease inhibitor) Roche	12.5 µl	Roche. Rotkreuz, Switzerland
PhosStop (phosphatase inhibitor)	25 µl	Roche
Phenylmethylsulfonylfluoride (PMSF) (protease inhibitor) (100mM) Sigma	5µl	Roche

3.6.2 *Membrane protein enriched fraction*

To isolate membrane fractions, cells were seeded into T75 or T150 cell culture flasks and grown up to a confluence of approximately 90 %. Cells were scratched into medium and collected into 50 ml tubes, which were centrifuged at 482 g at 4 °C for 8 minutes. The pellet was washed with 5 ml PBS and again centrifuged. During centrifugation, dounce- and neutralization buffers (**Table 9**) were prepared and protease and phosphatase inhibitors were added at the same concentration as described above (3.6.1). The pellet was resuspended in 1.5 ml dounce buffer and incubated on ice for 10 minutes. Afterwards, cells were filled into a

homogenisator and cell walls were mechanically destroyed by 70-100 slow pushes. The cell vitality indicating cell wall destruction was checked with trypan blue (Sigma-Aldrich) - at least 90% of the cells should be dead. Then 500 µl neutralization buffer was added and samples were centrifuged at 482 g for 8 minutes at 4°C. The supernatant, containing membrane and cytosolic fraction, was collected in ultra-centrifuge tubes (S100AT6) and the nucleic pellet was discarded. 40 µl ethylenediaminetetraacetic acid (EDTA) was added to the cytosolic fraction. The samples were equilibrated and centrifuged for 1h at 603,810 g in the SORVALL MX150+ Micro Ultracentrifuge (Thermo Fisher Scientific). The pellet containing the membrane fraction was resuspended in 75-100µl lysis buffer depending on the pellet size (**Table 8**) and sonicated with ultrasound pulses for 30 seconds until pellet was fully lyzed. The lysates were stored at -80 °C and 2.5 µl were set aside for protein determination.

Table 9 Buffers for membrane enriched fractions

Dounce buffer	
0.12 g Tris/HCl (10mM, pH 7.6)	0.12 g
0.01 g MgCl ₂ (0.5mM)	0.01 g
Dissolve in 100 ml ddH ₂ O	
<i>Add 25 µl/ml complete, 50µl/ml phosphostop and 10 µl PMSF before use</i>	
Neutralization buffer	
0.12 g Tris/HCl (10mM, pH 7.6)	0.12 g
0.01 g MgCl ₂ (0.5mM)	0.01 g
3.5 g NaCl (0.6M)	3.5 g
Dissolve in ddH ₂ O	
<i>Add 25 µl/ml complete, 50µl/ml phosphostop and 10 µl PMSF before use</i>	
EDTA (Ethylenediaminetetraacetic acid):	
0.25 M pH 7.6	

3.6.3 Cytosolic and Nuclear extracts

Isolation of cytosolic and nuclear extracts occurred according to the instructions given in the protocol of NE-PER Nuclear and Cytoplasmic Extraction reagents (Thermo Fisher Scientific, Waltham, Massachusetts, USA).

3.6.4 Protein determination

Protein concentrations were measured using the colorimetric “Pierce BCA Protein Assay Kit” (Thermo Fisher Scientific). For computing the calibration curve, a serial dilution row of bovine serum albumin (BSA) was measured. 2.5 µl of protein lysates were diluted 1:200 with ddH₂O and applied in triplets of 150 µl in a 96-well plate. Afterwards, samples were mixed with developing solution 1:2. After 1-2 hours of incubation (37 °C), the color change was measured either on the ASYS Expert Plus Microplate reader (Cambridge, UK) or on Tecan spectrophotometer by detecting the absorbance at 620 nm.

3.6.5 Sodium dodecyl sulfate polyacrylamide gel electrophoresis (SDS-PAGE)

For Western blot analysis, 8-15 µg of proteins were separated according to their molecular mass on 10 % polyacrylamide gels (**Table 10**).

Table 10 Acrylamide gels recipe

Separation gel (10 % Acrylamide)	
H₂O	3.65 ml
Acrylamide	1.875 ml
Tris/HCl 1.5M pH 8.8	1.875 ml
20 % SDS	75 µl
10 % Ammoniumperoxidesulfate (APS)	25 µl
Tetramethylenediamine (TEMED)	5 µl

Collecting gel (4.5 % Acrylamide)	
H ₂ O	1.56 ml
Acrylamide	0.281 ml
Tris/HCl 0.5 M pH 6.8	0,625 ml
20 % SDS	25 µl
10 % APS	12.5 µl
TEMED	2,5 µl

3.6.6 Western blot

After the protein samples have been separated according to their molecular weight, they were blotted onto polyvinylidenfluorid (PVDF) membranes using Trans Blot Turbo (Bio-Rad, Hercules, California, USA). In this procedure, electric voltage is used in order to transfer the negatively charged proteins from the gel onto the membrane. For semidry blotting, the PVDF membranes were activated with 100% methanol and the sandwich was built as follows:

1. Filter paper (Bjerrum buffer MeOH) (**Table 11**)
2. Activated membrane
3. Acrylamide gel
4. Filter paper (Bjerrum buffer with SDS (**Table 11**))

The blotting efficacy was evaluated by total protein staining with Ponceau solution. To avoid unspecific binding of the primary antibodies, the membranes were blocked with 0.5 % BSA and 1 % fat free powdered milk in Tris (hydroxymethyl) aminomethane (Tris) buffered saline with 0.1% Tween 20 (Bio-Rad) (TBST) for 1 h. Afterwards, membranes were washed with TBST three times for ten minutes each before primary antibodies were added (**Figure 20**)

All used buffers and reagents are listed in (**Table 11**).

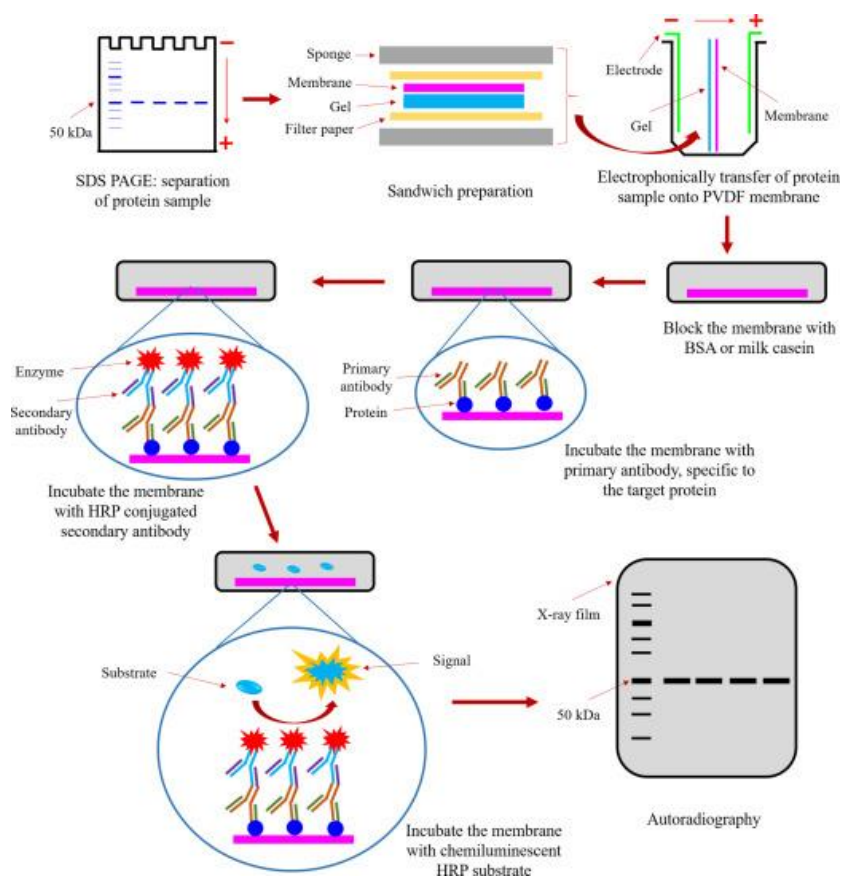


Figure 20 Western blotting
("Western Blotting - an Overview | ScienceDirect Topics" n.d.)

Table 11 Buffers and solutions for Western blotting

Buffers and solutions		
10*TBS	120 g Tris	VWR
	90 g NaCl	VWR
	Dissolve in 1 L ddH ₂ O and bring to pH 7.6	
1*TBST	100 ml 10*TBS	
	900 ml ddH ₂ O	
	1 ml Tween 20	Bio - Rad

10* Lämmli Elektrophoresis buffer	30 g Tris	VWR
	144 g Glycine	Sigma - Aldrich
	10 g SDS	Sigma Aldrich
	Dissolve in 1 L ddH ₂ O	
Bjerrumbuffer with Methanol	5.82 g Tris	VWR
	2.93 g Glycine	Sigma - Aldrich
	200 ml Methanol	VWR
	Bring to 1 L with ddH ₂ O	
Bjerrumbuffer with SDS	5.82 g Tris	VWR
	2.93 g Glycine	Sigma
	0.375 g SDS	Sigma
	Dissolve in 1 L ddH ₂ O	
4*Sample loading buffer	4 ml 99.5 % Glycerin	Sigma- Aldrich
	2 ml 2-Mercaptoethanol	Merck
	0.92 g SDS	Sigma- Aldrich
	0.2 mg Bromphenolblue	Merck
	2.5 ml 1M Tris-HCl (pH6.8)	
	Bring to 10 ml with ddH ₂ O and store aliquots at -20 °C	
Tris/HCl 1.5M pH8.8	18.2 g Tris(hydroxymethyl)-aminomethan in 100ml ddH ₂ O (pH8.8)	VWR

Tris/HCl 0.5M pH6.8	3 g Tris (hydroxymethyl)-aminomethan in 50ml ddH ₂ O (pH6.8)		VWR
Ponceau staining solution	Ponceau S	1 g	Sigma- Aldrich
	Acetic acid	50 ml	Merck
	ddH ₂ O	1 L	

3.6.7 Antibody incubation

Membranes were incubated overnight in primary antibody solution at 4°C. If not otherwise stated, antibodies were diluted 1:1000 in TBST with 3 % BSA. The next day, the membranes were washed three times with TBST. Afterwards respective (Rb, Ms) secondary antibodies conjugated to horseradish peroxidase (HRP) were added (1:10,000 in 1 % BSA/TBST) for an incubation time of 1 h. Finally, the membranes were again washed three times with TBST. Detection of the protein of interest was achieved by the reaction of the horseradish peroxidase (HRP) enzyme linked to the specifically bound secondary antibody with H₂O₂ and luminol reagent (**Table 12**). This reaction was visualized on an x-ray film in a dark chamber.

Table 12. Luminol

Luminol		
p- Coumaric acid	125 µl	Sigma-Aldrich
Luminol	250 µl	Sigma-Aldrich
1M Tris/HCl (pH 8.8)	5 ml	Merck/Sigma-Aldrich
ddH₂O	To final volume of 50ml	

Table 13 Used Antibodies

Primary Antibody (1:1000 in 3%BSA/TBST)	Source	Company
β -actin (1:2000 in 3%BSA/TBST)	Mouse	Sigma-Aldrich
Erk	Rabbit	Cell signaling (Danvers, Massachusetts, USA)
p-Erk (Tyr202/Ser204)	Rabbit	Cell signaling
FGFR4	Rabbit	Cell signaling
Lamin A/C		Cell signaling
S6	Mouse	Cell signaling
p-S6 (Ser240/244)	Rabbit	Cell signaling
Vimentin	Rabbit	Cell signaling
Secondary Antibody 1:10,000 in 1% BSA/TBST	Source	Company
α mouse antibody	goat	Genetech (San Francisco, California, USA)
α rabbit antibody	mouse	Santa Cruz (Dallas, Texas, USA)

3.7 Polymerase Chain reaction (PCR)

The polymerase chain reaction (PCR) is a technique applied for amplification of specific DNA fragments using specific primer pairs and a thermostable polymerase.

The three main steps during a PCR cycle are:

1. Denaturation (90-95 °C): dsDNA is denaturized into two single stranded molecules
2. Annealing (50-75 °C): Primer pairs bind to the target gene sequence on 3'OH
3. Elongation (72 °C): Polymerase elongates target gene sequence in 5'→3' direction

These steps are repeated for 30-55 cycles, followed by a final elongation step (**Figure 21**).

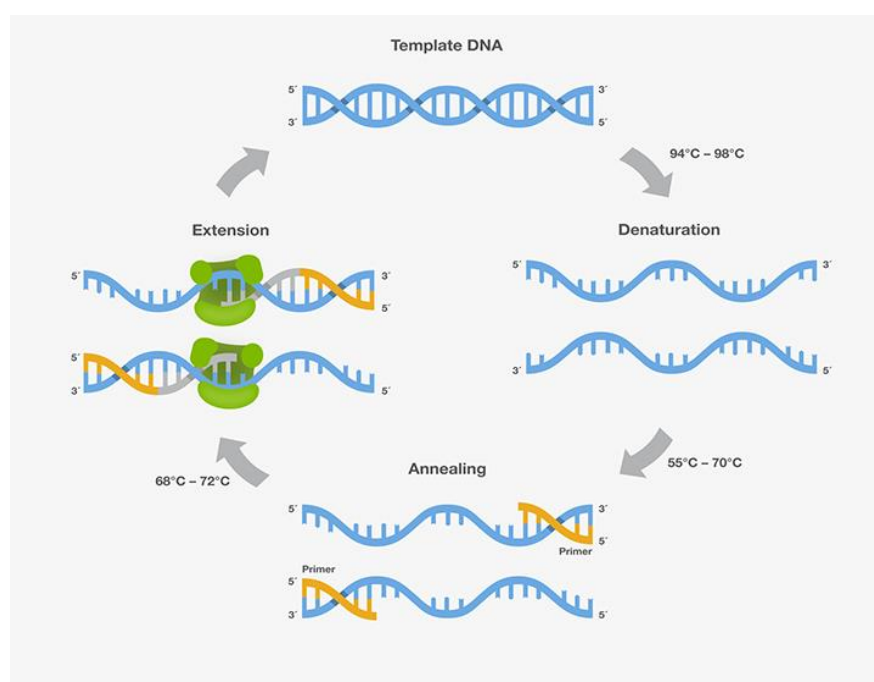


Figure 21 Polymerase chain reaction (PCR)

("Polymerase Chain Reaction (PCR) and Its Principle – The Science Info" n.d.)

3.7.1 RNA isolation with Trizol

For RNA isolation, medium was aspirated and cells were lysed in Trizol (Thermo Fisher Scientific). Afterwards, chloroform (Sigma-Aldrich) was added (1/5 of Trizol volume). The tubes were inverted and incubated for ten minutes at room temperature before they were centrifuged for 15 minutes at 12,000 g at 4 °C.

After centrifugation, RNA is solved in the aqueous upper phase of the triphasic content (chloroform phase), which is separated by an interphase from the organic, lower phase (Trizol

phase) containing proteins and DNA. The upper phase was collected in a new tube and cold isopropanol was added for RNA precipitation. The solution was incubated for ten minutes and then centrifuged for 15 minutes at maximum speed (30,279 g). The supernatant was discarded and the RNA pellet was washed twice with 80 % EtOH. Finally, the pellet was dissolved in nuclease-free H₂O to achieve a concentration in the range of 100-1000 ng/μl and stored at -80 °C. The next day RNA concentration was measured at Nanodrop ND-1000 (Thermo Fisher Scientific).

3.7.2 Reverse transcription of RNA to cDNA

Since a DNA template is needed for PCR reaction mRNA was converted into cDNA by reverse transcription. Therefore, 1 μg of RNA was diluted in H₂O to a final volume of 11 μl and incubated at 70 °C to remove remaining proteins. Then, 9 μl reverse transcription master mix were added (**Table 14**) and kept at 42 °C for at least 1.5 hours for reverse transcription.

Table 14 Reverse transcription master mix

1*MM for reverse transcription		
5* Transcription buffer	4μl	Fermentas, Thermo Fisher
Hexanucleotide	1μl	Invitrogen
dNTPs	1μl	GE Healthcare Life Sciences
Dithiothreitol (DTT)	2μl	Sigma Aldrich
Revert Aid Reverse Transcriptase (200 Units/μl)	1μl	Fermentas

3.7.3 Quantitative real time PCR (qPCR)

For a precise quantification the DNA amount was measured in a real-time setting. In order to detect amplified PCR products, a fluorescent signal, proportional to the amount of amplified DNA, is measured. In this study, SYBR Green and TaqMan probes were used as fluorescent probes.

Workflow SYBR green qPCR:

10 ng of cDNA was mixed 1:2 with 5 µl GoTaq qPCR Mastermix (Promega, Madison, Wisconsin, USA) and the primers [10 µM] for the gene of interest (primer sequences see below). Each sample was applied in triplets to a hard-shell 96-well qPCR plate (Bio- Rad). DNA levels were quantified and normalized to *ribosomal protein L41 (RPL41)* serving as housekeeping gene. To exclude contamination, a negative control was used containing RNase free water instead of sample DNA. The qPCR was performed on CFX96 Real time system Thermo Cycler (Bio- Rad) (**Table 15**). The results were evaluated using CFX maestro software (Bio- Rad) and processed according to the following formula:

$$2^{-\Delta CT} = 2^{-(CT \text{ target gene} - CT \text{ housekeeping gene})}$$

GFP (EGFP)

Forward: 5'– ACGTAAACGGCCACAAGTTC

Reverse: 5'– AAGTCGTGCTGCTTCATGTG

Klotho β (KLB)

Forward: 5'– AGATGTGCAGGGCCAGTTT

Reverse: 5'– GCCACAGACTCGGGCTTA

Vimentin (VIM)

Forward: 5'– CCAGATGCGTGAAATGGAAG

Reverse: 5'– TGAGTGGGTATCAACCAGAG

Snail (SNAIL)

Forward: 5'– CCCAATCGGAAGCCTAACTACAG

Reverse: 5'– CAGGTGGGCCTGGTCGTA

β – catenin (CTNNB1)

Forward: 5'– GTGCTATCTGTCTGCTCTAGTA

Reverse: 5'– CTTCTGTTTAGTTGCAGCATC

Ribosomal protein L41 (RPL41)

Forward: 5'- CAAGTGGAGGAAGAAGCGA

Reverse: 5'- TTACTTGGACCTCTGCCTC

Glyceraldehyde -3- phosphate dehydrogenase (GAPDH)

Forward: 5'- CGG GAA GCT TGT CAT CAA TGG

Reverse: 5'- GGC AGT GAT GGC ATG GAC TG

Table 15. PCR program (qPCR)

PCR program (qPCR)		
	50 °C	10 sec
Initial denaturation	95 °C	10 min
Cycle	95 °C	15 sec
	60 °C	10 min
	95 °C	10 sec
Melt curve	65 °C-95 °C	0.5 sec

50x

Quantitative real time PCR using TaqMan probes

For *FGFR4* expression on mRNA level qPCR using TaqMan probes (Thermo Fisher Scientific) was performed. In this setting a fluorogenic probe is used and signal detection is achieved by the 5' nuclease activity of the Polymerase leading to separation of the dye on the 5' end and the quencher on the 3' end of the probe. The fluorescent signal is measured and normalized to *β actin* levels as housekeeping gene like described above. cDNA dilution (1:25) was mixed with FAM/ROX qPCR Mastermix (**Table 16** and **Table 17**) (Thermo Fisher Scientific). Results were analyzed like described in 3.7.3.

Table 16. Mixture for 1 TaqMan PCR reaction

	Volume	Company
Maxima Probe qPCR Master Mix (2X)	5 µl	Thermo Fisher Scientific
FAM probe (<i>FGFR4</i> / β -actin)	0.5 µl	Thermo Fisher Scientific
cDNA (1:25)	5 µl	

TaqMan probes:

FGFR4-FAM: HS01106913_g1 (Applied Biosystems, Thermo Fisher Scientific)

β -actin (ACTB)-FAM: HS99999903 (Applied Biosystems, Thermo Fisher Scientific)

Table 17. PCR program (TaqMan PCR)

PCR program (TaqMan)		
	50 °C	2 min
Initial denaturation	95 °C	10 min
Cycle	95 °C	15 sec
	60 °C	1 min

} 55x

3.7.4 Restriction fragment length polymorphism PCR (RFLP PCR)

To test whether our generated cell models express the *FGFR4*-Gly or *FGFR4*-Arg allele of *FGFR4*, a PCR was performed (**Table 18** and **Table 19**) targeting *FGFR4* and subsequently a restriction enzyme was used specifically cutting in the region of interest (**Table 20** and **Figure 22**). Two samples carrying either the *FGFR4*-Gly or *FGFR4*-Arg variant served as positive controls. Additionally, GAPDH was used as positive control for the PCR and as housekeeping

gene (data not shown). For the RFLP PCR, first the region of interest was amplified using the following FGFR4 primers:

FGFR4

Forward: 5'- GAC CGC AGC AGC GCCC GAGG CCAGG TATA CG -3'

Reverse: 5' – AGA GGG AAGCG GG AGA GCTT CTGCA CAG TGG -3'

GAPDH (housekeeping gene)

Forward: 5`- CGG GAA GCT TGT CAT CAA TGG

Reverse: 5`- GGC AGT GAT GGC ATG GAC TG

Table 18 RFLP PCR Mastermix

Master mix for one PCR reaction:	
5*Q5 reaction buffer	4 µl
Q5 enhancer	4 µl
cDNA (undiluted)	1 µl
Forward primer (FGFR4)	2 µl
Reverse primer (FGFR4)	2 µl
dNTPs	2 µl
Q5 Polymerase	0.5 µl
Water (Nuclease free)	4.5 µl

Table 19 RFLP PCR program

PCR program (RFLP)		
Initial denaturation	95°C	12 min
	94 °C	30 sec
	66 °C	30 sec
	72 °C	40 sec
		5 cycles
	94 °C	30 sec
	62 °C	30 sec
	72 °C	40 sec
		35
Final elongation	72°C	7 min
Hold	4°C	infinite

Restriction digest with MspI

PCR amplified products were incubated with restriction enzyme MspI for 4 hours at 37 °C (*Table 20*).

Table 20 Restriction digest Master mix

Restriction mix (15µl/sample)	
H2O	2.5 µl
10* Tango buffer	1.5 µl
MspI (restriction enzyme)	1 µl
PCR product	10 µl

As *MspI* has the specific target sequence CCGG it has two restriction sites within the 168bp PCR product. The Gly388 variant contains the sequence CCGGG, therefore yielding an additional restriction site for *MspI*. In contrast, the 388Arg variant harbors CCAGG instead, leading to loss of one restriction site for *MspI*. Thus, restriction digest leads to three or two fragments in the FGFR4 Gly388 variant (87 bp+ 31 bp+ 50 bp), or 388Arg variant (118 bp + 50 bp), respectively (**Figure 22**).

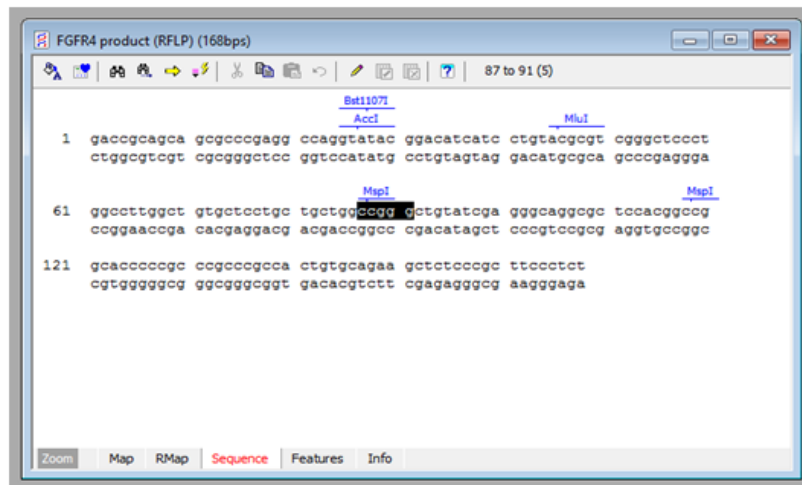
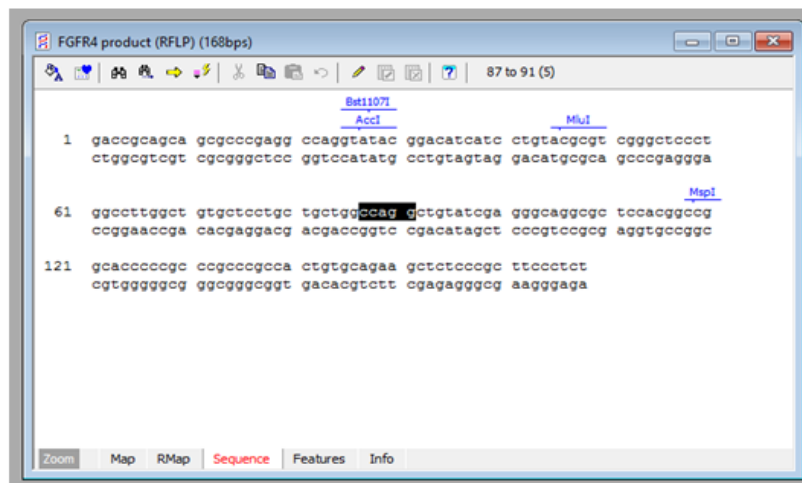
A**B**

Figure 22. RFLP PCR products and *MSPI* restriction sites in FGFR4-388Gly and FGFR4-388Arg variants. FGFR4 PCR product was analyzed with Clone Manager software for *MspI* restriction sites. G388R polymorphism results in change from guanine to adenine at position 89 and therefore only one restriction site for *MspI* in the FGFR4-Arg variant. Restriction results in three fragments in case of FGFR4-Gly (87 bp +31 bp + 50 bp) and two fragments in FGFR4-Arg variant (118 bp + 50 bp).

For evaluation, the digested as well as the undigested samples and the PCR product of the housekeeping gene were mixed with loading dye and loaded on a 15 % polyacrylamide gel. The gel was stained in an ethidium bromide bath and photographed with the software provided by Geldoc XR (Bio-Rad).

3.8 Knock-down of FGFR4 expression via RNAi

RNA interference (RNAi) is a process by which expression of a target gene is specifically silenced or knocked down by inactivation of the corresponding mRNA. Therefore, different molecules can be used. Small interfering RNAs (siRNA) physiologically derive from a longer double stranded (ds) RNA molecule transcribed in the nucleus. The ds precursor molecule is then binding to an endoribonuclease called DICER which cuts the RNA into smaller fragments of 20-30 bp length. These RNA fragments are then incorporated into an Argonaute protein resulting in formation of the RNA induced silencing complex (RISC). This complex is then directed to mRNAs which are complementary to the siRNA leading to degradation of the corresponding mRNA and thus gene silencing. However, artificial siRNA can also be used in an experimental setting (**Figure 23**).

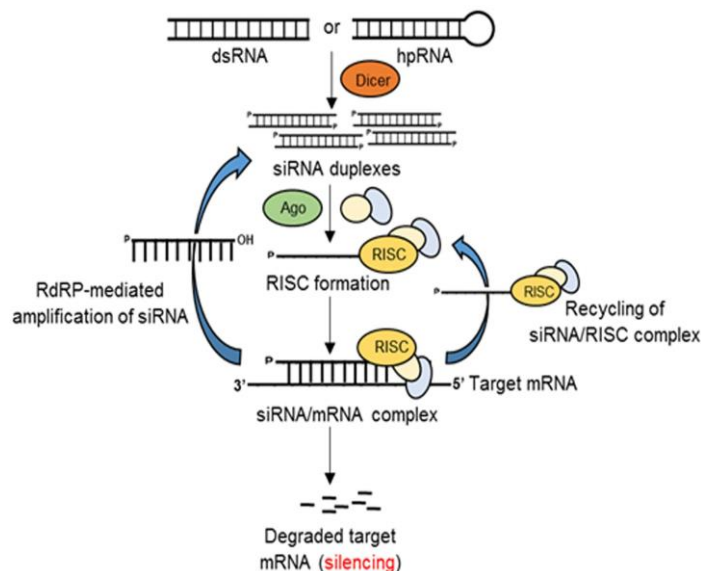


Figure 23 siRNA technique
(Hardham 2012)

Workflow

The transfection with siRNA and consequently the knock down of *FGFR4* was performed using X-fect transfection reagent (Takara, Mountain View, California, USA) and following the manufacturer instructions. As positive control for transfection, non- targeting scr siRNA was used (Dharmacon, Lafayette, Colorado, USA). An siRNA-pool mix targeting multiple parts of the *FGFR4* mRNA was purchased by Santa Cruz Biotechnology (Dallas, Texas, USA).

3.9 Fluorescence-activated cell sorting (FACS)

Fluorescence-activated cell sorting (FACS) is a commonly used high-throughput method to analyze cell population based on their morphological and physiological characteristics. Therefore, single cells are passing a narrow channel and are illuminated by a laser beam. Subsequently, the refracted and the emitted light are measured and fitted into a comprehensive picture (**Figure 24**).

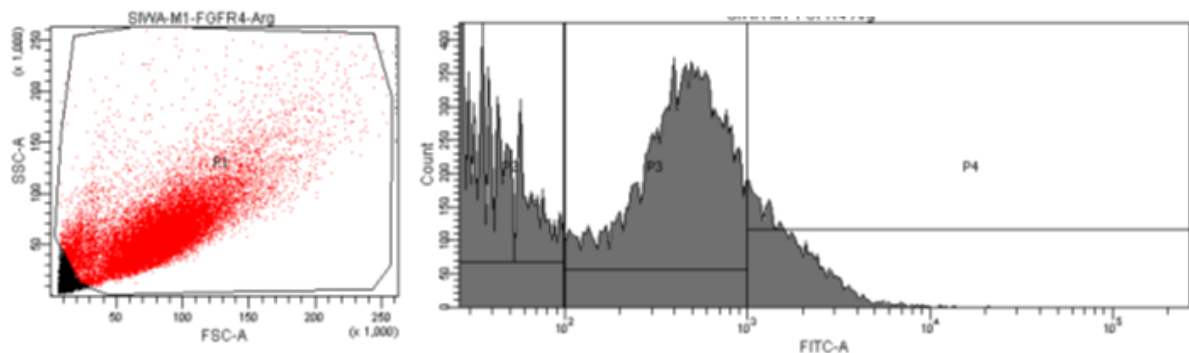


Figure 24 Exemplary FACS results

Exemplary FACS results:

Forward scatter/Side scatter: In this setting used for distinction of viable cells from apoptotic cells. Viable cells are represented by P1 population. Forward scatter (x-Axis) is used to distinguish cell populations by means of size and side scatter (y-Axis) by their inner complexity (granularity etc.).

Furthermore, the number of GFP (FITC) positive cells was analyzed. Based on the auto-fluorescent of non-transfected / non-transduced cells and the high fluorescence of GFP-

positive control cells, gates were introduced to divide the fluorescence spectrum into three different sections: FITC negative (P2), low positive (P3) and high positive (P4) cells.

3.10 In vivo tumor formation in severe combined immunodeficiency (SCID) mice



All animal experiments were approved by the ethic view board of the Medical University of Vienna and performed by holders of a completed FELASA course. For our experiments, SCID/CB17 (**Figure 25**) mice were used, characteristically harboring an acquired immune system deficiency. Specifically, those mice are lacking T- and B-lymphocytes as well as natural killer cells.

*Figure 25 SCID mouse
("001303 - NOD.CB17-Prkdc/J" n.d.)*

Workflow

The tumorigenicity of the different FGFR4-altered glioma cell models was tested female SCID/CB17 mice. 1×10^6 cells of SIWA-M1 (GFP and FGFR4-KD-GFP) were injected subcutaneously into the right flank of the mouse. Body weight and tumor growth was measured every second day using a micro caliper. When the humane end point was reached (defined by tumor size, mouse weight or general health conditions of the animal), mice were sacrificed by cervical dislocation. Thereafter, mice were dissected and organs (lung, liver, spleen, kidney, brain) and tumor were collected in histofix and histologically analyzed.

3.11 Statistical analysis

Data are presented either as mean \pm standard deviation (S.D.) or as mean \pm standard error of the mean (SEM). In vivo experiments were performed in groups of $n=4$.

Statistical significances between groups were either calculated with students t test or one- or two-way ANOVA using GraphPad Prism 5.0. In all cases p values were assigned according to the following characteristics: $p \leq 0.05$ were considered statistically significant (*), p values ranging from 0.01 to 0.001 as very significant (**) and those below 0.001 as highly significant (***).

4 Results

FGFR4 deregulation has been associated with tumor formation in a huge variety of cancers such as breast, lung and bladder cancer but also in rhabdomyosarcoma (Haugsten et al. 2016 ,Bange et al. 2002, da Costa Andrade et al. 2007).

FGFR activation drives various pathways like for example PI3K/Akt, STAT and the MAPK signaling. Hence, changes in FGFR expression and downstream signaling affect many cellular processes including cell proliferation, protein synthesis as well as epithelial-to- mesenchymal transition (EMT), thus tumor invasion and metastasis (Xian, Schwertfeger, and Rosen 2007) .

Previously, our group established a plethora of primary GBM and GS cell lines. Experiments from prior students in our lab have shown overexpression of FGFR4 in a subset of GBM and GS cell lines (**Figure 26**). To explore the impact of FGFR4 on cancer cell aggressiveness, cells were genetically modified by introduction of expression plasmids. As the Gly/Arg single nucleotide polymorphism (SNP) at position 388 (G388R) in the amino acid sequence of FGFR4 had been related to increased malignancy and invasiveness (Bange et al. 2002)(Yun et al. 2010), we aimed to overexpress these SNP variants in glioma cells. Furthermore, a point mutation in the kinase domain of the FGFR4 was introduced, resulting in a dominant-negative phenotype. This thesis works out the impact of FGFR4 inactivation on tumor promoting properties.

4.1 Endogeneous expression of FGFR4 in GBM and GS cell lines

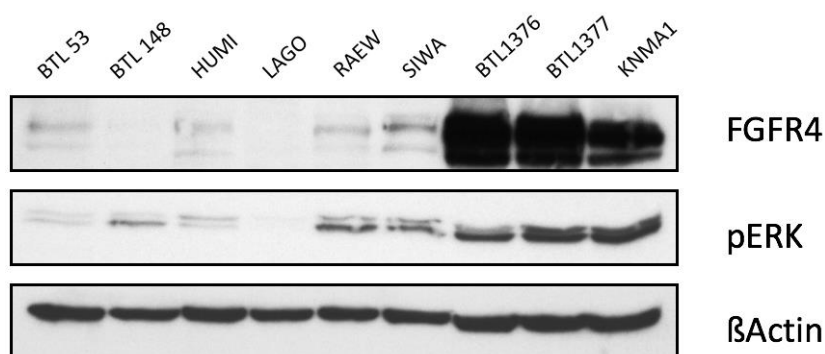


Figure 26 FGFR4 expression in glioma. FGFR4 and pERK expression levels in the indicated glioma cell lines were analyzed by Western blot analysis. β -actin served as housekeeping gene.

Different GBM and GS cell lines had been tested for their amount of FGFR4 protein expression by Western blot, revealing a distinct subgroup of FGFR4 over-expressing models. Highest expression levels were found in the GBM cell line SIWA and KNMA1 as well as in the GS cell lines BTL1376 and BTL1377 (**Figure 26**). These models have been selected for further establishment of FGFR4 kinase dead variants.

4.2 Determination of the endogenous *FGFR4* 388Gly / 388Arg status

Presence of the G388R SNP arginine variant in *FGFR4* has previously been connected to worse clinical outcome in breast cancer, head and neck squamous cell carcinoma and other forms of cancer (Bange et al. 2002), (Sylvia Streit et al. 2004), (da Costa Andrade et al. 2007; B. Xu et al. 2011; Bange et al. 2002; S Streit et al. 2006; Spinola et al. 2005). Therefore, we assessed the endogenous *FGFR4* G388R SNP status of selected glioma cell lines by RFLP PCR using the restriction enzyme *MspI*. In the case of *FGFR4* 388Gly, digestion results in three fragments (87bp + 31bp + 50bp), whereas presence of *FGFR4* 388Arg SNP leads to two fragments (118bp + 50bp). Based on the presented data, SIWA M1 as well as BTL1376 show all listed fragment sizes suggesting heterozygous allele presentations (**Figure 27**).

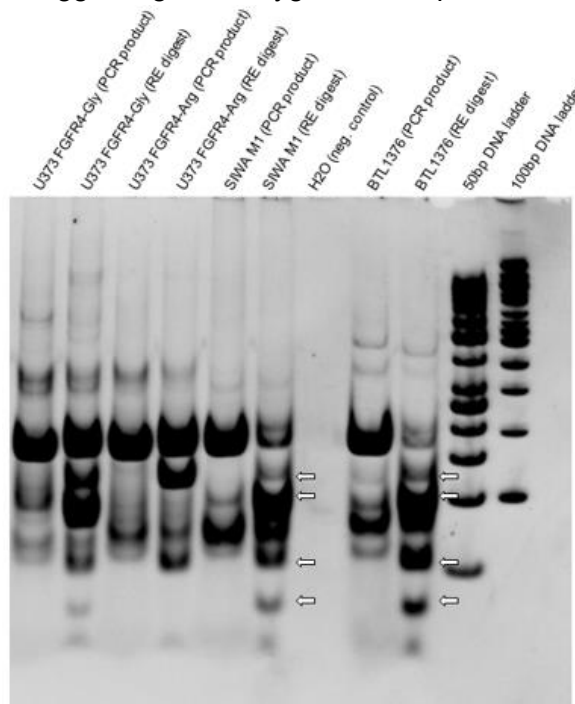


Figure 27. RFLP-PCR of *FGFR4* over-expressing glioma cells. The gel shows undigested PCR products of the indicated cell models loaded next to the respective *MspI*-digested fragments. U373 overexpressing either *FGFR4*-Gly or *FGFR4*-Arg served as positive controls for the respective receptor variant. A 50bp and a 100bp DNA ladder were used as indicated. RE = restriction enzyme (*MspI*), neg. = negative

4.3 Generation of FGFR4 over-expressing cellular models

GBM and GS cell lines, which are endogenously high in FGFR4 were used throughout this study. Stable integration of FGFR4 variants (3.2 and 3.4) into SIWA M1 (**Figure 28**) and BTL1376 (**Figure 29**) was achieved via retroviral transduction or presumably spontaneous integration after lipofection, respectively. Since GFP is C-terminally fused to each FGFR4 variant in one reading frame, it serves as reporter for FGFR4 expression. Cell lines expressing GFP only were used as controls. Up to now, the FGFR4-KA over-expressing cell model could not be established.

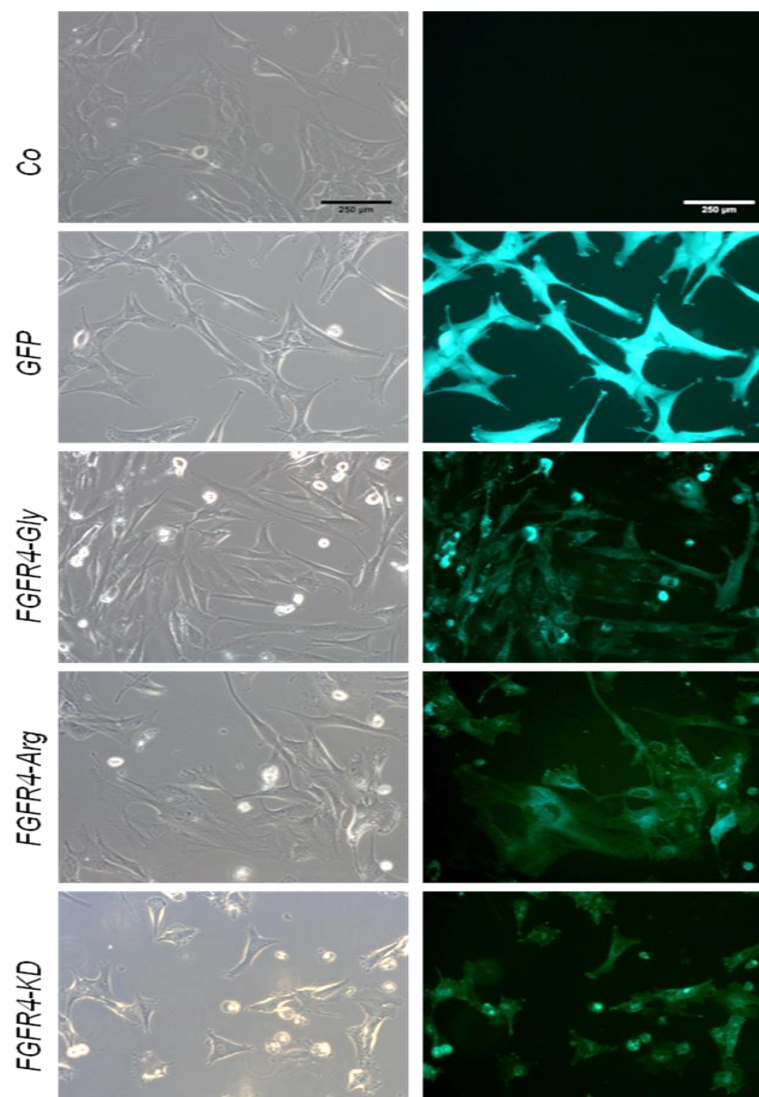


Figure 28. FGFR4-expressing SIWA M1 cell lines. SIWA-M1 cells were retrovirally transduced with the indicated FGFR4 variants or GFP only. Co indicates the non-transduced control cells. Microphotographs were taken with Nikon eclipse fluorescence microscope (Nikon Ti-S) using a 20x objective. Scale bar in first image refers to 250 μ m and can be applied to all included microphotographs.

Regarding the phenotype of the cell models, it might be worth to mention that the GS cell line, BTL1376, does not form a confluent cell layer under standard cell culture conditions. First, the cells form adherent clusters, however immediately detach and switch to 3-dimensional growth when space gets limited by neighboring cell clusters. This phenotype was observed in all models of BTL1376 but most strikingly in the FGFR4 dominant negative kinase dead (KD) variant.

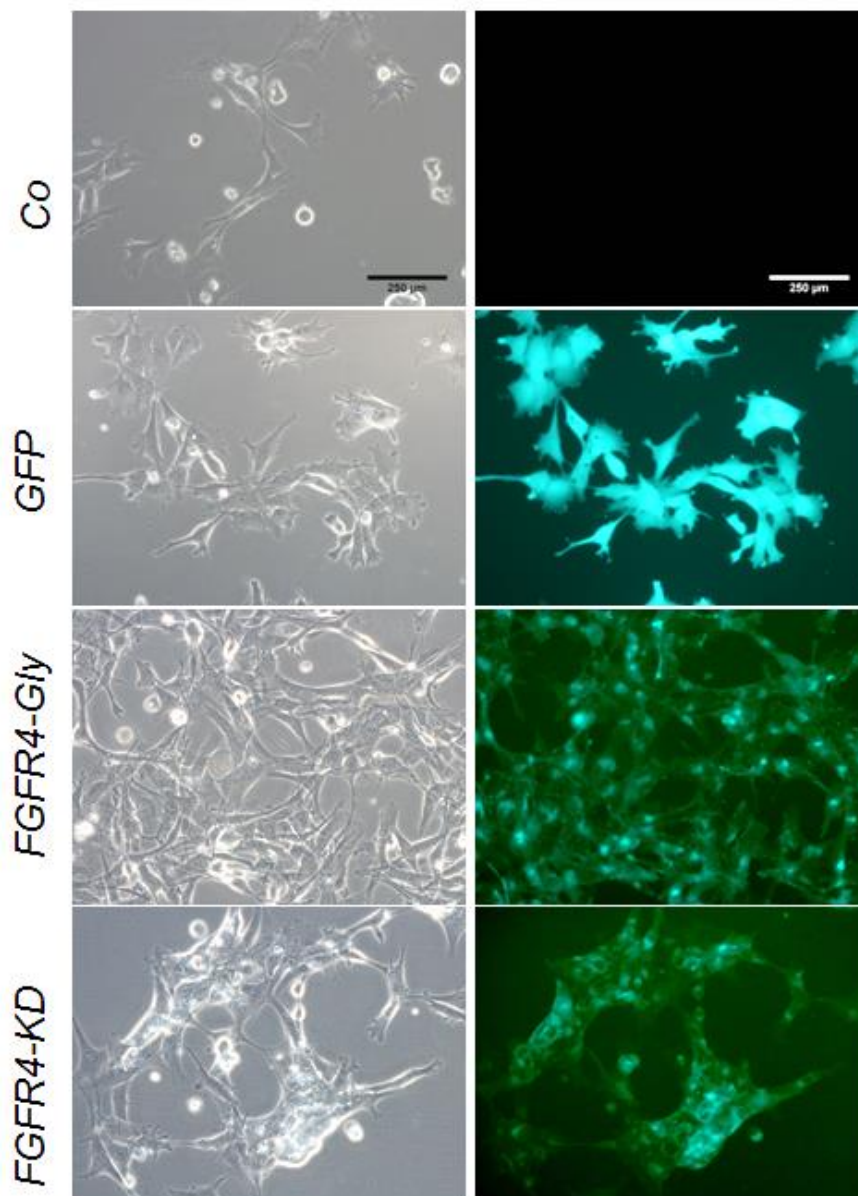


Figure 29. FGFR4-expressing BTL1376 cell models. BTL1376 cells had been created by lipofection and presumably spontaneous stable gene integration or GFP only. Co indicates the non-transfected control cells. Microphotographs were taken with Nikon eclipse fluorescence microscope (Nikon Ti-S) using a 20x objective. Scale bar in first image refers to 250μm and can be applied to all included microphotographs. Co = non-transfected control.

4.4 Localization of FGFR4 in ectopically over-expressing cell lines

Next, we assessed the intracellular localization of *FGFR4* upon ectopic overexpression of the altered *FGFR4* variants FGFR4-Gly, FGFR4- Arg and KD fused to GFP. WGA and DAPI were used as membrane and nuclear stains, respectively. In all ectopically over-expressing cell variants, FGFR4 was primarily expressed on the cell membrane, but also vesicular in the perinuclear space. (**Figure 30** and **Figure 31**).

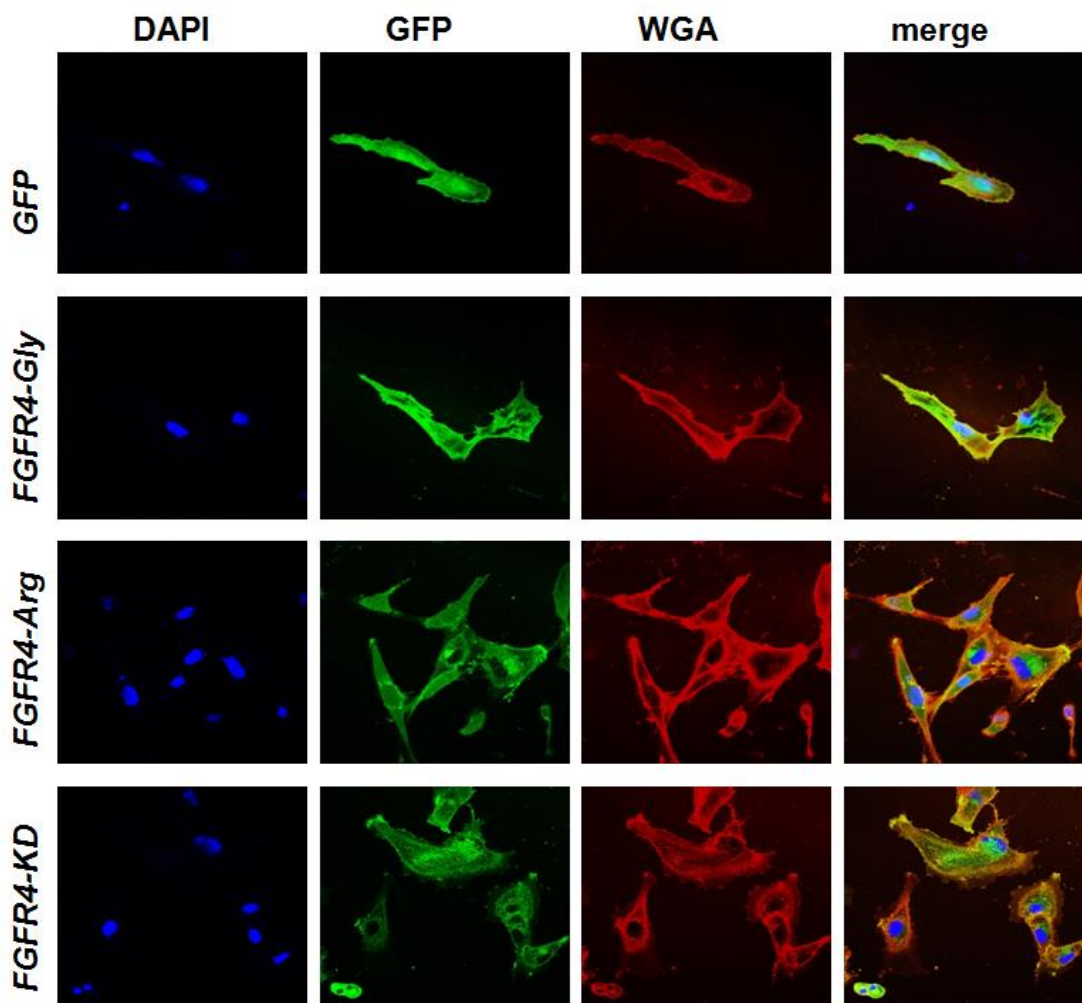


Figure 30. Confocal microphotographs of SIWA M1 cell models. SIWA-M1 GFP and the respective *FGFR4*-variants were observed as indicated. Cells were fixed with 4% PFA and membranes and nuclei were stained with WGA and DAPI, respectively. As plasmids encode an in frame fusion of the respective *FGFR4* variant to GFP, localization of ectopically overexpressed *FGFR4* can be visualized in fluorescent microscopy. Confocal imaging using LSM 700 microscope with 40x objective with oil showed localization of *FGFR4* in perinuclear vesicles and co-localization with WGA at the membranes.

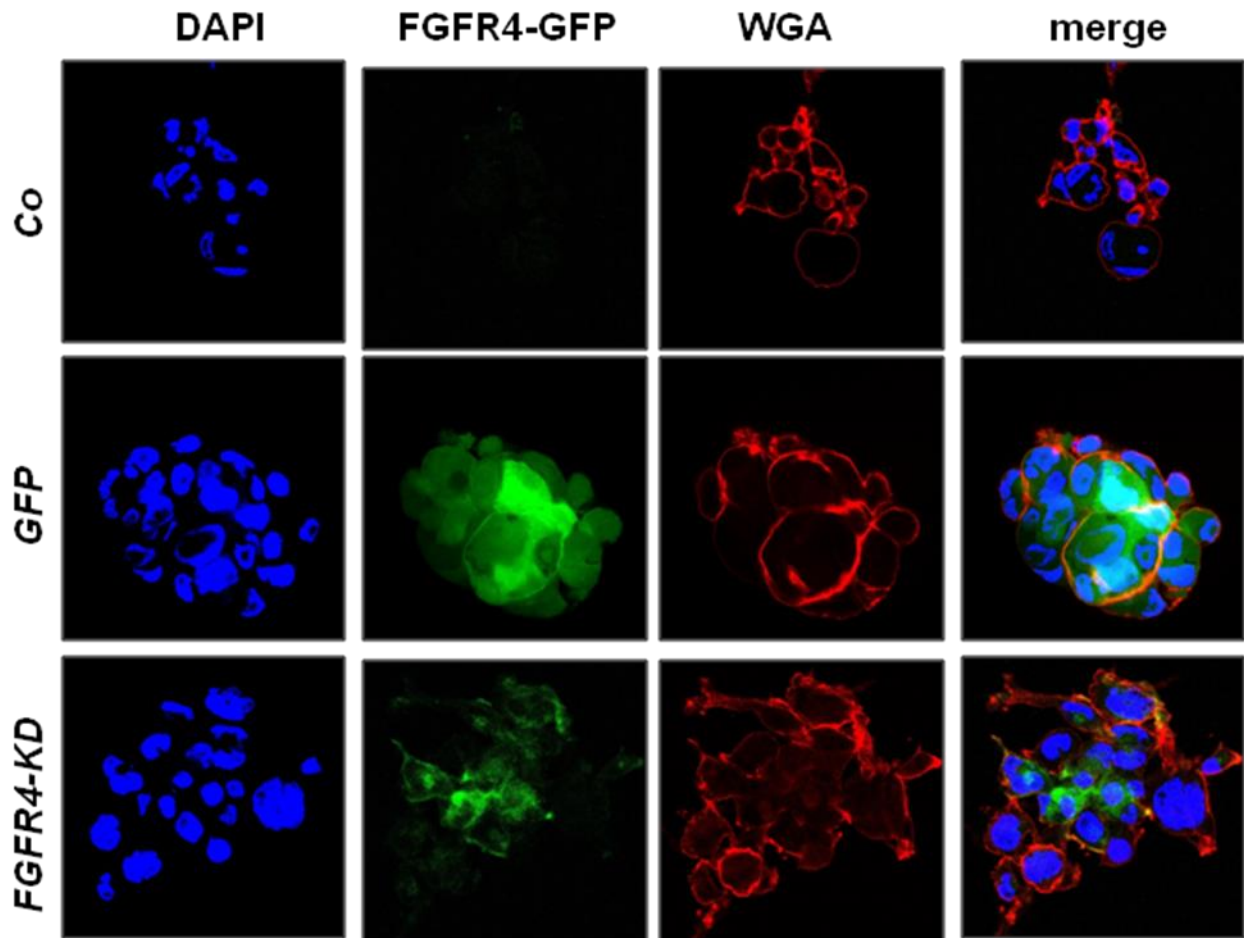


Figure 31. Confocal microphotographs of BTL1376 cell models. BTL1376 GFP and the respective FGFR4-variants were observed as indicated. Cells were fixed with 4% PFA and membranes and nuclei were stained with WGA and DAPI, respectively. As plasmids encode an in frame fusion of the respective FGFR4 variant to GFP, localization of ectopically overexpressed FGFR4 can be visualized in fluorescent microscopy using LSM 700 microscope. Confocal imaging using 63x objectives with oil showed localization of FGFR4 in perinuclear vesicles and co-localization with WGA at the membranes.

For further investigations regarding localization of FGFR4 in the cells, protein extracts from different cellular compartments of SIWA M1 and BTL1376 were isolated in addition to whole protein lysates (tot. prot.). FGFR4 levels were highly overexpressed in the KD variant as indicated in the cytoplasmic fractions but also in the whole-cell protein lysates as well as in the nuclear extracts (**Figure 32**). This finding confirming perinuclear localization of the receptor as previously observed in confocal microscopy.

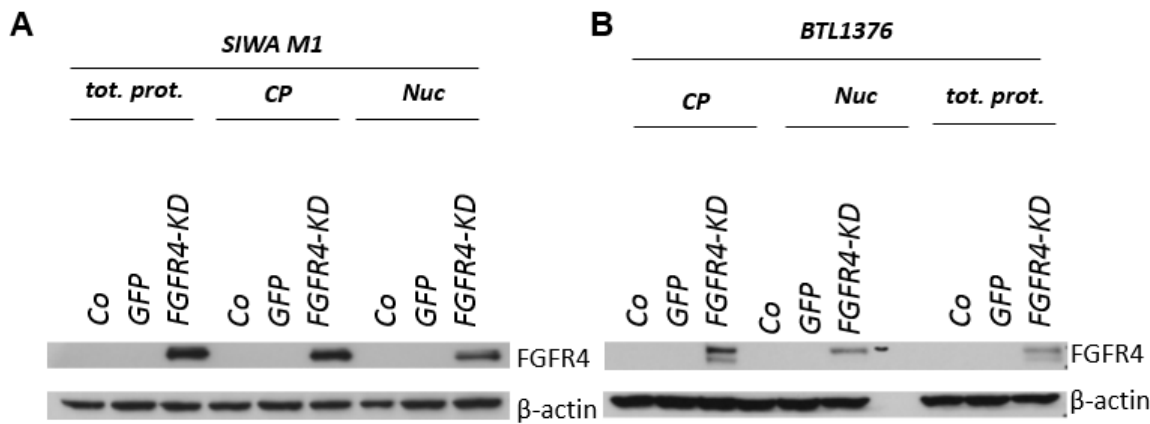


Figure 32. Western blot of total protein, cytoplasmic and nuclear extracts from SIWA M1 and BTL1376. Cytoplasmic and nuclear extracts were isolated. Furthermore, total protein extracts were analyzed. Expression of FGFR4 was observed in the respective cellular fractions of SIWA M1 (A) and BTL1376 (B) as indicated. β -actin served as a loading control in both cell lines. Tot.prot = total protein extracts; CP = cytoplasmic extracts; Nuc = nuclear extracts; Co = non-transduced control.

Since FGFR4 is a membrane-bound receptor, membrane fractions of FGFR4-variants expressing SIWA M1 as well as control cells were isolated. FGFR4 expression was analyzed comparing the basal protein levels to FGFR4 levels after 24h of serum starvation. Interestingly, we found that FGFR4 was enhanced after starvation in all cell lines harboring a functional FGFR4. In contrast, in the FGFR4-KD variant starvation did not result in expression changes. Furthermore, the FGFR4-KD variant was highly expressed on the cell membrane already under standard cell culture conditions (**Figure 33**).

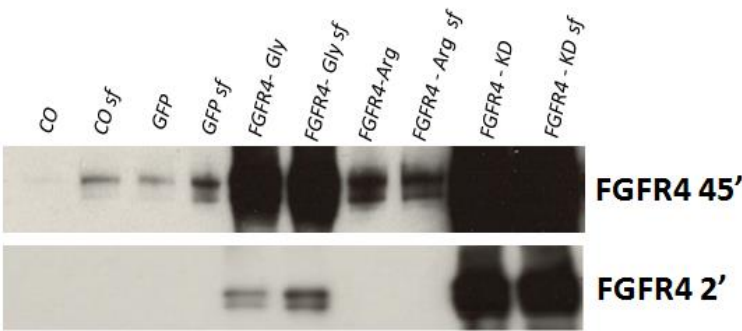


Figure 33. Membrane fractions of SIWA M1. Membrane fractions were isolated and analyzed for FGFR4 expression by Western blot. Two different exposure times are shown. Cells were starved for 24h prior to membrane fraction isolation. Co = non-transduced control; sf = serum - free

4.5 FGFR4 expression levels in genetically modified cell lines

FGFR4 over- expression was proved by qPCR, flow cytometry and Western blot analyses.

Quantitative real-time PCR (qPCR)

FGFR4 levels of the genetically modified SIWA M1 and BTL1376 descendants were quantified by qPCR. Corroboratively, *GFP* levels of the described cell models were analyzed (**Figure 34 C+D**). Since *GFP* is naturally expressed in transduced cell lines only, it was undetectable in the non-transduced controls of either cell line, proving the specificity of the PCR reaction. Both results prove *FGFR4* (over)expression upon genetic modification in all variants including *FGFR4*-Gly, -Arg and -KD. (**Figure 34 A+B**)

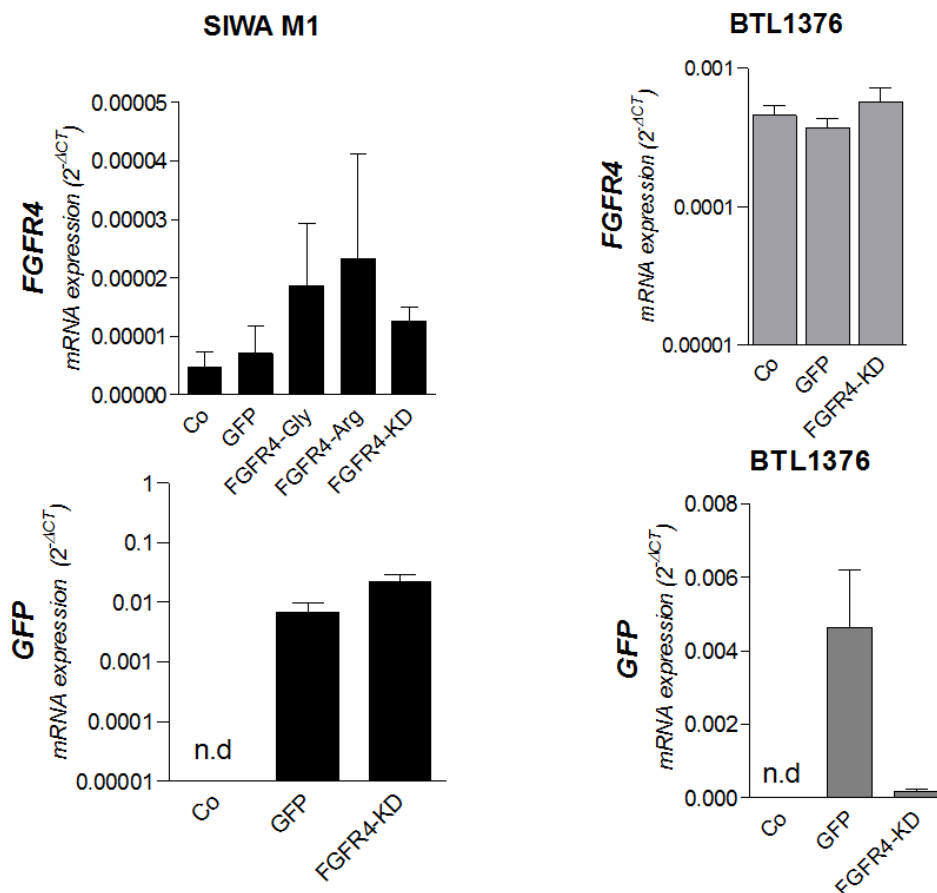


Figure 34. qPCR results indicating *FGFR4* and *GFP* expression levels. (A+B) TaqMan PCR was performed and *FGFR4* expression of non-transduced SIWA M1 (A) and BTL1376 (B) control (Co) as well as in *FGFR4*-variants expressing models and *GFP* is shown. Expression of *FGFR4* was normalized to *ACTB* (β -actin) used as housekeeping gene. (C+D) SYBR green qPCR targeting *GFP* was performed in the indicated cell models SIWA M1 (C) and BTL1376 (D). Expression was normalized to *RPL-41* serving as housekeeping gene. Results are given as as $2^{-\Delta CT}$ normalized to the respective housekeeping gene (mean \pm SD). n.d. = not detected; Co = non-transduced control.

Quantification of GFP-positive cells by flow cytometry

The ectopically introduced plasmids encoding *FGFR4* are fused to *GFP*, which can be measured by flow cytometry. GFP positivity is indicated by fluorescein-5-isothiocyanat (FITC) levels.

Gates were applied according to the auto-fluorescence levels of the respective non-transduced cells. Based on these ranges, viable cells of the novel *FGFR4*-altered cell lines were classified as FITC negative, low positive and high positive cell populations. Thus, transduction efficiency (% FITC positive cells from all viable cells) was analyzed. Interestingly, SIWA M1 *FGFR4*-KD variant showed nearly 100% transduction efficiency, while in the two SNP variants, -Gly and -Arg, efficiency was varying between 50 and 60% (**Figure 35** and **Figure 37**).

In BTL1376 cells, transfection efficiency was about 60% both in the *FGFR4*-KD as well as in the -Gly variant (**Figure 36** and **Figure 37**).

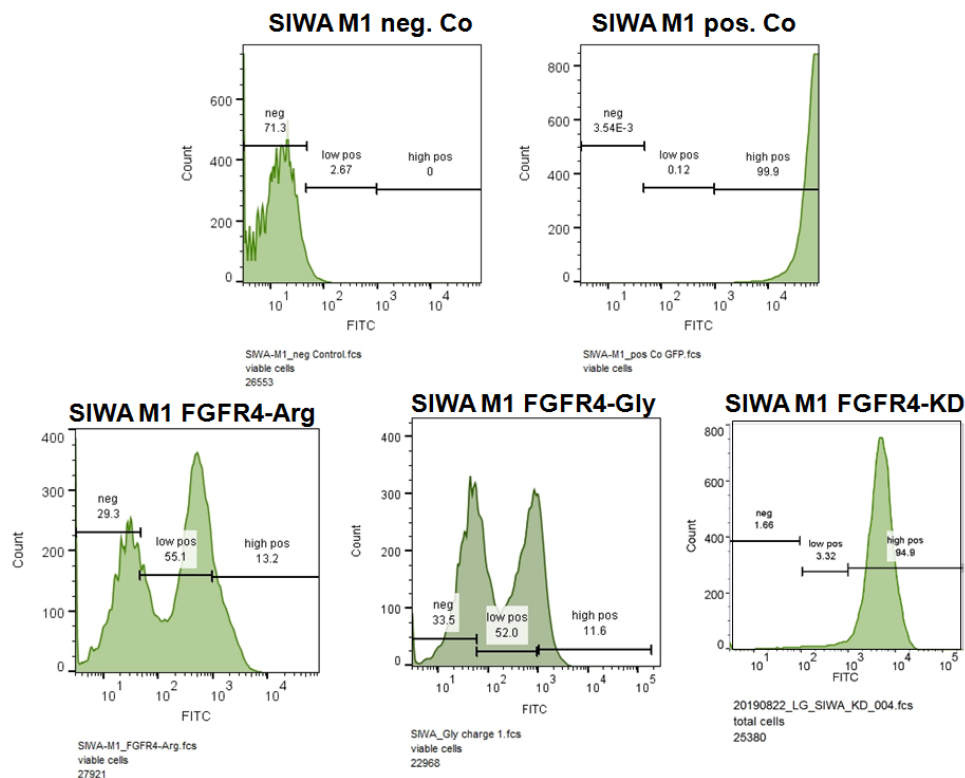


Figure 35 Flow cytometry analysis of SIWA M1 cell models. Results of SIWA M1 control (A), GFP (B), Arg (C), Gly (D) and KD (E) are given above. Viable cells were measured and divided into sub-populations based on expression of GFP (FITC). Gates for FITC negative, low positive and high positive cells were applied based on the autofluorescence of the negative controls. Values in the graphs indicate % of viable cells in the indicated sub-population.

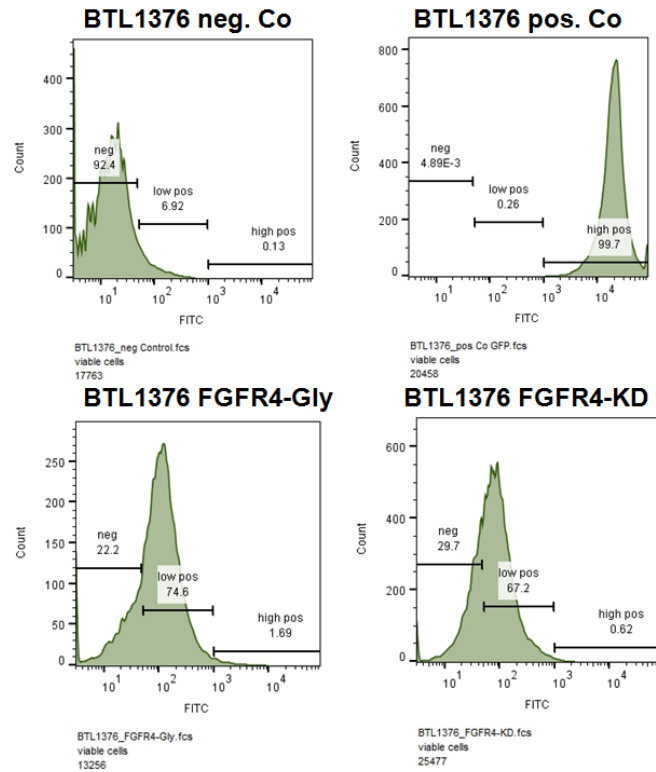


Figure 36 Flow cytometry analysis of BTL1376 cell models. Results of BTL1376 control (A), GFP (B), Gly (C) and KD (D) are given above. Viable cells were measured and divided into sub-populations based on expression of GFP (FITC). Gates for FITC negative, low positive and high positive cells were applied based on the autofluorescence of the negative controls. Values in the graphs indicate % of viable cells in the indicated sub-population.

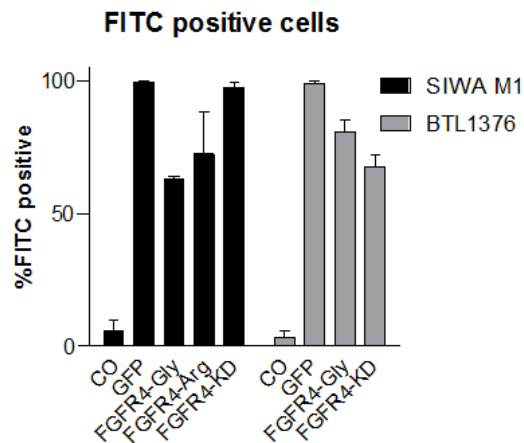


Figure 37 Analysis of FITC positive cells measured by FACS analysis. The graph indicates the percent of FITC positive cells of the respective cell lines from all viable cells. Non-transduced/ non-transfected controls were used to measure cells' autofluorescence. Cells that were transduced with GFP only served as positive controls. Results are given as mean \pm SD from two independent experiments. CO = non-transduced controls.

Western blot

Furthermore, ectopic overexpression of FGFR4 with the KD variant of SIWA M1 and BTL1376 was detected on protein levels by Western blot analysis (**Figure 38**). The data confirm prior results obtained from the qPCR as well as from flow cytometry, as FGFR4-KD is highly overexpressed as compared to the respective control cells.

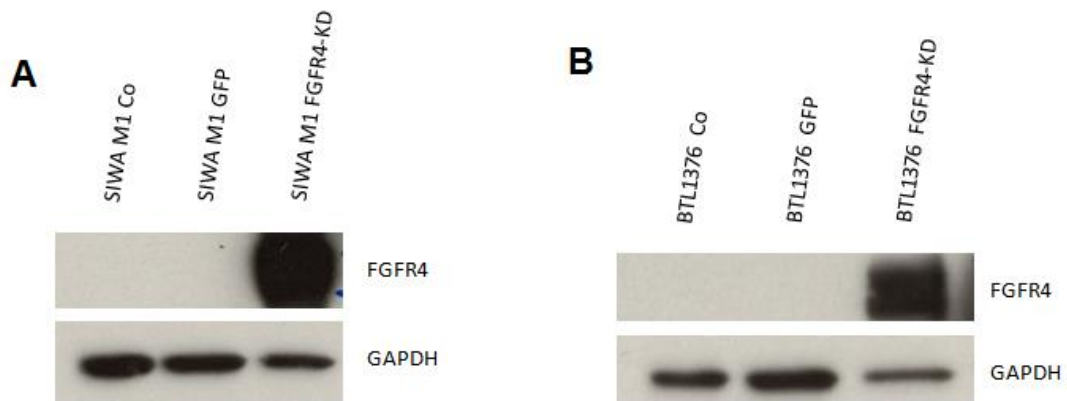


Figure 38. Western blots showing overexpression of FGFR4 in the KD variant. Western blot analysis detecting FGFR4 in SIWA M1 (A) and BTL1376 (B) as well as in their GFP and KD variants. GAPDH served as loading control. Co = non-transduced control.

Taken together, the data shown so far prove the successful transduction of FGFR4-Gly, -Arg and KD into the endogenously FGFR4-high cell lines SIWA M1 and BTL1376, thus the expression plasmids have been stably integrated into the genomes. Nevertheless, the aim of the thesis was to dissect the role of FGFR4 activity and the impact of FGFR4 impairment in these cell lines. Therefore, the main part of this thesis will focus on the FGFR4-KD variant of the cell lines. Nevertheless, for some experiments we found profound differences between the two variants of the G388R polymorphism, thus these results will also be included.

4.6 Klotho beta (*KLB*) is co-regulated with FGFR4 expression in BTL1376

Interaction of FGFs with their receptors is mediated and stabilized by different co-factors. While canonical FGFs depend on HSPG to interact with FGFRs, the endocrine FGF family consisting of FGF15/19, FGF21 and FGF23 relies on presence of klotho family members, like klotho α and klotho β (*KLB*) (Ornitz and Itoh 2015). As *KLB* is known to mediate interaction between FGFR4 and its specific ligands, FGF19 and FGF23, we analyzed the impact of ectopic overexpression of FGFR4 on *KLB* levels. Accordingly, we found elevated *KLB* mRNA levels in BTL1376 after introduction of the FGFR4-KD overexpression plasmid as compared to the non-transfected and the GFP control (**Figure 39**).

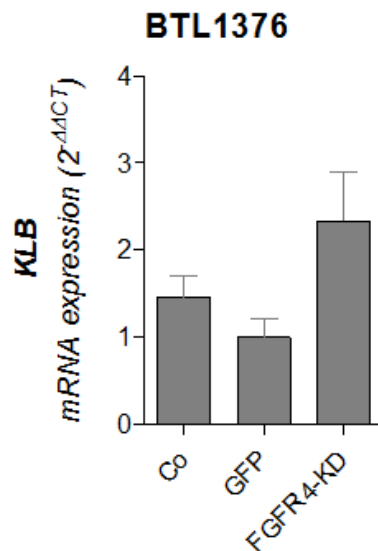


Figure 39. *KLB* expression levels in BTL1376. *KLB* expression was quantified using qPCR. Expression has been normalized to RPL-41 as a housekeeping gene and is shown as $2^{-\Delta\Delta CT}$ normalized to the GFP control. Co= non-transfected control.

Furthermore, *FGFR4* was knocked down in the endogenously *FGFR4*-high GBM model SIWA M1 as well as in an additional ectopically *FGFR4*-overexpressing glioma line (U373-Gly). Preliminary results from that experiment show that knock-down of *FGFR4* is directly linked to downregulation of *KLB*. These findings suggest that *KLB* mRNA expression is co-regulated with *FGFR4* (**Figure 40**). However, this experiment has to be validated in future studies.

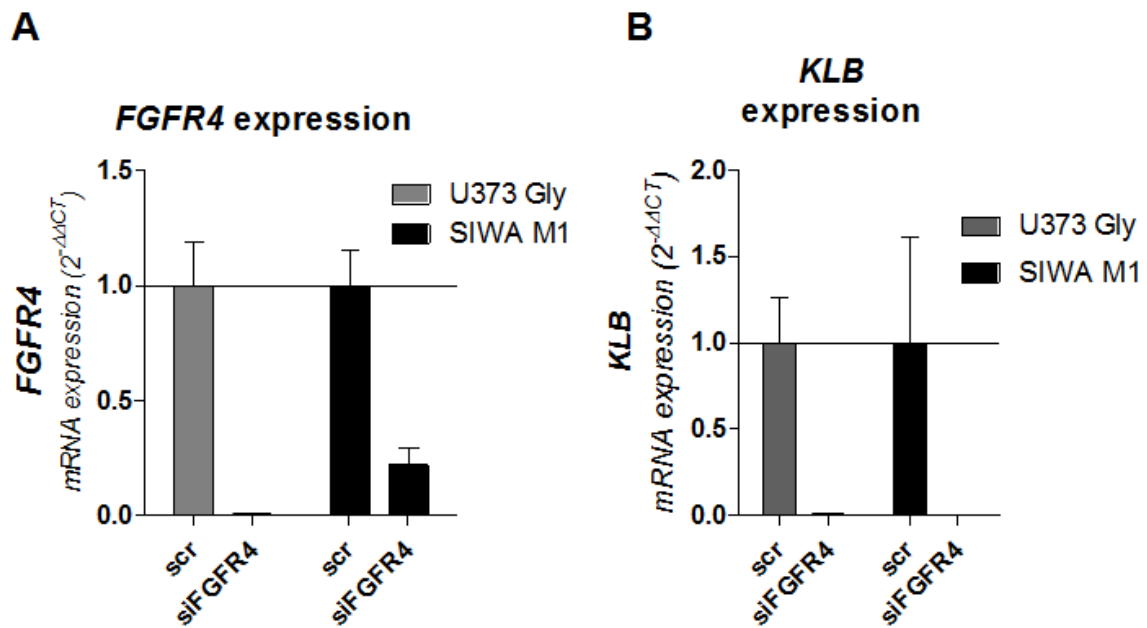


Figure 40. *KLB* expression upon knock-down of *FGFR4* in U373 *FGFR4*-Gly and SIWA M1. *FGFR4* and *KLB* expression was quantified using qPCR. Expressions have been normalized to *ACTB* (β -actin) or *RPL-41* as a housekeeping gene, respectively, and are shown as $2^{-\Delta\Delta CT}$ normalized to the scr control. Scr = scrambled.

4.7 Functionality of FGFR4 kinase-dead variant and impact on downstream signaling

In order to investigate the consequences of FGFR4 inactivation by introduction of a kinase dead FGFR4 variant, Western blot analyses was performed, focusing on expression and activation of receptor downstream signaling pathway members.

FGFRs, such as FGFR4 act in many different pathways affecting cellular growth, protein synthesis, survival and migration (Heinzle et al. 2014). Therefore, they are involved in many intracellular signaling cascades activating pathways like MAPK signaling, STAT3 and PI3K/Akt signaling. Indeed, introduction of the kinase-dead FGFR4 variant resulted in decreased activity of S6 in as compared to the GFP control in SIWA M1 but also in BTL1376. Since in SIWA M1 FGFR4 overexpression could not be detected in FGFR4-Arg variant, it is most likely that the expression was lost during cell culture propagation. Therefore, in further experiments freshly thawed FGFR4-Arg clones were used (**Figure 41**).

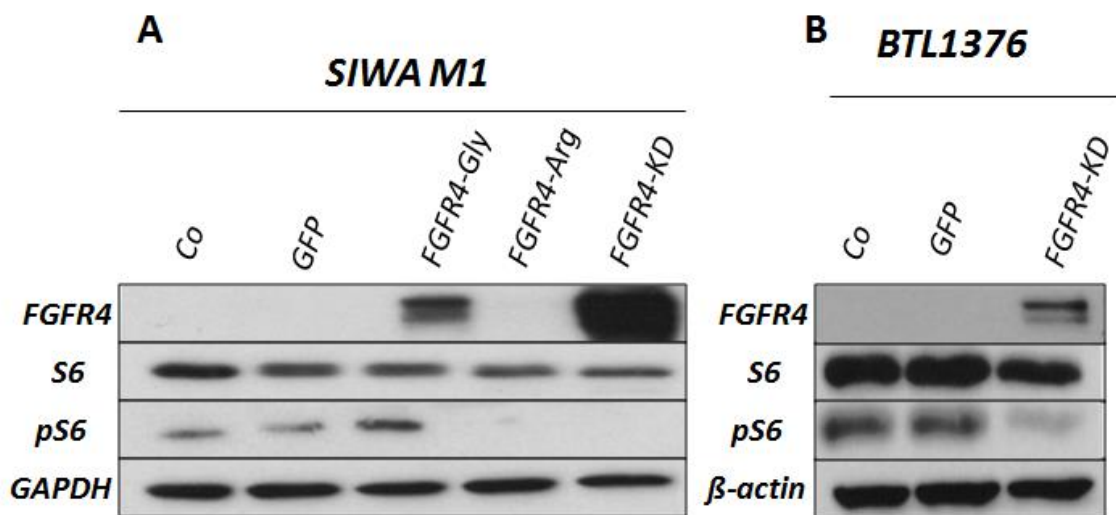


Figure 41. Western blot showing FGFR4 expression and downstream signaling in SIWA M1 and BTL1376. Protein lysates of the indicated cell lines were isolated and analyzed regarding FGFR4 expression and activation of the downstream signaling molecule S6. GAPDH and β -actin served as loading controls as indicated. Co = non-transduced control.

Since FGFR4 activity is mainly mediated by ligand binding, stimulation assays were executed. Thereby, we aimed to dissect the differences between non-transduced and GFP control cells as well as FGFR4 KD in response to the receptor-activating ligand FGF2. It is worth to mention, that FGF2 is binding and activating not only FGFR4 but also the other members of FGFRs. Next, downstream signaling of FGFR4 was analyzed by a siRNA approach. Upon knock-down and incubation for 48 hours, cells were starved in serum-depleted medium for 24 hours before they were stimulated with FGF2 for 15 min. Subsequently, protein lysates were isolated and analyzed on Western blots. FGFR4 expression was analyzed to confirm the knock- down. While FGFR4 levels were drastically decreased in the FGFR4-KD variant, the non-transduced control as well as the GFP control cells did not show an FGFR4 specific band on Western blot even after long exposure. Nevertheless, membrane fractions confirmed FGFR4 overexpression in these cell lines, which was even enhanced after serum starvation. Indeed, basal deactivation of FGFR4 in KD led to decreased activation of S6 and MAPK signaling as compared to both non-transduced and GFP controls. Strikingly, FGF2 stimulation was not capable to activate S6 downstream signaling upon knock-down of *FGFR4* in all cell lines, indicating functional knock- down of *FGFR4*. Nevertheless, activation of ERK1/2, a downstream effector of the MAPK signaling pathway, could still be achieved by FGF2. (**Figure 42**)

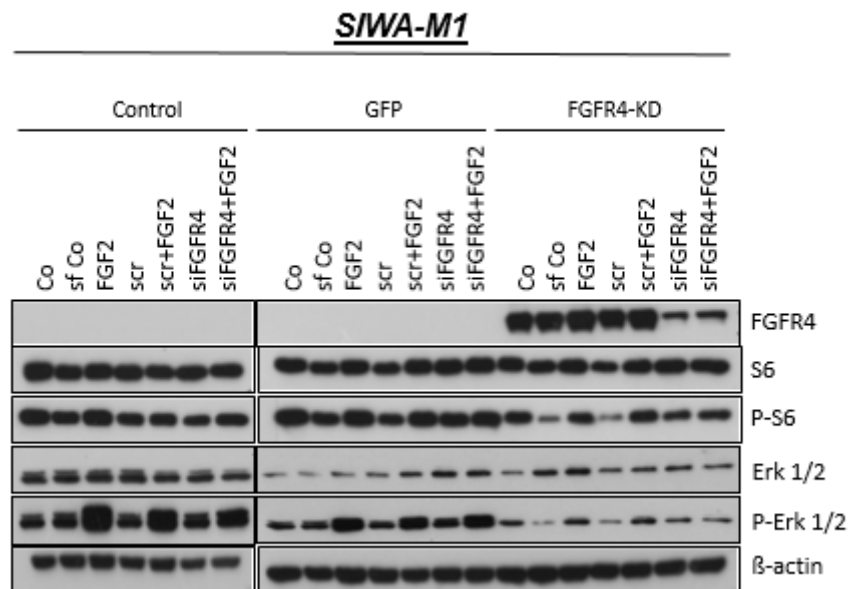


Figure 42. Western blot after knock-down of FGFR4 followed by stimulation with FGF2. After 48h upon FGFR4 knock-down, cells were starved with serum-free medium. The next day, starved cells were stimulated with FGF2 [100ng/ml] for 15 minutes before proteins were isolated. Expression levels of FGFR4 as well as effects on downstream signaling upon knock-down and stimulation were investigated. β -actin served as loading control. Co = control, sf Co = serum-free control, scr = scrambled

4.8 Effects of FGFR4 inactivation on two-dimensional growth

4.8.1 Clone formation capacity

Since FGFR signaling drives many cellular processes like growth and proliferation (Heinzle et al. 2014), the generated cell models were tested regarding their two-dimensional clone formation capacity. Therefore, cells were seeded in very low density and tested for their capacity to form clones out of single cells. Colony formation capacity assays performed in endogenously FGFR4 over-expressing cells SIWA M1 and BTL1376 as well as FGFR4-KD expressing cells elucidated significant differences between the KD variant and the respective GFP control. In either cell line downregulation of FGFR4 signaling in the KD variant resulted in significantly impaired clone formation capacity (**Figure 43**).

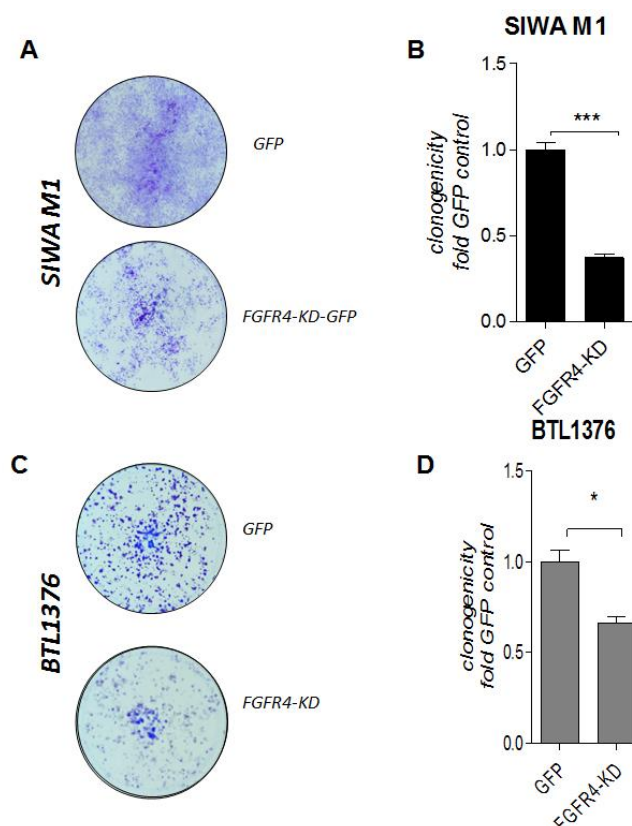


Figure 43 Colony formation assays upon FGFR4 inactivation. SIWA M1 (**A + B**) and BTL1376 (**C + D**) control cells as well as either FGFR4-KD variant were seeded and incubated for seven days until clones had formed. Subsequently, cells were stained with crystal violet. Photographs were taken using the Nikon D7200 camera. The percentage of the total well areas covered with cells as shown in (**A and C**) were quantified using Image J. Results are given as fold change compared to GFP (control) set to 1 as indicated (**B and D**). Statistical analyses were performed using unpaired student's t- tests ($p < 0.05 = *$; $p < 0.01 = **$; $p < 0.001 = ***$). Data in graphs are shown as mean \pm SD.

4.8.2 Impact of stimulation and inhibition of FGFR on clone formation capacity

To assess the influence of FGFs on proliferation and clone formation capacity, stimulation assays were performed. Therefore, cells were seeded in low density and incubated for two days before FGFs [50ng/ml] were added. After seven days under normal cell culture conditions, cells were fixed, stained with crystal violet and quantified. While FGF2 binds to all kind of FGFRs, FGF23 has high affinity for FGFR4 (Grabner et al. 2017; Wyatt and Drüeke 2016). Accordingly, the globally acting FGF (FGF2) triggered proliferation of the KD variant, while FGF23 did not stimulate colony formation. In contrast, the GFP variant showed response to both FGFs. Another aspect of this experiment was to test the endogenously FGFR4 high cells BTL1376 and its FGFR4-KD model with the RTKI ponatinib in a long-term treatment setting. Although the kinase dead variant appeared a little more sensitive to ponatinib treatment, no profound differences to the GFP control cells could be found. As ponatinib serves as a multi-kinase inhibitor, other targets could be blocked in this setting. For further experiments a more specific FGFR4 inhibitor shall be used (**Figure 44**).

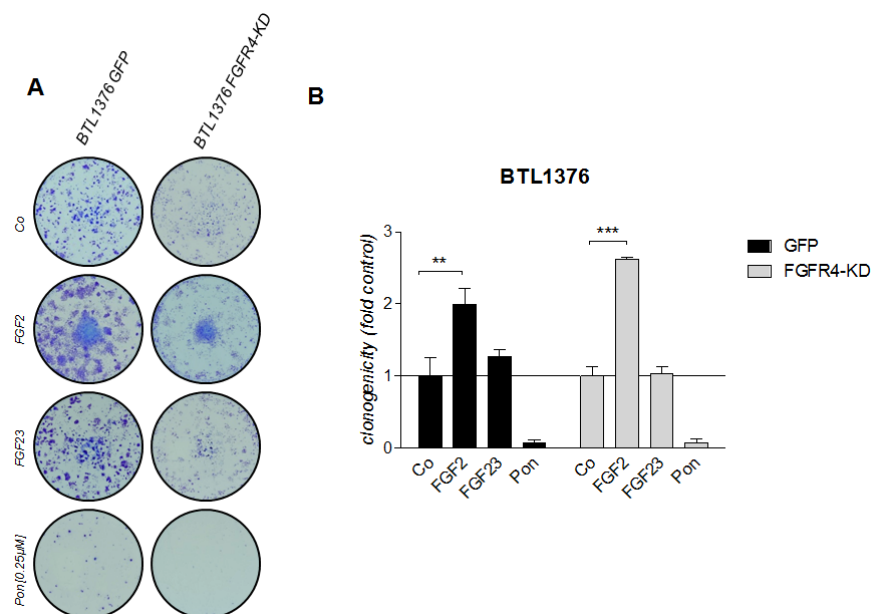


Figure 44. Stimulation assay BTL1376 with FGF2 and FGF23. (A) Cells were seeded in low density and stimulated with FGF2 or FGF23 [50ng/ml] two days after seeding. Additionally, response to ponatinib [0.25μM] was investigated. Clone formation was observed every day. One week after treatment cells were fixed and stained with crystal violet. (B) Graph indicates response to stimulation with FGFs and inhibition with ponatinib. An algorithm designed for R was used to quantify amount of cells in the well by counting black pixels of the binary images. Values were normalized to the untreated control of the respective cell line set to 1. Results are given as Mean +/- SD. Co = untreated control; Pon = ponatinib.

4.9 Effects of FGFR4 inactivation on three-dimensional growth

To investigate the ability of our cell models to grow in an undifferentiated manner and to form neurospheres, cells were seeded in serum-free neurobasal medium supplemented with growth factors (NB+) in ultra-low attachment plates. The ability to form spheres under such conditions is associated with stem cell like characteristics, which is referred to as stemness. As FGFR4 also plays a major role in differentiation (Bennasroune et al. 2004), (Heinzle et al. 2014), we aimed to test if the ectopically FGFR4 over-expressing cell lines, including KD, differ from the GFP controls.

Another important aspect in this regard is whether the cells are capable to re-differentiate back when they are transferred to non-treated cell culture plates in serum-containing growth medium. Concerning this aspect, our major interest was whether the kinase dead variant was impaired in re-differentiation compared to GFP control. Although the FGFR4-KD was capable to form spheres after two days in stem cell medium, re-differentiation was impaired. In SIWA M1 as well as in BTL1376 the GFP controls were capable to re-differentiate back to their original phenotypes (**Figure 45** and **Figure 46**)

4.9.1 Sphere formation and re-differentiation upon inactivation of FGFR4 in BTL1376

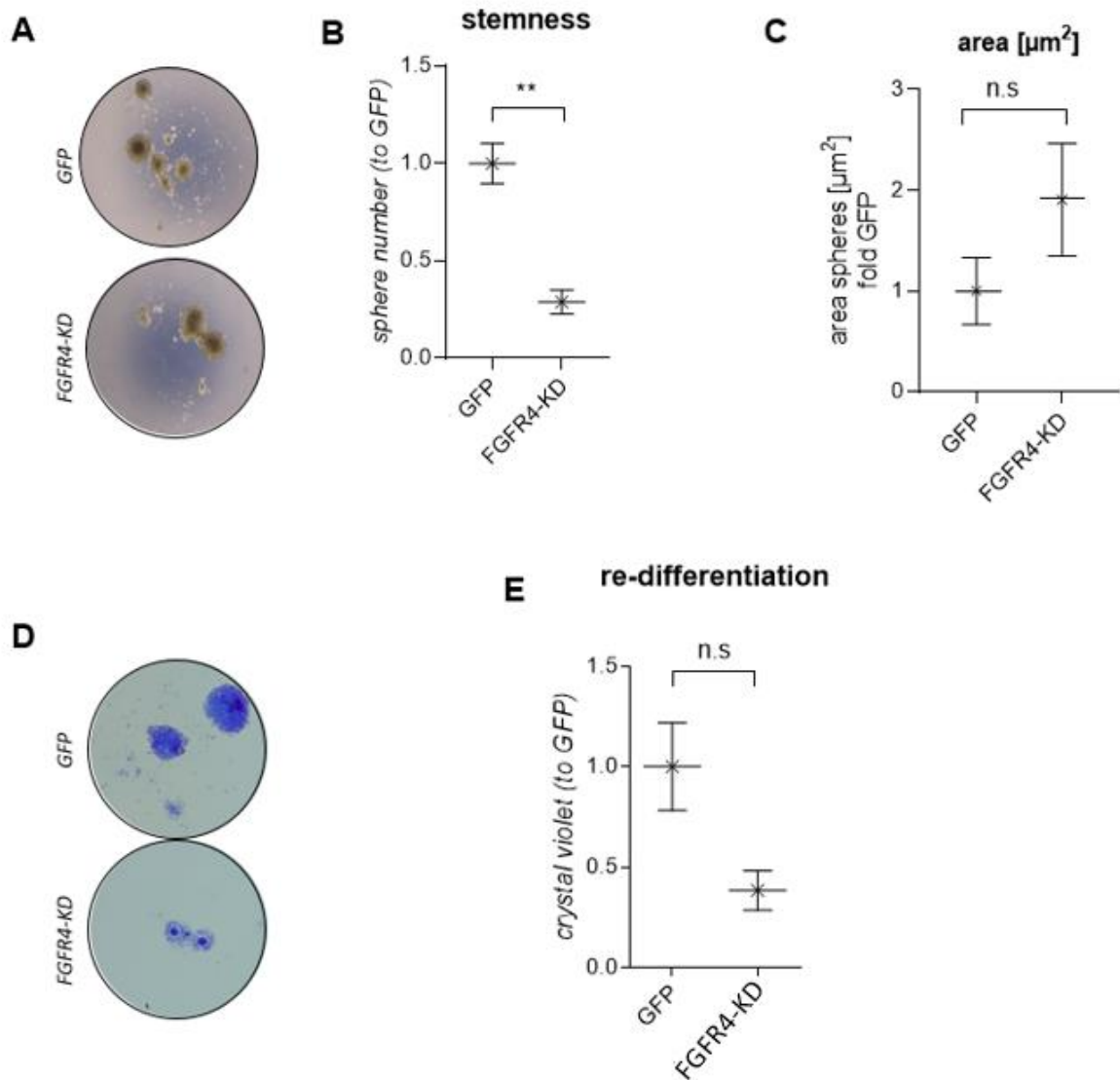


Figure 45. Sphere formation assay BTL1376. Cells were seeded in NB+ medium and incubated for two days in ultra-low attachment plates. Microphotographs were taken in order to observe sphere formation using the Zeiss AxioCam ICc5 (**A**). Image J software was used analyzing number (**B**) and area (**C**) of the spheres. After three days spheres were transferred to non-treated cell culture plates in RPMI10 medium and tested for their capacity of re-differentiation. After re-settlement and re-differentiation of the cells, medium was aspirated and cells were stained with crystal violet and photographed using Nikon D7200 camera (**D**). (**E**) Graph indicates amount of re-differentiated cells calculated by analyzing the integrated density using Image J. Statistical analysis was performed using an unpaired student's *t*-test (n.s.= not significant; $p < 0.05$ =*; $p < 0.01$ =**; $p < 0.001$ =***). All results are given as mean \pm SEM.

4.9.2 Sphere formation and re-differentiation upon inactivation of FGFR4 in SIWA M1

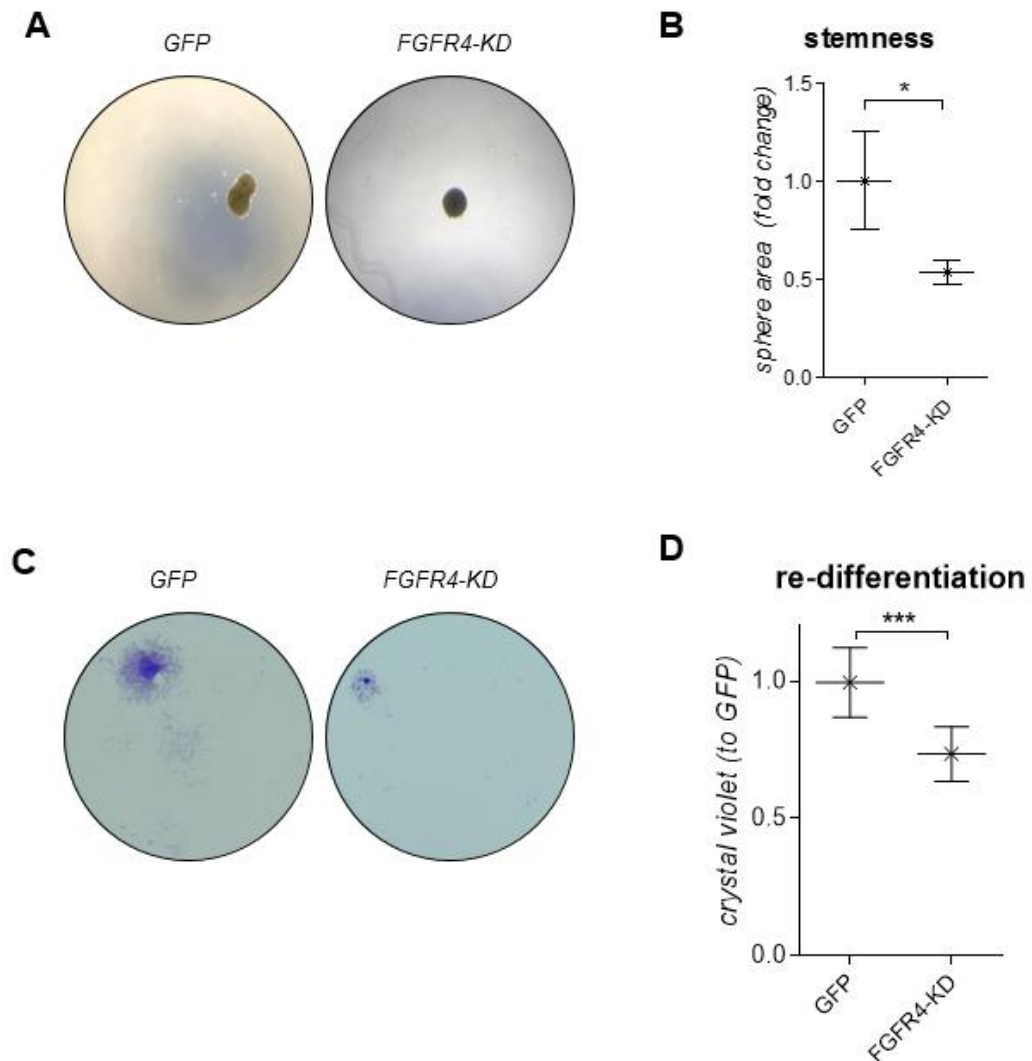


Figure 46. Sphere formation assay SIWA M1. Cells were seeded in NB+ and incubated for two days in ultra-low attachment plates. Photographs were taken in order to observe sphere formation using the Zeiss AxioCam ICc5 (**A**). Image J software was used analyzing area of the spheres, given as mean \pm SD. (**B**).

After three days spheres were transferred to normal cell culture plates in normal RPMI medium and tested for their capacity of re-differentiation. After re-settlement and re-differentiation of the cells medium was aspirated and cells were stained with crystal violet (**C**).

(**D**) Graph indicates amount of re-differentiated cells calculated by analyzing the integrated density using Image J given as Mean \pm SD. Statistical analysis was performed using an unpaired student's t- test ($p < 0.05$ =*; $p < 0.01$ =**; $p < 0.001$ =***).

4.9.3 Sphere formation with stimulation of FGFR4 via FGF23 in SIWA M1

For further investigation of the role of FGFR4 in sphere formation, we examined the response to FGF23 regarding spheroid growth. Therefore, FGF2 in NB+ medium was substituted by FGF23. Since FGF23 directly targets FGFR4 (Grabner et al. 2017; Wyatt and Drüeke 2016), we examined differences between the GFP and the KD variant. Accordingly, sphere formation was not induced in the KD clones after stimulation with FGF23, but was slightly enhanced in the GFP control cells. Corroboratively with data shown before, the FGFR4-KD showed impaired re-differentiation capability as compared to the GFP control cells (**Figure 47**). Stimulation with FGFs did not show effects on re-differentiation in either cell line (data not shown).

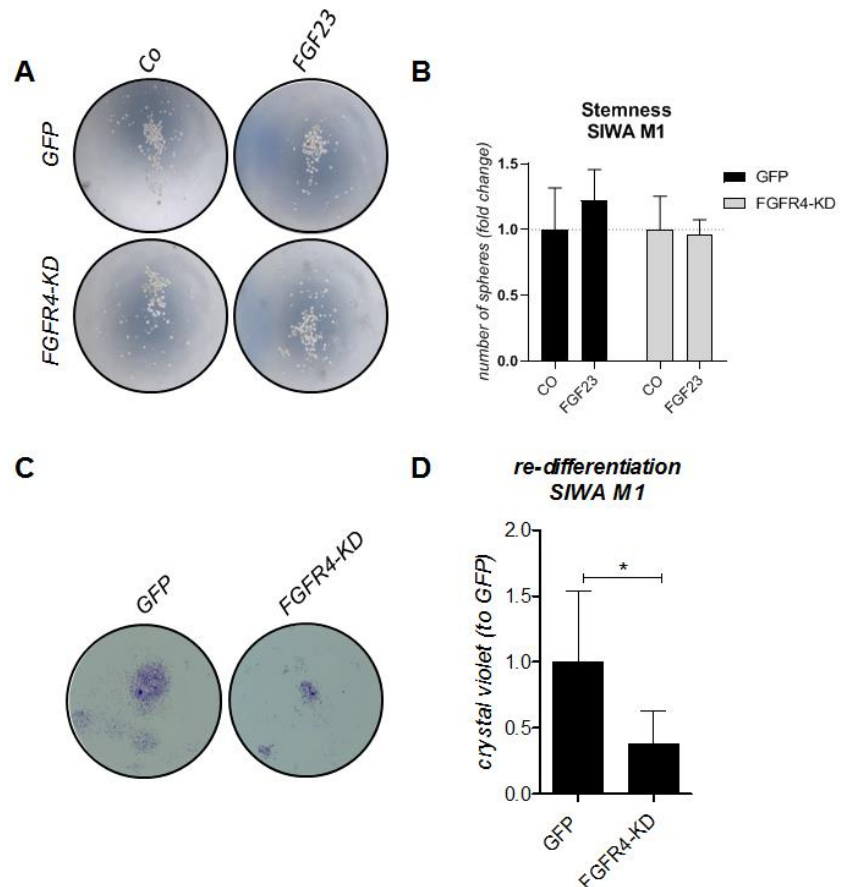


Figure 47. Sphere formation assay SIWA M1 with stimulation via FGF23. Cells were seeded in NB+ medium supplemented with EGF, L-glutamine, N2 and B27 but lacking FGF2. To allow sphere formation prior to stimulation cells were incubated for 24h before FGF23 was added (50ng/ml). (A) Photographs were taken one day after stimulation and formed spheres were counted using ImageJ software. (B) Graph indicates number of spheres normalized to the unstimulated control of the respective cell line set to 1. Results are presented as mean \pm SD. (C) For re-differentiation, spheres were transferred to RPMI10 medium into non-treated cell culture plates and incubated for 7 days for re-differentiation before cells were stained with crystal violet. Photographs were taken using Nikon 7200 camera. (D) Re-differentiation was analyzed by computing the area covered by cells using an algorithm designed for R. Results are given as mean \pm SD. Statistical analysis was performed using an unpaired student's t- test ($p < 0.05 = *$; $p < 0.01 = **$; $p < 0.001 = ***$).

4.10 *In vivo* aggressiveness of FGFR4-inactivated SIWA-M1

Since two- as well as three-dimensional growth experiments revealed major differences between the FGFR4-KD model and the GFP control, we investigated the *in vivo* tumor formation capacities of the cells. Therefore, our FGFR4-KD modified SIWA M1 model as well as the GFP control cells were injected subcutaneously into four SCID/CB17 mice per group. One mouse per group developed a thymic tumor, which was based on literature most corresponding to thymic lymphomas (Custer, Bosma, and Bosma 1985), therefore these mice were euthanized prior to the study endpoint and were censored in our analyses. According to the FELASA guidelines of animal care, mice were sacrificed when their weights drastically dropped, when tumor sizes exceeded 2 cm in one direction or when they were in noticeable worsening health conditions. Mice weights were stable throughout the experiment. In the FGFR4-KD group in one mouse no tumor engraftment was observed and in the two remaining mice, the tumorigenicity was significantly impaired. Remarkably, the tumor growth was significantly reduced in the FGFR4-KD tumor-bearing mice as compared to the GFP control. Mice with tumors of FGFR4-KD cells had a significantly improved survival time as compared to the GFP control (**Figure 48**).

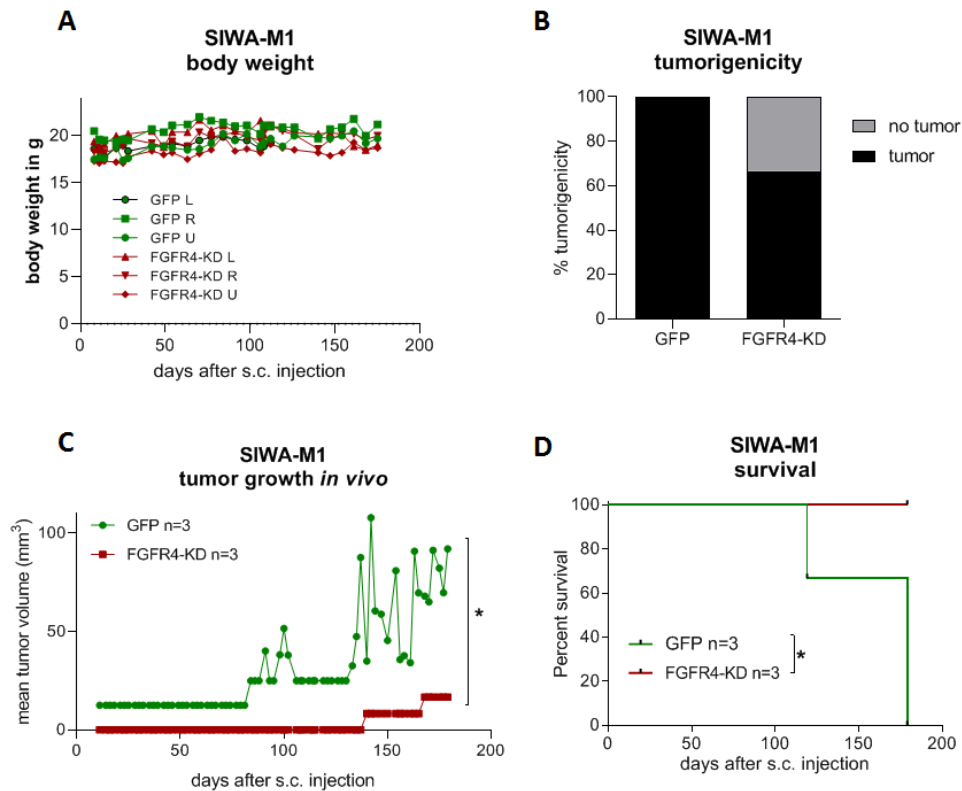


Figure 48. In vivo tumor formation of SIWA M1 cell models. Cells were subcutaneously injected into SCID/CB17 mice and tumors were grown for 180 days until the experiments' endpoint was reached as depicted. **(A)** Body weights of mice was steadily observed throughout the experiment. Graph shows body weight in grams (g) of each included mouse. **(B)** Tumorigenicity of indicated cell models (n=3 per group) is given in percent. **(C)** Tumor growth was monitored at every third day after injection and mean tumor volumes of every cell model are depicted. Two-way ANOVA (Bonferroni test) was used for significance measurement ($p < 0.05 = *$; $p < 0.01 = **$; $p < 0.001 = ***$). **(D)** Kaplan Meier curves are depicted showing overall survival of mice in each group (n=3 per group). Statistical analysis was performed using log-rank (Mantel-Cox) test ($p < 0.05 = *$; $p < 0.01 = **$; $p < 0.001 = ***$). S.c.=subcutaneous; U = unmarked; L= left-ear marked; R=right-ear marked.

4.11 Sensitivity of FGFR4 modified cell models towards receptor inhibition

To test whether FGFR4 overexpression influences susceptibility to certain receptor tyrosine kinase inhibitors (RTKIs), cell viability assays were performed. Most RTKIs act via inhibition of downstream signaling by blocking the ATP-binding pocket of the RTK (Mohammadi et al. 1997). For that reason, we were interested whether inactivation of the kinase domain in the FGFR4-KD variant influences sensitivity towards such inhibitors. Therefore, the multi tyrosine

kinase inhibitors ponatinib and nintedanib as well as the FGFR4-specific inhibitors BLU9931 and BLU554 were tested. Surprisingly, viability assays using the mentioned RTKIs revealed that FGFR4-KD is most sensitive. Exemplary results are depicted below (**Figure 49**). This suggests FGFR4 non-kinase impacts and/or compensatory upregulation of other FGFR molecules. To precisely dissect the underlying mechanisms, further analyses are required.

SIWA M1

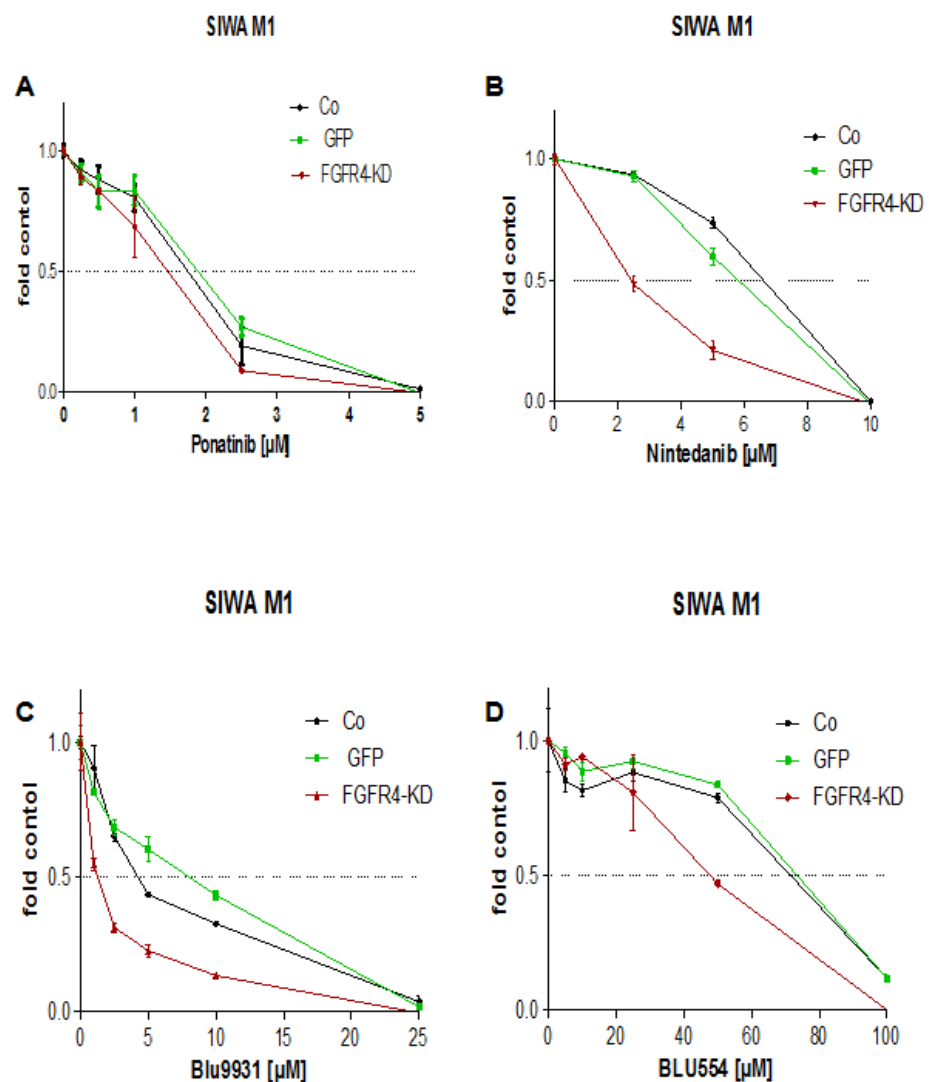


Figure 49. Cell viability assays of SIWA M1. Non-transfected control (Co), GFP-only as well as FGFR4-KD cells were seeded and treated with increasing concentrations of RTKIs on the next day. FGFR4-targeting compounds ponatinib (A), nintedanib (B), as well as BLU9931 (C) and BLU554 (D) were used. After 72h, cell viability was measured (MTT assay). Graphs show the sensitivity of the cells to different RTKIs and data were normalized to the respective untreated control set to 1. Values are presented as mean \pm SD. Co = non-transduced control.

In order to explore sensitivity of our cell models towards the used RTKIs, IC₅₀ values have been calculated. IC₅₀ values represent the required drug concentration for 50% proliferation inhibition and are therefore used to define the potency of the drug. IC₅₀ values of ponatinib, nintedanib, BLU9931 and BLU554 in the non-transduced control, GFP and FGFR4-KD model are given below (**Figure 50** and **Table 21**).

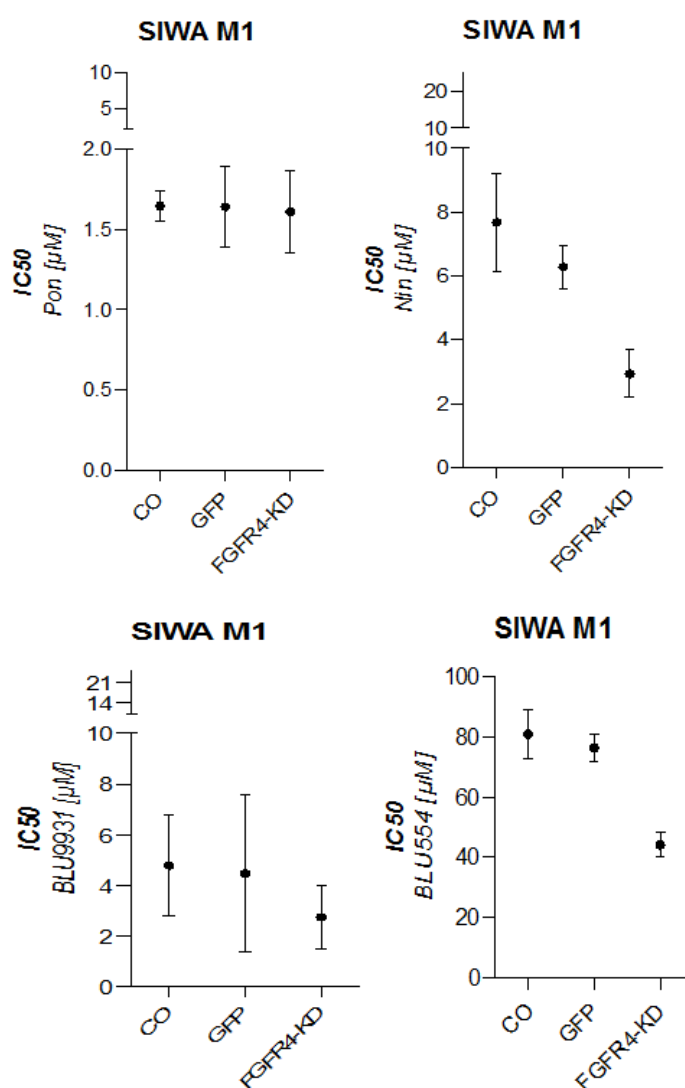


Figure 50. Graphical IC₅₀ presentation of the indicated RTKIs in SIWA M1 cell models. IC₅₀ values have been calculated using GraphPad Prism 5. Y-axes show the applied drug concentrations. IC₅₀ values of each cell model are shown as mean \pm SD. Co= non-transduced control;

Table 21. IC50 table of different RTKIs in SIWA M1 models

<u>Cell line</u>	<u>Ponatinib</u> <u>[μM]</u>	<u>Nintedanib</u> <u>[μM]</u>	<u>BLU9931</u> <u>[μM]</u>	<u>BLU554</u> <u>[μM]</u>
	<u>Mean</u> <u>+/- SD</u>	<u>Mean</u> <u>+/- SD</u>	<u>Mean</u> <u>+/- SD</u>	<u>Mean</u> <u>+/- SD</u>
<u>SIWA M1 Co</u>	1.648 +/- 0.093	7.674 +/- 1.518	4.784 +/- 1.979	80.925 +/- 8.179
<u>SIWA M1 GFP</u>	1.642 +/- 0.255	6.283 +/- 0.676	4.705 +/- 3.09	76.499 +/- 4.436
<u>SIWA M1 FGFR4- KD</u>	1.610 +/- 0.256	2.935 +/- 0.734	2.754 +/- 1.272	44.146 +/- 4.151

BTL1376

As the GS cell line BTL1376 grows partially as spheres, an ATP assay was used to examine sensitivity towards RTKIs. Drug concentrations were adjusted to the new cell line, as BTL1376 is much more sensitive towards all inhibitors as compared to SIWA M1. Interestingly, we observed that pan RTKIs as well as drugs targeting specifically FGFR4, like Blu9931 and Blu554, could drive cells into spheroid growth, especially in the FGFR4-Gly variant (**Figure 51B**). This effect has also been investigated in a previous clonogenic experiment for treatment with ponatinib (data not shown). Nevertheless, the presented results originate from one single experiment, which therefore have to be validated (**Figure 51**).

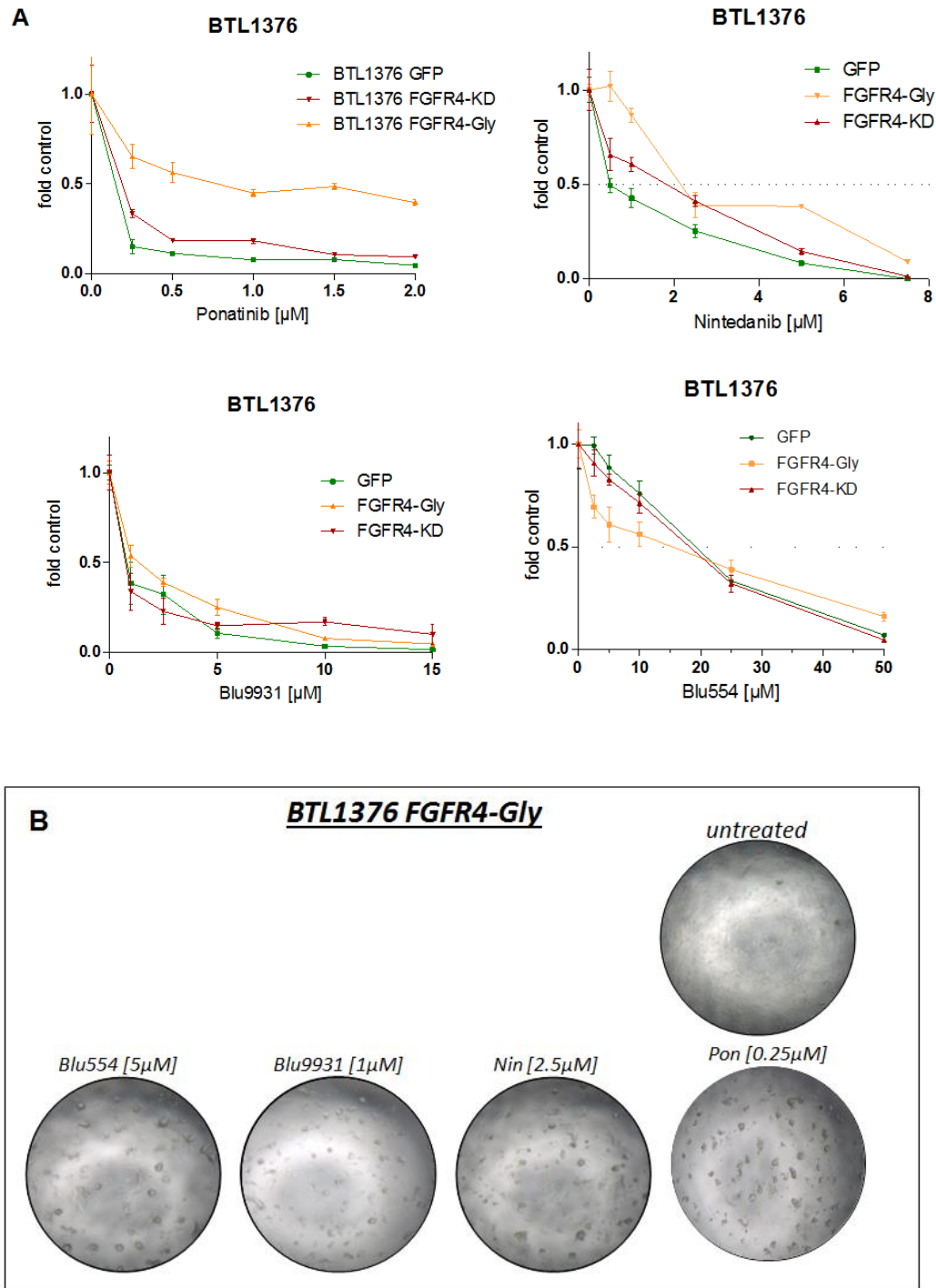


Figure 51. Sensitivity of BTL1376 towards RTKIs. GFP control, FGFR4-Gly as well as FGFR4-KD cells were seeded and treated with increasing concentrations of RTKIs on the next day. (**A upper panels**) FGFR4-targeting compounds ponatinib and nintedanib, as well as (**A lower panels**) BLU9931 and BLU554 were used. After 72h, cell viability was measured (ATP assay). Graphs show the sensitivity of the cells to different RTKIs and data were normalized to the respective untreated control set to 1. Values are presented as mean \pm SD. (**B**) Microphotographs taken after 72h of drug incubation show spheroid growth pattern of the FGFR4-Gly variant in response to RTKIs.

4.12 Inhibition of FGFR4 downstream signaling by Ponatinib

To evaluate the impact of the RTKs ponatinib on FGFR downstream signaling, Western blot analysis was performed. Since ponatinib is active already in comparably low concentrations in the FGFR4 high expressing SIWA M1 cell line, cells were treated with 1 or 2.5 μ M ponatinib and incubated for 27h before proteins were isolated. FGFR4 expression levels are rather enhanced in response to ponatinib in the FGFR4-Gly and FGFR4-KD variants while it seems to be degraded in the FGFR4-Arg model. Upon ponatinib treatment, activation of the downstream signaling molecule S6 is clearly diminished in FGFR4-Gly, -Arg as well as in control cell lines. Interestingly, in the FGFR4-KD variant S6 activation was not equally attenuated in response to high ponatinib concentrations (**Figure 52**).

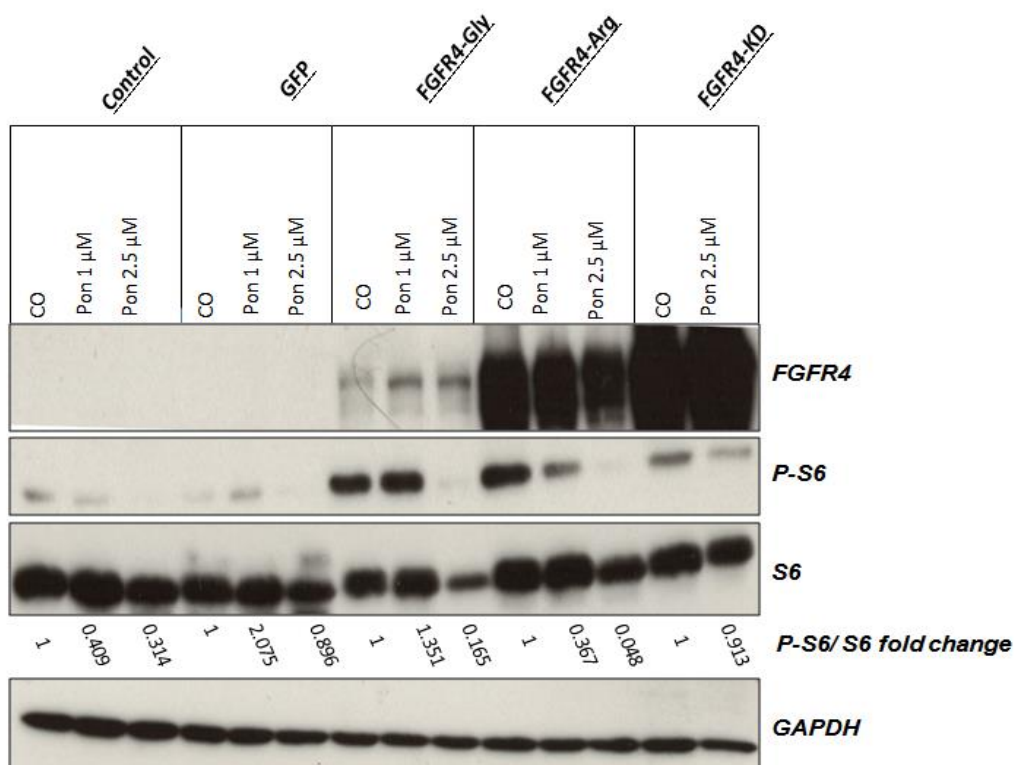


Figure 52. Downstream signaling in FGFR4 modified SIWA M1 cell models upon ponatinib treatment. Western blot shows effects of ponatinib treatment on FGFR downstream signaling in the indicated cell lines. Cells were treated with 1 μ M or 2.5 μ M ponatinib, as indicated, and incubated for 27h. Total protein extracts were obtained and effects on FGFR4 expression as well as downstream signaling were analyzed upon inhibition. GAPDH served as loading control.

S6 and p-S6 expression levels were quantified and normalized to the respective loading control using ImageJ. Values indicate S6 activation upon ponatinib treatment normalized to the respective untreated control. CO = untreated control, Pon = ponatinib

4.13 Investigation of migration and invasion capacity of FGFR4 modified glioma cells

Since FGFR4 is involved in processes like cell migration and invasion (Bennasroune et al. 2004), (Heinzle et al. 2014), we analyzed these properties correspondingly. Therefore, cells were seeded in serum-free medium in transwells where they had to migrate through a fine-mashed membrane attracted by serum-supplemented medium, which was only present in the bottom well. For invasion assays the membrane was previously coated with matrigel, generating an additional barrier for the cells. Strikingly, FGFR4-KD variant showed distinctly reduced migratory and invasive potential as compared to the GFP control in SIWA M1 as well as in BTL1376 cell lines (**Figure 53** and **Figure 54**).

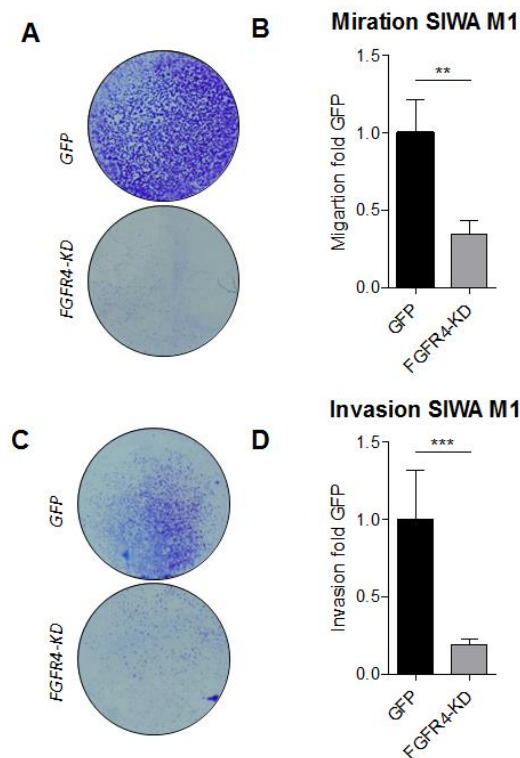


Figure 53. Migration / invasion assay in SIWA M1 FGFR4 altered cell models. Cells were seeded in serum-free medium in transwells and incubated for 72 h to allow cells to migrate through the pores of the membrane. Subsequently, migrated cells in the bottom well were stained with crystal violet. Photographs of one representative well taken using Nikon D7200 are depicted in (A) representing migrated and (C) invaded cells. (B, D) Photographs were analyzed with ImageJ. Graphs indicate amount of migrated (B) or invaded (D) cells. Results are given as mean \pm SD and normalized to the GFP control set to 1. Statistical analysis was performed using unpaired student's t-tests ($p < 0.05 = *$; $p < 0.01 = **$; $p < 0.001 = ***$).

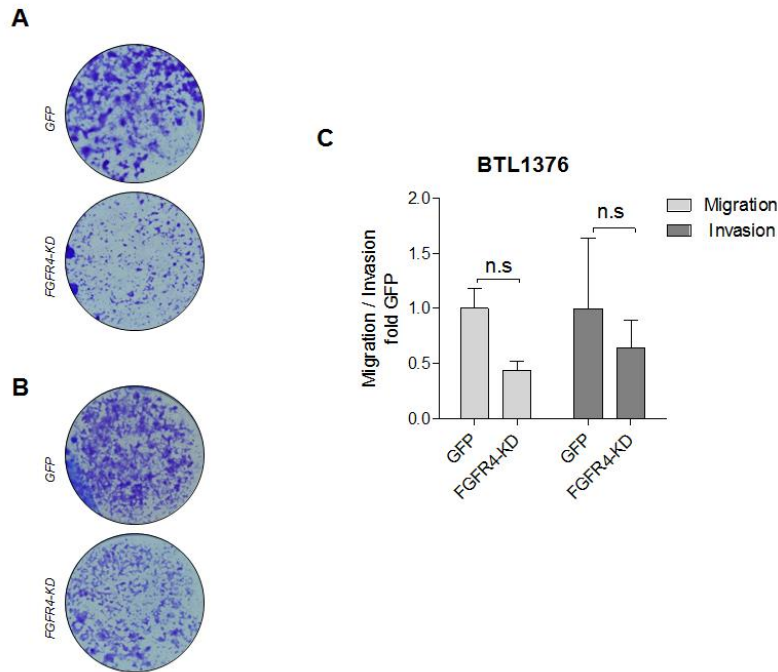


Figure 54. Migration / invasion assay in BTL1376 FGFR4 altered cell models. Cells were seeded in serum-free medium in transwells and incubated for 72 h to allow cells to migrate through the pores of the membrane. Subsequently, migrated cells in the bottom well were stained with crystal violet. Photographs of one representative well taken using Nikon D7200 are depicted in **(A)** representing migrated and **(B)** invaded cells. **(C)** Photographs were analyzed using integrated density analyzed with Photoshop software. Graphs indicate amount of migrated or invaded cells as indicated. Results are given as mean \pm SEM and normalized to the GFP control set to 1. Statistical analysis was performed using unpaired student's *t*-tests (n.s. = not significant).

As the migratory potential was significantly impaired in the FGFR4-KD as compared to SIWA-M1 GFP, we next performed scratch assays. Using live cell imaging, our cell models were tested regarding their wound healing capacity. Therefore, cells were seeded as a confluent monolayer, scratches were made and cells were steadily followed in real time. Subsequently, the gap closure time was measured. Indeed, the FGFR4-KD variant showed significantly impaired motility and efficiency in gap closure as compared to the GFP control and the non-transduced control (**Figure 55**).

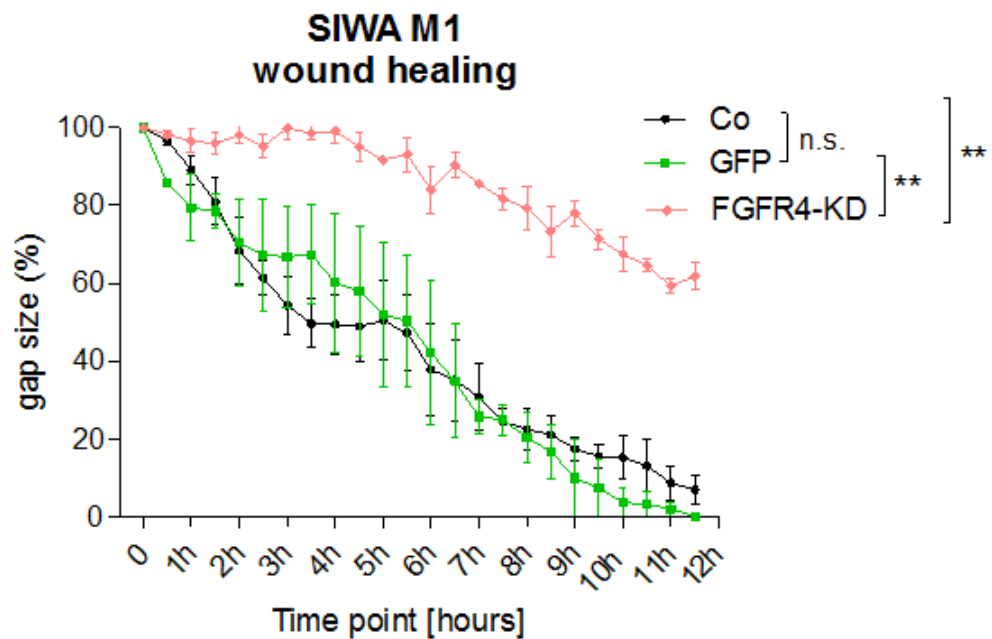


Figure 55. Wound healing analysis of SIWA M1. Cells were seeded as confluent monolayer. Scratches were made and microphotographs were taken in a time interval of 30 minutes with 10x objective. Two independent measurements of the same well were analyzed using T scratch software and results are given as mean \pm SD. Statistical analysis was performed using one-way ANOVA. (n.s.= not significant; $p < 0.05$ =*; $p < 0.01$ =**; $p < 0.001$ =***). Co = non-transduced control.

4.14 Analysis of epithelial and mesenchymal cell markers upon FGFR4 modulation

On the one hand, the here presented findings suggest that inactivation of FGFR4 in the FGFR4-KD cell variants strongly regulates sphere-formation potential and re-differentiation capacity. On the other hand, FGFR4-KD also impairs cells migration and motility. Therefore, as a next step, we were interested whether FGFR4 inactivation influences other cancer cell migration associated processes like epithelial to mesenchymal transition (EMT). We assessed expression of different mesenchymal markers in all novel FGFR4 modulated cell models on RNA- as well as on protein-levels. Surprisingly, we found major differences among the GBM cell line SIWA M1 and the GS model BTL1376.

Vimentin is a component of the cytoskeleton which has been linked to cell migration and is predominantly expressed in mesenchymal cells (“Vimentin - an Overview | ScienceDirect Topics” n.d.). In SIWA M1, expression of vimentin was elevated in the FGFR4-KD variant on RNA level as well as on protein level. Furthermore, also other EMT markers revealed elevated levels of *SNAI1* (*snail*) and *CTNNB1* (β -catenin) mRNA in the FGFR4-KD variant, suggesting a more mesenchymal phenotype upon inactivation of FGFR4 in SIWA M1 models. Furthermore, major differences regarding EMT marker expression could be found between the FGFR4-Gly and -Arg variant. While the FGFR4-Gly variant favors a mesenchymal phenotype by upregulation of all investigated markers, the -Arg variant displays the most epithelial phenotype within the SIWA-M1 panel, as suggested by downregulation of the mentioned mesenchymal cell markers (**Figure 56**).

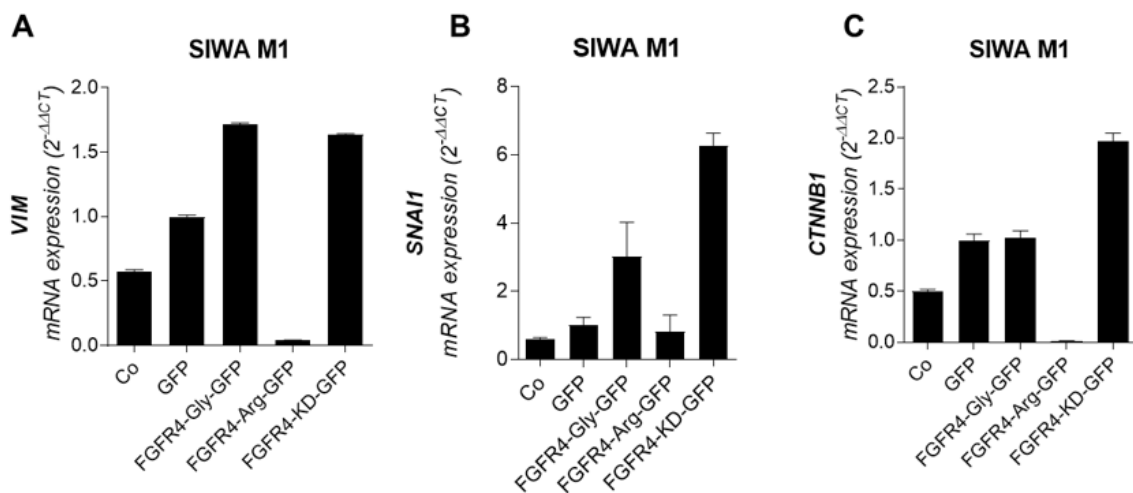


Figure 56. mRNA expression levels of EMT markers in SIWA M1 models. Expression levels of EMT markers (A) vimentin (VIM), (B) snail (SNAI1) and (C) β -catenin (CTNNB1) were analyzed by qPCR and normalized to the housekeeping gene RPL-41. Graphs show expression levels of EMT markers in the different FGFR4 altered models in SIWA M1 as well as in the non-transduced control (Co) and GFP only. Data are given as $2^{-\Delta\Delta CT}$ normalized to the GFP control. Co = non-transduced control.

Conversely, inactivation of FGFR4 in the GS model BTL1376 resulted in a rather epithelial phenotype. Compared to the GFP control, BTL1376 FGFR4-KD showed decreased mRNA expression levels of *VIM*, *SNAI1* and *CTNNB1* (**Figure 57**).

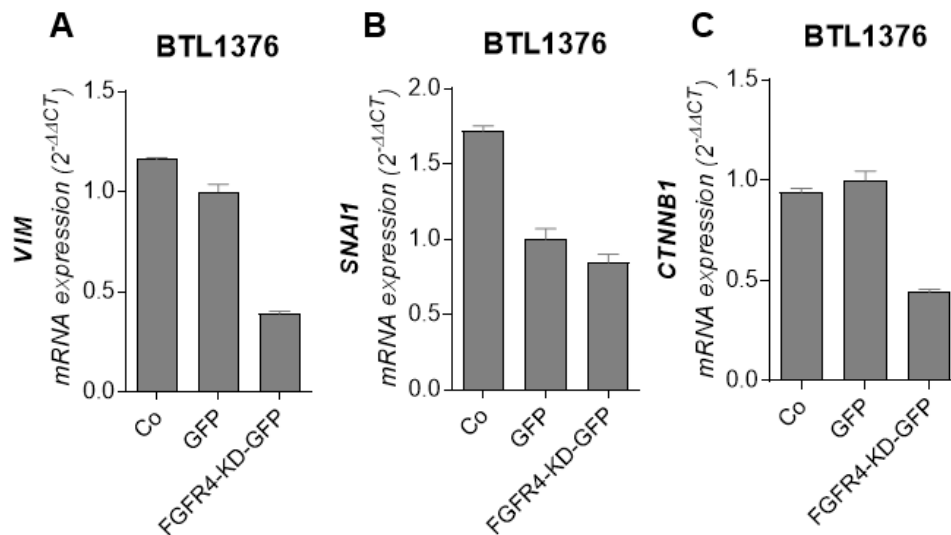


Figure 57. Expression of EMT markers in BTL1376. Expression levels of EMT markers (A) vimentin, (VIM) (B) snail (*SNAI1*) and (C) β -catenin (*CTNNB1*) were analyzed by qPCR and normalized to the housekeeping gene *RPL-41*. Graphs show expression levels of EMT markers in the FGFR4-KD model as well as the non-transduced control (Co) and GFP only. Data are given as $2^{-\Delta\Delta CT}$ normalized to the GFP control.

Since we discovered major differences in EMT marker expression between the altered FGFR4 models and the respective GFP controls, we were further interested in the consequences of *FGFR4* knock-down in the novel SIWA M1 cell models. Therefore, *FGFR4* was knocked down in SIWA M1 cell models ectopically over-expressing FGFR4 as well as the non-transduced controls using an siRNA approach. qPCR confirmed successful knock-down of *FGFR4*. Again, focusing on mesenchymal markers, we found downregulation of the EMT markers *VIM*, *SNAI1* and *CTNNB1* upon knock down of *FGFR4* in the FGFR4-KD variant and the ectopically over-expressing FGFR4-Gly variant. Interestingly, in the FGFR4-Arg variant knock-down of *FGFR4* resulted in slight upregulation of mesenchymal markers, thus a more mesenchymal phenotype. Expression of other mesenchymal markers like *CTNNB1* and *SNAI1* follow this trend. Knock-down of *FGFR4* was not successful in the GFP control (data not shown). Although the non-transduced control showed downregulation of *VIM*, *SNAI1* and *CTNNB1* levels were rather upregulated after knock-down of FGFR4 (**Figure 58**).

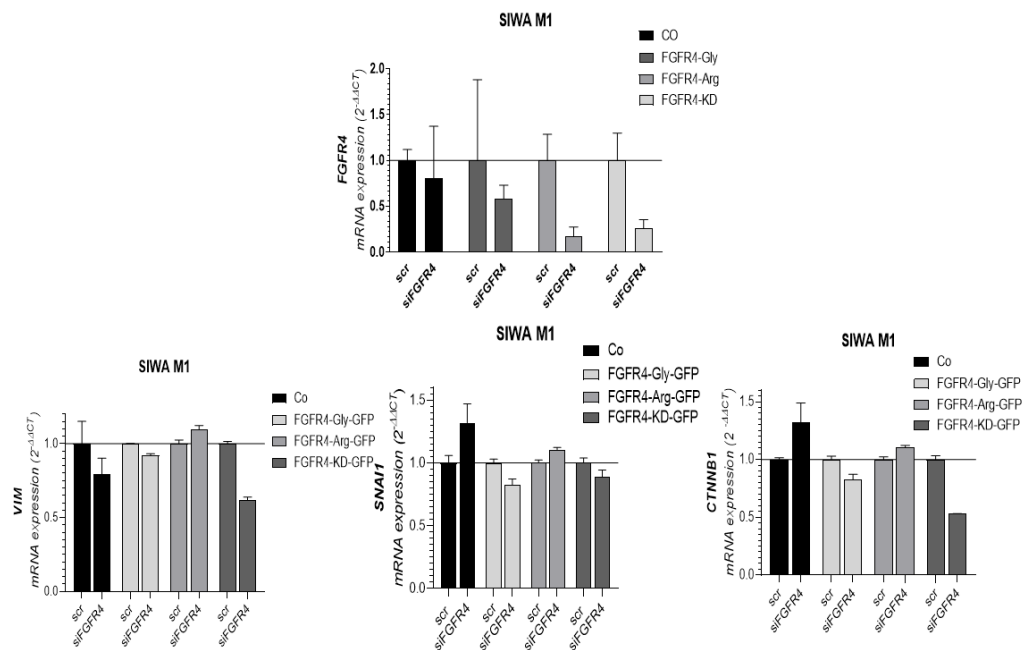


Figure 58. EMT marker expression after knock-down of FGFR4 in SIWA M1. Analysis of (A) *FGFR4* and EMT marker (B) vimentin (*VIM*), (C) snail (*SNAI1*) and (D) β -catenin (*CTNNB1*) expression levels after knock-down of *FGFR4* in SIWA M1 cell models. EMT marker expression levels have been normalized to scr and are given as $2^{-\Delta\Delta CT}$. Co = non-transduced control; scr = scrambled.

On protein level, EMT marker analysis of SIWA M1 cells revealed overexpression of vimentin in the FGFR4-inactivated model compared to the GFP control. In agreement with the previous qPCR data shown above, knock-down of *FGFR4* resulted in attenuated vimentin levels compared to basal expression profiles in case of the KD variant, which was even enhanced by stimulation with FGF2. This effect was not present in the GFP control. Furthermore, stimulation with FGF2 after starvation resulted in vimentin hyper-expression in the GFP model (**Figure 59**)

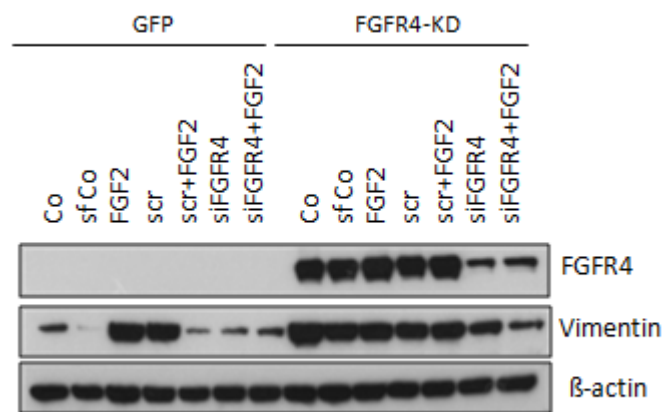


Figure 59. Western blot analysis of vimentin expression in SIWA M1 upon knock-down of FGFR4. Besides analysis of FGFR4 expression of the EMT marker vimentin was analyzed after knock-down of FGFR4. This Western blot has been shown previously focusing on the effect of FGFR4 knock-down on downstream signaling. β -actin served as loading control. Co = Control, sf Co = serum-starved control, scr = scrambled

5 Discussion

With an incidence of 17 million new diagnosed cases and a mortality rate of around 9.6 million deaths worldwide in 2018 (“Worldwide Cancer Statistics | Cancer Research UK” n.d.), cancer is ranked as the leading cause of death in high-income countries (Dagenais et al. 2019). As cancer is mainly driven by aberrant regulation of pathways involved in cell cycle or survival (Sever and Brugge 2015), overexpression or constitutive activation of receptor tyrosine kinases (RTKs) are characteristic features in various cancer types (Sever and Brugge 2015). Besides epidermal growth factor receptors (EGFR), vascular endothelial growth factor receptors (VEGFR) and platelet-derived growth factor receptors (PDGFR) (Butti et al. 2018), also FGFRs are among those receptors which are often deregulated in cancer (Butti et al. 2018). As FGFRs are involved in many cellular pathways driving proliferation, survival, differentiation and migration (Chae et al. 2017), constitutive activation of FGFRs in cancer cells is known to enhance tumor formation and aggressiveness. Up to now, 5 members of the FGFR family are known (Zhou et al. 2016). While the existence and function of FGFR5 are critically discussed in literature (Regeenes et al. 2018; Sleeman et al. 2001; Zhou et al. 2016; Gnatenko, Kopantsev, and Sverdlov 2017), expression and deregulation of the other family members have been proposed to influence tumorigenesis and progression. Overexpression of FGFR4 has been previously reported in prostate, colon, liver cancer and rhabdomyosarcoma (Harris et al. 2018; Chae et al. 2017). Furthermore, a SNP in the coding region of FGFR4 leading to an amino acid substitution at codon 388 (glycine to arginine, G388R) has been identified (Falvella et al. 2009; Wimmer et al. 2019; W. Xu et al. 2010). Presence of the arginine variant of this SNP has been correlated to enhanced tumor progression and poor survival (Spinola et al. 2005; Bange et al. 2002) in other tumor entities but not in GBM (Mawrin et al. 2006). Recent studies in our lab revealed a subset of GBM especially GS tumors, that exhibit massive overexpression of *FGFR4*. GBM and GS belong to the group of astrocytic CNS tumors with highly diverse cell populations and therefore remain difficult to treat. As the gold standard therapy including the alkylating drug temozolomide is only successful in a subgroup of patients harboring *IDH* mutations or *MGMT* promoter methylations (SongTao et al. 2012, Li et al. 2016, Szopa et al. 2017) discovery of new molecular targets and new therapeutic approaches are urgently needed for these cancer patients.

FGFR4 is variably expressed among glioma

Alterations in *FGFRs* including amplifications and translocations have been linked to different types of cancer including myeloma, lung cancer, breast cancer and gastric cancer (Chae et al. 2017). *FGFR4* protein expression has also been linked to increased malignancy in astrocytic tumors as only tumors of grades III and IV showed detectable *FGFR4* expression. Furthermore, patients harboring grade III or IV tumors with *FGFR4* overexpression had a worse overall survival (Yamada et al. 2002). Previous findings by our group have demonstrated that *FGFR4* is heterogeneously expressed among malignant glioma (grade IV) including GBM and GS. Both *in silico* as well as *in vitro* analyses of primary and immortalized cell lines revealed a distinct *FGFR4*-overexpressing subgroup within glioma.

Heterozygous expression of FGFR4 G388R variants in GBM and GS cell lines

The *G388R* polymorphism, in which a glycine is substituted by an arginine at position 388 located in the transmembrane domain, has been proposed to enhance tumor cell motility and metastasis in different types of cancer (da Costa Andrade et al. 2007; Taylor et al. 2009; Bange et al. 2002). Although *FGFR4*-Arg variant has been correlated to tumor aggressiveness and invasiveness in other cancer types, the impact of the SNP in glioma remains widely unknown. Prior to genetic *FRFR4* manipulation, we assessed the endogenous *FGFR4* SNP status of our used cell lines SIWA M1 and BTL1376. RFLP PCR revealed presence of both alleles in either cell line, indicating that both cell lines are heterozygous, thereby expressing one (or more) alleles of either variant. This observation fits well to previous data by Mawrin *et al.*, where the *FGFR4*-Arg variant appears rarely in GBM, however, heterozygous SNP presentations and *FGFR4*-Gly were equally distributed within this tumor entity (Mawrin et al. 2006). Nevertheless, expression of the *FGFR4*-Gly variant seems to be much stronger as compared to the *FGFR4*-Arg variant in both cell lines suggesting a shift in allele coverage at this sequence site. This finding might also contribute to the transduction efficacy in case of the *FGFR4*-Gly retroviral expression plasmid in both of the investigated cell lines. Expression of both mentioned variants increases the genetic diversity within the cell, which might be beneficial for evolutionary adaptation to mutations and tumor formation.

Generation of FGFR4-overexpressing cell clones

Since previous data in our group identified a subgroup of GBM and GS cell lines harboring a distinct FGFR4 overexpression, we assumed a possible role of FGFR4 in tumor onset and/or progression of this GBM subgroup. Therefore, two of these FGFR4-high cell lines were selected to generate ectopically FGFR4 overexpressing cell models via stable integration of genetically altered *FGFR4* expression plasmids, either by spontaneous integration via lipofection or by retroviral transduction. On the one hand, we aimed to dissect the role of G388R in glioma. On the other hand, we introduced an FGFR4 variant harboring a loss of function point mutation in the kinase domain resulting in a dominant-negative phenotype and thus inhibition of FGFR4 downstream signaling. Each *FGFR4* variant was fused to *GFP* as reporter for efficient transduction/transfection and for localization of FGFR4 within the cell.

In the GBM cell line, SIWA M1, stable integration of the altered FGFR4 variants was achieved via retroviral transduction and transduction efficiency was analyzed using different quantitative and semi-quantitative methods. Quantitative real-time PCR and Western blot proved overexpression of all FGFR4 *variants* i.e. the KD variant and the SNP variants. Since GFP is C-terminally fused to each *FGFR4* variant, successfully transduced cells were quantified by flow cytometry. Interestingly, we saw that FGFR4 overexpression in the two SNP variants FGFR4-Gly and FGFR4-Arg was lost in parts of the cell population, presumably by recombination. In case of the FGFR4-KD transduction efficiency was rather high. Since SIWA M1 is endogenously FGFR4-high and based on our data even heterozygous for G388R, we assume that it does not depend on the artificially modified FGFR4 variant encoding either of the two SNP variants and might have therefore lost it during cell culture propagation. Still, since the kinase inactivated form led to highly efficient transduction, we assume that integration of the dominant negative form of FGFR4 might have any secondary beneficial effects for the tumor cell line, like for example upregulation of other RTKs to compensate for inactivated FGFR4 signaling.

In the GS cell line BTL 1376, transduction efficiency was varying between 60-80% in the FGFR4-KD as well as in the FGFR4-Gly variants. On the one hand, BTL1376 express higher levels of FGFR4, even higher as SIWA M1, points towards a major role of the receptor in this cell line. Therefore, BTL1376 might be more susceptible towards inactivation of FGFR4. On the other hand, BTL1376 is also high in expression of other FGFRs, like FGFR1 (data not shown), kinase inactivation might be compensated by activation of FGFR1.

Since FGF19 and FGF23, which target FGFR4 specifically, depend on members of the klotho family in order to interact with FGFR4, we analyzed *KLB* mRNA expression of the different BTL1376 models. Interestingly, *KLB* levels were increased in the ectopically FGFR4 overexpressing KD variant, indicating that *KLB* is co-regulated with FGFR4 expression independent from its kinase-dependent functions or that cells try to reconstitute FGFR4 downstream signaling by upregulation of the cofactors needed for receptor activation.

Conversely, a knock-down experiment in SIWA M1, as well as in a ectopically overexpressing cell model U373 Gly revealed that upon knock-down of *FGFR4* *KLB* expression was downregulated, indicating co- regulation of these two molecules.

Localization of FGFR4 predominantly on the membrane and in vesicles in the perinuclear space

As FGFR4 belongs to the family of RTKs, it is expected to localize primarily at the plasma membrane. Nevertheless, FGFRs can be internalized and translocated to the perinuclear space upon activation by their ligands (Auciello et al. 2013). Different theories regarding kinase dependency of FGFR internalization have been investigated. On the one hand, studies performed by Auciello *et al.* showed that activation of FGFRs and thus activation of downstream signaling via FRS2 α and Src kinase leads to clathrin dependent receptor internalization. Subsequently, upon activation of Eps8, a target of Src kinase, FGFRs get translocated to the perinuclear recycling and degradative compartments (Auciello et al. 2013). On the other hand, studies on FGFR1 internalization performed by Reilly et. al. proved cell-cycle dependent localization of FGFR1 that was neither dependent on FGF stimulation nor on tyrosine kinase activity, thereby suggesting a novel mechanism of receptor internalization (Reilly, Mizukoshi, and Maher 2004). This finding was also supported by Opalinski *et.al.* who proved that close proximity of two FGFR monomers could induce internalization rather than ligand binding or transphosphorylation of the kinase domains (Opaliński et al. 2017). Using confocal microscopy, we found *FGFR4* being located on the cell membrane in all ectopically FGFR4 overexpressing cell lines as well as in vesicles in the perinuclear space. Although these perinuclear vesicles were also observed in the FGFR4–KD, the receptor was much more stabilized at the membrane compared to the FGFR4–Gly and FGFR4–Arg variants. Corroboratively, protein analyses of FGFR4-modulated SIWA M1 membrane fractions

revealed that inactivation of FGFR4 in the KD variant resulted in stabilization of the receptor on the membrane pointing towards a role of the kinase activity in receptor internalization (Monsonogo-Ornan et al. 2002). Nevertheless, cytoplasmic and nuclear fractions of both cell lines proved overexpression of FGFR4 in the KD variant in both compartments, supporting perinuclear localization seen in confocal microscopy. Taken together, these data indicate that internalization of FGFR4 is diminished upon receptor inactivation and that receptor activation/kinase activity might be essential for internalization. Moreover, membrane fractions isolated from SIWA M1 models proved membrane localization of FGFR4 in all models. Furthermore, we found that FGFR4 is recruited to the membrane upon serum starvation in all FGFR4 variants but not in the KD variant, indicating an induced survival mechanism of the cells in order to maintain downstream signaling and proliferation. Furthermore decreased receptor internalization upon serum starvation again strengthens previous findings, that receptor internalization depends on its activation (Monsonogo-Ornan et al. 2002). Strikingly, FGFR4 levels were highest upon receptor inactivation in the KD variant and starvation did not change expression levels. These findings confirm the predicted dominant-negative receptor function and diminished receptor internalization.

Impaired downstream signaling upon dominant-negative inactivation of FGFR4

FGFR4 drives many cellular signal pathways like MAPK and PI3K/Akt pathway, thus regulating various cellular functions including cell proliferation, survival and migration. As we were interested to investigate whether genetic modification of *FGFR4* changes these cancer driving pathways, we looked at S6 activation levels in the novel generated cell models as readout of the PI3K/AKT pathway. The FGFR4-KD variant harbors a point mutation within the kinase domain of the FGFR4 with leads to a loss of receptor function and, furthermore, to dominant-negative FGFR4 molecules. According to our expectations, we found decreased activation of S6 in the KD variant of SIWA M1 and BTL1376. These results prove that FGFR4-KD had successfully been introduced into the above-mentioned cell lines and that the kinase function of FGFR4 is crucial for S6 activation, thus loss of function of the FGFR4 leads to impaired S6 signaling. Apart from that, we found that overexpression of FGFR4 was lost in the FGFR4-Arg variant of SIWA M1, also resulting in diminished activation of S6. Since cells were still GFP positive (data not shown), it is most likely that cells might have lost the genetically altered receptor due to recombination processes. Therefore, a new charge was freshly thawed and

used for further experiments. The fact that cells recombined the FGFR4-Arg variant strengthens our hypothesis that the endogenously high coverage of the FGFR4-Gly SNP as compared to the FGFR4-Arg SNP in the SIWA M1 as well as in the BTL1376 models rather adapts to a FGFR4-Gly hyper-expression.

To further investigate dependency of PI3K and MAPK signaling on FGFR4 activity, we knocked down *FGFR4* in the overexpressing SIWA M1 cell lines using a siRNA approach. Concerning activation of FGFR downstream signaling upon knock-down of *FGFR4*, we stimulated the transfected cells, as well as the non-transfected controls with FGF2, which targets all kind of FGFRs. Thereby we assessed the response of our cell models to knock-down of *FGFR4* and whether cells aim to overcome signaling deprivation upon knock-down via upregulation of other FGFRs. First of all, this experiment elucidated significant differences regarding MAPK and S6 signaling in the FGFR4-KD model as compared to the control cell models. Attenuated activation of Erk1/2 and S6 in the non-transfected KD- controls indicates successful inactivation of endogenous FGFR4-mediated growth and survival signals in these cell lines. Furthermore, decreased protein expression levels of FGFR4 proved successful knock-down in the FGFR4-KD, which could not be overcome by stimulation via FGF2. Although we did not see FGFR4 expression in total protein extracts of the control cell lines, membrane fractions proved overexpression of FGFR4 in all cell models, which was even enhanced upon serum starvation, which also fits well to the hypothesis that receptor activation is necessary for its internalization (Monson-Orran et al. 2002). Accordingly, we saw that the stimulatory effect on MAPK signaling as well as S6 activation were decreased after knock-down of *FGFR4* in both control cell lines compared to the respective non-transfected controls, indicating functionality of the knock-down. These findings strengthen our hypothesis that FGFR4 activity plays a crucial role in proliferation and survival in this GBM cell line. Nevertheless, we assume that also other RTKs might be driving these pathways, as signaling was still active after knock-down and even enhanced by stimulation via FGF2. Moreover, this experiment revealed major differences in response to stimulation with FGF2 on a basal level as well as upon knock-down of *FGFR4*. Interestingly, addition of FGF2 in the FGFR4-KD model did not result in comparable stimulatory effect as seen in the control cell lines, indicating that non-functional FGFR4 monomers could also impair downstream signaling by interaction with other RTKs. Formation of heterodimers of FGFR4 with other family members, especially with FGFR3, has also been postulated in other studies (Brewer, Mazot, and Soriano 2016; Paur et al. 2015; Lang and Teng 2019). Accordingly, knock-down of FGFR4 had the opposite effect in the FGFR4-KD model

as compared to the control cell lines, as we observed that knock-down of dominant-negative *FGFR4* resulted in increased activation of S6 signaling as also MAPK signaling compared to the serum free controls. This suggests, that knock-down of the ectopically overexpressed, non-functional FGFR4 resulted in reconstitution of downstream signaling of other RTKs as interaction with kinase-inactivated FGFR4 is impaired. Conclusively, stimulation with FGF2 resulted in increased p-S6 levels after knock-down of FGFR4 in the KD model. Moreover, we saw that p-S6 as well as MAPK signaling were significantly attenuated upon serum starvation, suggesting that activation of FGFR4 downstream signaling is essential for the cells to overcome serum deprivation.

Impact of FGFR4 signaling on two – and three-dimensional growth

Next, we investigated whether modulation of FGFR4 and thus overexpression of different FGFR4 variants impacts cellular functions indicating an important role of FGFR4 in GBM and GS cell pathology. Therefore, changes in the proliferation capacity and clonogenic survival potential of the FGFR4-positive GBM cell models upon FGFR4 modulation were compared between FGFR4-KD cell line and the GFP control in clone formation assays. The clonogenicity of the generated cell models was elaborated on a basal level as well as under different stimulating and inhibitory conditions including FGFs and FGFR-targeting compounds, respectively. Indeed, we found that expression of the FGFR4-KD variant resulted in significantly decreased proliferative potential in SIWA M1 as well as in the BTL1376 cell line, corroborating our previous protein analyses were MAPK activation and therefore proliferation was impaired by inactivation of the FGFR4 kinase domain. Decreased ERK1/2 activity in the FGFR4-KD variant was also shown in Western blot analysis not only on basal levels but also after knock down of FGFR4. The impact of FGFR4 on colony formation capacity has already been reported in other cancer types, like for example in hepatocellular carcinoma (French et al. 2012). In addition to analyses of basal clone formation capacity upon FGFR4 modulation, FGFs or the TKI ponatinib were added in the FGFR4 variants of the GS model BTL1376 and the proliferation was analyzed. Stimulation with FGF2, also known as basic FGF, a growth factor known to bind to all FGFRs, resulted in growth stimulation in the FGFR4-KD variant as well as in the GFP control. Since BTL1376 is also highly expressing other FGFRs, such as FGFR1 (data not shown), the significant proliferation stimulation via FGF2 especially in the FGFR4-KD variant can most likely be explained by alternative receptor activation. Contrary to FGF2, FGF23 is known to predominantly activate FGFR4 (Wyatt and Drüeke 2016; Itoh, Ohta,

and Konishi 2015; Grabner et al. 2017). Accordingly, we saw proliferation stimulation in the GFP control but not in the FGFR4-KD variant, again suggesting dominant negative inhibition of FGFR4 signaling in the KD variant. The FGFR targeting compound ponatinib was highly active at very low concentrations (250 nM) in the endogenously FGFR4 high expressing cell model BTL1376. Application of ponatinib did not reveal major differences between BTL1376 GFP and FGFR4-KD. Nevertheless, we saw that treatment with ponatinib drives the BTL1376 models into a more pronounced spheroid shape. This phenotype has also been observed in cell viability assays and will therefore be discussed later.

Spheroid growth and the ability to grow in an undifferentiated state are often associated with stem cell properties of cancer cells, a phenomenon referred to as “stemness”. In sphere formation assays, we assessed the ability of our FGFR4-variants expressing cell models to form neuro-spheres in serum-deprived neuro-basal medium in low-attachment plates. In SIWA M1, inactivation of FGFR4 resulted in decreased stemness in the FGFR4-KD variant compared to the GFP control as indicated by both, reduced sphere number and sphere area. In contrast, inactivation of FGFR4 in case of the KD variant rather led to a more pronounced spheroid shape in the BTL1376, which was also observed in 2D cell culture, where cells tended to grow as spheres already. Thus, directing cells into neuro-sphere formation was highly efficient in the BTL1376 FGFR4-KD variant as the spheres number was lower, however, the sizes of the spheres was increasing as compared to the GFP control. Since FGFR4 also drives pathways acting in differentiation, we further investigated the ability of our cell models to re-differentiate back to their original phenotype. Herein, we could prove impaired re-differentiation capacity in the FGFR4-KD models in SIWA M1 as well as in BTL1376 cell lines, suggesting a major role of FGFR4 signaling in differentiation. Impact of FGFR4 stimulation on sphere formation was investigated by adding FGF23, thereby directly activating FGFR4 in SIWA M1 cell models. While FGF23 could stimulate spheroid growth in the GFP variant, stimulation showed no effect in the FGFR4-KD model, proving a dominant negative FGFR4 inactivation in the KD variant. Taken together, these data suggest that FGFR4 contributes to GBM cell stemness and plasticity. The role of FGFR4 driven signaling cascades, like the PI3K and the MAPK pathway, in spheroid growth and re- differentiation of GBM cell lines have already been described by Sunayama *et al* (Sunayama et al. 2010).

FGFR4 inactivation reduces tumorigenicity and tumor aggressiveness in vivo

To assess the role of FGFR4 activity on *in vivo* tumor formation, kinase inactivated (KD) FGFR4 expressing and GFP control cell models of SIWA M1 were injected subcutaneously into SCID mice. Tumorigenicity and tumor growth were constantly observed and analyzed. In agreement with previous data proving that FGFR4 functionality is crucial for two- and three-dimensional growth, the FGFR4-KD model was less successful in tumor formation and showed significantly impaired tumor growth as well as animal overall survival as compared to the GFP control. FGFR4 overexpression has already been associated with tumorigenicity and tumor progression in various other cancer types like prostate, colon and hepatocellular carcinoma as well as rhabdomyosarcoma (Chae et al. 2017). Herein we report, for the first time, that dominant negative FGFR4 (KD) GBM xenografts show significantly impaired tumorigenicity and tumor growth *in vivo*. Dependency of FGFR4 activity on *in vivo* tumor formation have already been reported in rhabdomyosarcoma (S. Q. Li et al. 2013; Crose et al. 2012) and hepatocellular carcinoma (Gauglhofer et al. 2014; French et al. 2012).

FGFR4 inactivation alters susceptibility towards RTKIs

In contrast to our expectations, cell viability assays revealed increased sensitivity of the FGFR4-KD variant towards pan-FGFR inhibitors ponatinib and nintedanib as well as FGFR4-specific inhibitors BLU9931 and BLU554. Different hypotheses regarding this hypersensitivity are under current investigation in our group and need to be further worked out in detail. As most RTKIs bind to the ATP binding pocket in the kinase domain of their target (Levitzki and Gazit n.d., Tucker et al. 2014), alteration of the kinase domain in the KD variant might have resulted in conformational changes altering the binding site of the drug. Furthermore, upregulation of other RTKs compensating for FGFR4 inactivity in the KD variant could result in the observed hypersensitivity towards multi RTKIs ponatinib and nintedanib. Nevertheless, the response to FGFR4 specific drugs BLU9931 and BLU554 remains enigmatic. This effect has been observed in both cell lines although it was more pronounced in SIWA M1. In general, the GS cell line BTL1376 was distinctly more sensitive towards all of the tested RTKIs in accordance with the profoundly higher expression of FGFR4. The BTL1376-KD variant appeared to be more resistant towards ponatinib and nintedanib, whereas inhibition via BLU9931 and BLU554 did not reveal major differences between the FGFR4-KD and the GFP

control. Nevertheless, the ectopically overexpressing FGFR4-Gly subline was more sensitive towards specific inhibition of FGFR4, indicating that expression levels of this receptor might play a role in mediating TKI sensitivity. Apart from that, cell viability assays in BTL1376 revealed that inhibition of RTK signaling as well as inhibition of FGFR4 could drive cells into spheroid growth, especially in the ectopically overexpressing FGFR4-Gly variant. This phenotype has been previously observed in a clonogenic assay, where treatment with ponatinib could induce sphere formation in all cell models following a 24h treatment, suggesting that inhibition of RTKs might induce stem cell characteristics in these cells. This effect was observed in the FGFR4-Gly variant as well as to some extent in the control cell lines but not in the FGFR4-KD variant. This suggests that FGFR4 activity might be essential for this phenotype. Nevertheless, due to the high expression of FGFR4 as well as FGFR1 in BTL1376, cells died after 72h even at lowest ponatinib concentrations.

To assess effects of RTK inhibition by ponatinib on FGFR4 downstream signaling, Western blot analysis was performed after treatment of the FGFR4 modified glioma models with two different concentrations of ponatinib. Analysis of FGFR4 expression in the ectopically overexpressing models showed that FGFR4 is rather degraded upon increasing ponatinib concentration in the FGFR4-Arg variant, whereas in the FGFR4-Gly and FGFR4-KD variant the receptor was rather stabilized. Stabilization of FGFR4 after ponatinib treatment has been observed in crystallography studies. The complex formed by FGFR4 with ponatinib was characterized by a small dissociation constant and is therefore considered as relatively stable (Tucker et al. 2014). As ponatinib binds to the ATP binding pocket of the FGFR, interaction is mainly depending on the structure of the kinase domain. The differences seen in receptor stability upon ponatinib treatment suggest that besides the K504M mutation affecting the kinase domain of the FGFR4-KD variant, the *G388R* polymorphism in the transmembrane domain might also affect kinase domain structure and, thus, probably interaction with ponatinib.

Furthermore, SIWA M1 variants were treated with 1 and 2.5 μ M ponatinib for 27 hours. Activation of S6 was decreased at highest ponatinib concentrations in all overexpressing cell models as well as in the controls but to a lesser extent in the FGFR4-KD variant. This suggests functionality of the dominant-negative point mutation as inhibition of FGFR signaling does not show same effects in the FGFR4-KD variant as compared to the other FGFR4 over-expressing cell models, hence pointing towards increased resistance of the kinase dead variant to ponatinib treatment. These results are opposing to the results obtained from cell viability

assays, where we observed that FGFR4-KD cells are rather hypersensitive towards ponatinib. However, it has to be mentioned that cell viability in MTT assays was analyzed following 72h drug incubation, whereas proteins for this Western blot were isolated 27h after treatment. This might suggest that ponatinib acts in a time-dependent manner. Moreover, the dominant negative mutation in the kinase domain can influence binding of ponatinib to *FGFR4*. Since this mutation impairs optimal binding of ponatinib to FGFR4 (data not shown), complex stability might be changed either to a more or a less stable form. This hypothesis is supported by data originating from studies on conformational selectivity of EGFR inhibitors like erlotinib, which proved that erlotinib can bind to the kinase domain of EGFR in its active as well as in its inactive conformation (Park et al. 2012).

FGFR4 activation is essential for processes like cell migration, invasion and EMT

Another aspect of this work was to investigate our cell models for their migratory potential. We assessed the migratory potential of the kinase inactivated variant expressing models of both cell lines BTL1376 and SIWA M1 compared to the respective GFP controls. Strikingly, we saw decreased migratory and invasive capacity in the FGFR4-KD models of either cell line, indicating that FGFR4 activity indeed is essential for migration of tumor cells. Furthermore, migration and invasion assays, as well as a wound healing assays conducted in live cell experiment, proved decreased migratory potential of SIWA M1 and BTL1376 cell lines upon inactivation of FGFR4. Decreased migratory potential as well as impaired wound healing capacity after FGFR4- silencing has already been reported in Nasopharyngeal carcinoma (Shi et al. 2015a).

In confocal fluorescence microscopy images as well as in nuclear and membrane fractions in Western blot we found that nuclear trafficking was impaired in the FGFR4-KD variant. This, together with the dominant-negative kinase function, would also explain the diminished migratory and invasive capacity seen in migration, invasion, and wound healing assays. The latter hypothesis is supported by a study postulating that FGFR1 mediated migration is associated with transport from the membrane to the nucleus upon activation (Turkington et al. 2014). Similar, nuclear localization of EGFR has been associated with enhanced migratory potential and poorer prognosis in ovarian cancer (Xia et al. 2009).

Surprisingly, analyses of the mesenchymal markers *VIM*, *SNAI1* and *CTNNB1* revealed elevated mRNA levels in the FGFR4-KD variant as compared to GFP control in SIWA M1 cell models. As FGFR4 is involved in pathways driving cells into EMT and FGFR4 inactivation resulted in decreased migratory potential we would have expected that kinase inactivation resulted in a more epithelial phenotype. Therefore, high levels of vimentin, as also seen in the KD variant in Western blot analysis, were contradictory to our expectations. Nevertheless, we assume that inactivation of FGFR4 signaling in this cell line might have resulted in compensatory upregulation of other RTKs also explaining high sensitivity to RTKIs in cell viability assays. Furthermore, we saw in flow cytometry that transduction efficiency of the novel generated cell models of SIWA M1 was not always 100%, as the FGFR4-Gly and the -Arg variants might have lost part of their FGFR4 overexpression, what was also seen in Western Blot. As SIWA M1 is assigned to the panel of FGFR4-high cell lines in GBM, it might not even need the altered FGFR4 variant and therefore it might be lost by recombination event. Interestingly, the FGFR4-KD variant was the only FGFR4 modified plasmid, which was 100% stably integrated, although the dominant-negative alteration should be rather negative for the cells. Hence, it might be assumed that integration of the KD variant could have some secondary beneficial effects for cell growth, like for example induction of compensatory upregulation of other RTKs. As EMT is not only induced by FGFR4 signaling but also by other RTKs and TGF β signaling (Gonzalez and Medici 2014), upregulation of other RTKs, compensating for FGFR4 inactivation could result in a more mesenchymal phenotype. However, the FGFR4-KD variant performed worse in migration assays as compared to the GFP control, indicating that FGFR4 activity might still be indispensable for any essential step initiating EMT, or this effect might also be caused by increased sensitivity towards serum starvation or decreased proliferative potential also seen in two- and three-dimensional growth assays. Nevertheless, since our FGFR4 inactivated cell models are impaired in proliferation, they might be switching to a more mesenchymal phenotype by upregulation of other RTKs. Especially IIIc splice variants of other FGFRs have been associated with a more mesenchymal, migratory phenotype (Holzmann et al. 2012). Since only the IIIc variant of FGFR4 exists, a potential switch to the IIIc variants of other FGFRs might be proposed to compensate FGFR4 dysfunction, thereby achieving upregulation of mesenchymal markers. However, these hypotheses need to be dissected by additional experiments.

Another aspect regarding the transfection experiments is that the FGFR4-KD overexpression plasmid additionally contains the SNP coding for glycine at position 388. Since the FGFR4-Gly variant of SIWA M1 cell line appeared to strongly induce mesenchymal markers, we postulate that this might be a protein-dependent phenotype, which is caused by non-kinase rather than kinase-mediated functions of the FGFR4 molecule. Accordingly, overexpression of mesenchymal markers has also been previously detected in U373 FGFR4-Gly, another ectopically overexpressing glioma cell model (data not shown). Interaction of the two different SNP variants of the FGFR4 with members of the extracellular matrix-interacting proteins, including metalloproteases, was already suggested. Facilitated migration and invasion in surrounding tissue by FGFR4 in a kinase-independent fashion has already been reported by Sugiyama et al., who showed that FGFR4 could still interact with MT1-MMP even upon kinase deletion (Nami Sugiyama et al. 2010).

Interestingly, GBM cells expression the FGFR4-Arg variant showed downregulation of all tested mesenchymal markers, indicating that the FGFR4-Arg variant supports a more epithelial phenotype. Since FGFR4-Arg has been associated with increased invasiveness and tumor cell motility in other cancer forms (Bange et al. 2002; S Streit et al. 2006; Peláez-García et al. 2013), this would be a novel and GBM-related finding, which might be specific for neuronal tissues.

Interestingly, knock-down of *FGFR4* in the SIWA M1 FGFR4 overexpressing cell models resulted in decreased mRNA levels of *VIM*, *SNAI1* and *CTNNB1* in case of the FGFR4-Gly variant as well as the FGFR4-KD variants, while it increased mesenchymal marker expression after loss of the FGFR4-Arg variant. Although we saw that SIWA M1 is heterozygous for *G388R*, RFPL data suggested that the FGFR4-Gly variant might be present at a higher copy number in this cell line. Therefore, the effect of knock-down of FGFR4 was presumably predominantly targeting the FGFR4-Gly variant causing obviously downregulation of EMT markers, since FGFR4-Gly variants have been shown to favor a mesenchymal phenotype. These results suggest that, according to our prior hypothesis, the SNP in the transmembrane region of FGFR4 indeed might contribute to epithelial versus mesenchymal differentiation balance by kinase-independent mechanism. Accordingly, *FGFR4* knock-down in the FGFR4-Arg overexpressing cell line resulted in slight upregulation of EMT markers, suggesting that FGFR4-Arg might support a more epithelial differentiation phenotype.

Comparable effects as on EMT marker expression at the mRNA level were found after FGFR4 inactivation as well as knock-down by protein analyses. Inactivation of FGFR4 in the FGFR4-KD model led to increased vimentin expression, which could be attenuated by knock-down of the ectopically overexpressed kinase-dead receptor. This would again strengthen our hypothesis that either ectopically overexpressed inactive FGFR4 resulted in upregulation of other compensatory RTKs favoring a mesenchymal state or that kinase independent mechanisms might support expression of mesenchymal markers probably by vimentin stabilization at the plasma membrane. Regarding the GFP control cell line, stimulation with FGF2 resulted in remarkable increased vimentin expression. Since this effect was attenuated after knock-down of *FGFR4*, this points towards a major role FGFR4 in EMT-driving processes. Increased invasiveness upon MAPK pathway activation via stimulation with FGF2 has been reported in a study on mesothelioma by Schelch *et al.* at our institute (Schelch et al. 2018). Accordingly, in the FGFR4 kinase inactivated model, vimentin expression could not be stimulated by FGF2 upon knock-down of FGFR4. Still, since the stimulatory effect of FGF2 was not present in the kinase inactivated model, we suggest that FGFR4 kinase function is essential for vimentin expression or its stabilization. However, knock-down of *FGFR4* resulted in attenuated vimentin levels in either cell line. Although, based on previous RFLP PCR data, SIWA M1 is heterozygous for *G388R*, expression of the FGFR4-Gly variant showed higher expression levels in this cell line. Therefore, we suppose that knock-down of FGFR4 might have targeted the FGFR4-Gly variant predominantly. Consequently, the decreased expression levels of vimentin and other mesenchymal makers might be caused by shifting to the FGFR4-Arg variant, thus favoring a more epithelial phenotype.

Contrary to SIWA M1 cells, inactivation of FGFR4 in BTL1376 resulted in downregulation of mesenchymal markers *VIM*, *SNAI1* and *CTNNB1*. This suggests that FGFR4 activity is essential to initiate EMT in this cell line. Furthermore, the GS cell line BTL1376 has been shown to be not only high in FGFR4 levels but also high in expression of other RTKs like FGFR1 (data not shown). Therefore, compensation for loss of FGFR4 activity is not as essential in BTL1376 as compared to SIWA M1 because cells can also drive most FGFR4 related pathways via FGFR1. Decreased levels of mesenchymal markers and therefore decreased migratory potential can also be observed in migration and invasion assays. Impaired EMT induction upon knock-down of FGFR4 in nasopharyngeal carcinoma was already reported by Shi *et al.* (Shi et al. 2015a).

6 Conclusion

Taken together, the data elaborated in this master thesis point towards a major role of FGFR4 activity on proliferation, differentiation and migration in a subgroup of gliomas especially concerning three-dimensional growth and invasion, suggesting that targeting FGFR4 in this highly aggressive subgroup of GBM might be a feasible treatment approach.

7 Abstract

Glioblastoma multiforme and gliosarcoma are the most frequent malignant brain tumors in adults accounting for approximately 45%. With a 5-year overall survival rate of <5% despite therapy, alternative therapeutics for GBM and gliosarcoma are urgently needed. Fibroblast growth factor receptors are receptor tyrosine kinases, which have become of major interest for cancer research in the last years. Inhibitors targeting receptor tyrosine kinases or even fibroblast growth factor receptors have successfully been implicated into clinics and are used in cancer therapy. Interestingly, we have identified a subgroup of glioma with Fibroblast growth factor receptor 4 overexpression, suggesting a driving function of the receptor molecule. Therefore, the aim of the study was to further dissect the role of Fibroblast growth factor receptor 4 on tumor aggressiveness.

Glioma cell lines harboring endogenously high Fibroblast growth factor receptor 4 expression levels were used. Additionally, plasmids containing different variants of this receptor had been generated and were stably integrated into the tumor models genomes by retroviral transduction. Besides two SNP variants, which are known to influence tumor aggressiveness in many cancer types, also a dominant negative point mutation in the kinase domain of Fibroblast growth factor receptor 4 was introduced, leading to downregulation of downstream signaling. Therefore, ectopically overexpressing Fibroblast growth factor receptor 4 glioma cell variants were analyzed regarding their tumor aggressiveness using different growth and proliferation assays.

Investigating the role of Fibroblast growth factor receptor 4 activity in glioma cells by comparing the kinase dead cell line to the endogenously high Fibroblast growth factor receptor 4 control cell lines has shown that impaired downstream signaling interferes with proliferation, re-differentiation and invasion. Furthermore, we have shown that activation of Fibroblast growth factor receptor 4 signaling partially drives the cells into epithelial to mesenchymal transition (EMT) state, which plays a role in tumor progression.

Conclusively, our data suggest that Fibroblast growth factor receptor 4 could serve as a promising therapeutic target in glioma and is strongly associated with glioma aggressiveness.

8 Zusammenfassung

Glioblastome und Gliosarkome gehören zu den häufigsten und aggressivsten Gehirntumoren im Erwachsenen. Trotz maximaler Therapieeskalation beträgt die durchschnittliche Lebenserwartung unter 15 Monate. Da die bisher in der Klinik angewendeten Standardtherapiemethoden nur in einer Subgruppe von Patienten den gewünschten Effekt erzielen, ist die Entwicklung neuer Therapieansätze von außerordentlicher Dringlichkeit. Fibroblastische Wachstumsfaktorrezeptoren gehören zur Familie der Rezeptor-Tyrosinkinasen, deren Expression oder Aktivität in Tumoren oft dereguliert sind. Frühere Experimente in unserem Labor konnten nachweisen, dass eine Gruppe von Glioblastomen und Gliosarkomen besonders hohe Expression von fibroblastischem Wachstumsfaktorrezeptor 4 zeigt. Folglich liegt das Ziel dieser Arbeit darin, die Auswirkungen der Überexpression und Aktivität von fibroblastischen Wachstumsfaktorrezeptor 4 auf Wachstums- und Aggressivitätsmerkmale des Glioblastom zu untersuchen.

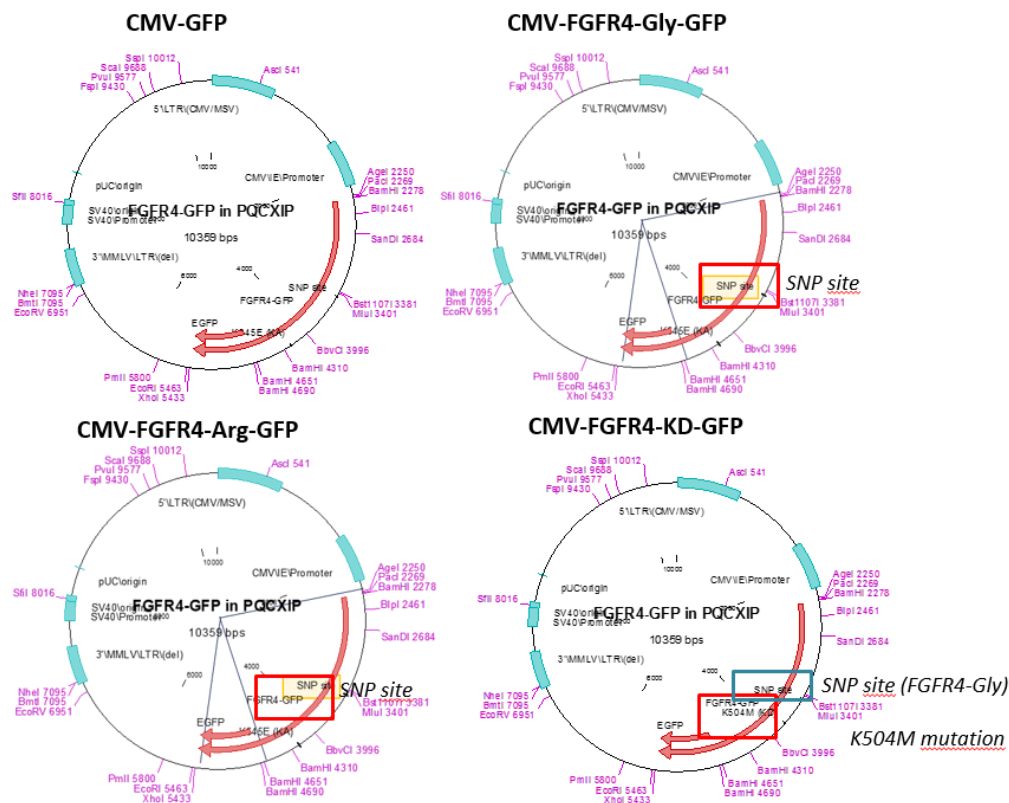
Um die Rolle der Rezeptoraktivität in den basal fibroblastischen Wachstumsfaktorrezeptor 4 überexprimierenden Zelllinien zu prüfen, wurden verschiedene genetisch modifizierte Varianten des Rezeptors stabil in das Genom der Gliomzelllinien eingebracht. Neben einem Einzelnukleotid-Polymorphismus, der bereits in anderen Krebsformen mit erhöhter Aggressivität in Verbindung gebracht wurde, wurde auch eine Kinase-inaktivierte und somit dominant-negativ wirkende Variante von fibroblastischen Wachstumsfaktorrezeptor 4 exprimiert.

Inaktivierung der Kinase Domäne hatte signifikant hemmende Effekte auf das aggressive Verhalten der Krebszellen hinsichtlich zwei- und dreidimensionalen Wachstum, Differenzierung und Migration sowie Tumorigenität *in vivo*. Des Weiteren konnte gezeigt werden, dass die Aktivität von fibroblastischem Wachstumsfaktorrezeptor 4 Auswirkungen auf den Phänotyp der Zellen hat. Ein regulierender Einfluss auf den Prozess der epithelialen zur mesenchymalen Transition wurde als zugrunde liegender Mechanismus nachgewiesen.

Zusammenfassend weisen die Ergebnisse dieser Arbeit fibroblastischem Wachstumsfaktorrezeptor 4 als einen wichtigen Regulator der Aggressivität einer Subgruppe von in Gliomen aus. Dessen Inhibierung stellt somit eine neue, vielversprechende Möglichkeit in der Glioblastom Therapie dar.

9 Appendix

As already mentioned, four different variants of genetically altered *FGFR4* variants had been used. However, the KA form was not efficiently integrated in the used cell models, therefore the thesis focused on the two different SNP variants as well as on the *FGFR4*-KD model, carrying a point mutation (K504M), leading to a dominant negative loss of function mutation in the kinase domain. The four genetically modified *FGFR4* variants had been cloned using In-fusion cloning (Takarabio, Kusatsu, Japan) into a pQCXIP (Addgene, Watertown, Massachusetts, USA) retroviral backbone. Thereby, *FGFR4* gene was fused to the CMV promoter as well as to the green fluorescent protein (GFP) reporter in such a way that the start and stop codon of the target gene was removed. Therefore, the CMV-*FGFR4*-GFP is in one reading frame. Characteristically, this plasmid harbors a cytomegalovirus (CMV) promoter leading to strong ubiquitous expression of the altered *FGFR4* gene. In addition, pQCXIP harbors an ampicillin bacterial resistance cassette as well as a puromycin (**Figure 16**) selectable marker allowing selection for cells with a stably integrated *FGFR4* variant in their genomes. Retroviral plasmids of the respective *FGFR4* variants as well as GFP control are depicted below.



10 Abbreviations

ALT	<i>Alternative lengthening of telomeres</i>
AP2	<i>Activating protein 2</i>
APS	<i>Ammoniumperoxidesulfate</i>
BA	<i>Bile acid</i>
Bcl-2	<i>B-cell lymphoma 2</i>
bFGF	<i>basic FGF</i>
BSA	<i>Bovine serum albumine</i>
CLSM	<i>Confocal laser scanning microscopy</i>
CMV	<i>Cytomegalovirus</i>
CNS	<i>Central nervous system</i>
CP	<i>Cytoplasm</i>
CTLA-4	<i>Cytotoxic T- Lymphocyte associated protein 4</i>
CTNNB1	<i>β-catenin</i>
DAPI	<i>4', 6-Diamidin-2-phenylindol</i>
DMSO	<i>Dimethylsulfoxide</i>
DTT	<i>Dithiothreitol</i>
ECM	<i>Extracellular matrix</i>
EDTA	<i>ethylenediaminetetraacetic acid</i>
EGF	<i>Epidermal growth factor</i>
EGFR	<i>Epidermal growth factor receptor</i>

EMT	<i>Epithelial to mesenchymal transition</i>
EndEMT	<i>Endothelial to mesenchymal transition</i>
env	<i>Envelope (retroviral scaffold proteins)</i>
FACS	<i>Fluorescence-activated cell sorting</i>
FBS	<i>Fetal bovine serum</i>
FGF	<i>Fibroblast growth factor</i>
FGFR	<i>Fibroblast growth factor receptor</i>
FGFR4-Arg	<i>FGFR4 with arginine at position 388</i>
FGFR4-Gly	<i>FGFR4 with glycine at position 388</i>
FGFR4-KD	<i>FGFR4 with loss of function mutation in kinase domain</i>
FITC	<i>fluorescein-5-isothiocyanat</i>
S.D.	<i>Standard Deviation</i>
FRS2α	<i>FGFR substrate 2α</i>
G388R	<i>Glycine changed to Arginine at position 388</i>
Gag	<i>Groups specific antigen for retroviral particles</i>
GAPDH	<i>Glyceraldehyde-3-phosphatedehydrogenase</i>
GBM	<i>Glioblastoma multiforme</i>
GCF	<i>GC factor</i>
GFP	<i>Green fluorescent protein</i>
GS	<i>Gliosarcoma</i>
GSK3β	<i>Glycogen synthase kinase 3</i>

HBS	<i>HEPES buffered saline</i>
HGG	<i>High grade glioma</i>
HRP	<i>horseradish peroxidase</i>
IDH1/2	<i>Isocitrate dehydrogenase 1/2</i>
Ig	<i>Immunoglobulin</i>
KLB	<i>Klotho beta</i>
LGG	<i>Low grade glioma</i>
MAPK	<i>Mitogen activated protein kinase</i>
MGMT	<i>O⁶-Methylguanin-DNA-Methyltransferase</i>
MHC	<i>Major histocompatibility complex</i>
MMP	<i>Matrix Metalloprotease</i>
MT1-MMP	<i>Membrane type 1 Metalloprotease</i>
NADH	<i>Nicotinamideadeninedinukleotide</i>
Nav	<i>voltage gated sodium channel</i>
NB+	<i>Neurobasal</i>
N-CAM	<i>Neural cell adhesion molecule</i>
Nuc	<i>Nucleus</i>
PBS	<i>Phosphate buffered saline</i>
PCR	<i>Polymerase chain reaction</i>
PD1	<i>Programed cell death protein -1</i>
PDGF	<i>Platelet derived growth factor</i>
PDGFR	<i>Platelet derived growth factor receptor</i>

PET	<i>Polyethylene terephthalate</i>
PFA	<i>Paraformaldehyde</i>
PI3K	<i>PI-3-Kinase</i>
PLCy	<i>Phospholipase Cy</i>
PMSF	<i>Phenylmethylsulfonylfluoride</i>
Pol	<i>Polymerase (retroviral)</i>
PVDF	<i>polyvinylidenfluorid</i>
RFLP	<i>Restriction fragment length polymorphism</i>
RISC	<i>RNA induced silencing complex</i>
RNAi	<i>RNA interference</i>
RPL41	<i>Ribosomal protein L41</i>
RTK	<i>Receptor tyrosine kinases</i>
RTKI	<i>Receptor tyrosine kinase inhibitors</i>
s.c.	<i>Sub- cutaneous</i>
SCID	<i>Severe combined immunodeficiency</i>
Scr	<i>scrambled</i>
SDS	<i>Sodium dodecyl sulfate</i>
SEM	<i>Standard error of the mean</i>
Sf	<i>Serum-free</i>
SH2 domain	<i>Src homology-2</i>
siRNA	<i>Small interfering RNA</i>
SNAI1	<i>Snail</i>

SNP	<i>Single nucleotide polymorphism</i>
Sp1	<i>specify protein 1</i>
STAT	<i>Signal transducer and activator of transcription</i>
TACC	<i>Transforming acidic coiled coil</i>
TCA	<i>Tricarboxylic acid</i>
TEMED	<i>Tetramethylenediamine</i>
TERT	<i>Telomerase reverse transcriptase</i>
TGFα	<i>Transforming growth factor α</i>
TMZ	<i>Temozolomide</i>
Tot.prot	<i>Total protein extracts</i>
Tris	<i>Tris(hydroxymethyl)-aminomethane</i>
TSP	<i>Transcription start point</i>
VEGF	<i>Vascular endothelial growth factor</i>
VIM	<i>Vimentin</i>
VEGFR	<i>Vascular endothelial growth factor receptor</i>
WGA	<i>Wheat germ agglutinine</i>
WHO	<i>World health organization</i>

11 Bibliography

- "001303 - NOD.CB17-Prkdc/J." n.d. Accessed December 9, 2019.
<https://www.jax.org/strain/001303>.
- Ahmad, Imran, Tomoko Iwata, and Hing Y. Leung. 2012. "Mechanisms of FGFR-Mediated Carcinogenesis." *Biochimica et Biophysica Acta (BBA) - Molecular Cell Research* 1823 (4):850–60. <https://doi.org/10.1016/j.bbamcr.2012.01.004>.
- Ansell, Anna, Lovisa Farnebo, Reidar Grénman, Karin Roberg, and Lena K Thunell. 2009. "Polymorphism of FGFR4 in Cancer Development and Sensitivity to Cisplatin and Radiation in Head and Neck Cancer." *Oral Oncology* 45 (1). Pergamon:23–29. <https://doi.org/10.1016/J.ORALONCOLOGY.2008.03.007>.
- Arora, Amit, and Eric M Scholar. 2005. "Role of Tyrosine Kinase Inhibitors in Cancer Therapy." *The Journal of Pharmacology and Experimental Therapeutics* 315 (3). American Society for Pharmacology and Experimental Therapeutics:971–79. <https://doi.org/10.1124/jpet.105.084145>.
- Arrieta, Víctor A., Fabio Iwamoto, and Rimas Lukas. 2019. "Can Patient Selection and Neoadjuvant Administration Resuscitate PD-1 Inhibitors for Glioblastoma?" *Journal of Neurosurgery*.
<https://doi.org/https://doi.org/10.3171/2019.9.JNS192523>.
- Auciello, Giulio, Debbie L Cunningham, Tulin Tatar, John K Heath, and Joshua Z Rappoport. 2013. "Regulation of Fibroblast Growth Factor Receptor Signalling and Trafficking by Src and Eps8." *Journal of Cell Science* 126 (Pt 2). Company of Biologists:613–24. <https://doi.org/10.1242/jcs.116228>.
- Baird, A., and P. Böhlen. 1991. "Fibroblast Growth Factors." In *Peptide Growth Factors and Their Receptors I*, 369–418. New York, NY: Springer New York.
https://doi.org/10.1007/978-1-4612-3210-0_7.
- Bange, Johannes, Dieter Prechtel, Yuri Cheburkin, Katja Specht, Nadia Harbeck, Manfred Schmitt, Tatjana Knyazeva, et al. 2002. "Cancer Progression and Tumor Cell Motility Are Associated with the FGFR4 Arg(388) Allele." *Cancer Research* 62 (3). American Association for Cancer Research:840–47.
<http://www.ncbi.nlm.nih.gov/pubmed/11830541>.
- Barriere, Guislaine, Pietro Fici, Giulia Gallerani, Francesco Fabbri, and Michel Rigaud. 2015. "Epithelial Mesenchymal Transition: A Double-Edged Sword." *Clinical and Translational Medicine* 4. Springer:14.
<https://doi.org/10.1186/s40169-015-0055-4>.
- Batchelor, Tracy T., A. Gregory Sorensen, Emmanuelle di Tomaso, Wei-Ting Zhang, Dan G. Duda, Kenneth S. Cohen, Kevin R. Kozak, et al. 2007. "AZD2171, a Pan-VEGF Receptor Tyrosine Kinase Inhibitor, Normalizes Tumor Vasculature and Alleviates Edema in Glioblastoma Patients." *Cancer Cell* 11 (1). Cell Press:83–95. <https://doi.org/10.1016/J.CCR.2006.11.021>.
- Bennasroune, Amar, Anne Gardin, Dominique Aunis, Gérard Crémel, and Pierre Hubert. 2004. "Tyrosine Kinase Receptors as Attractive Targets of Cancer Therapy." *Critical Reviews in Oncology/Hematology* 50 (1). Elsevier:23–38.
<https://doi.org/10.1016/J.CRITREVONC.2003.08.004>.
- Bray, Freddie, Jacques Ferlay, Isabelle Soerjomataram, Rebecca L. Siegel, Lindsey

- A. Torre, and Ahmedin Jemal. 2018. "Global Cancer Statistics 2018: GLOBOCAN Estimates of Incidence and Mortality Worldwide for 36 Cancers in 185 Countries." *CA: A Cancer Journal for Clinicians* 68 (6):394–424. <https://doi.org/10.3322/caac.21492>.
- Brewer, J Richard, Pierre Mazot, and Philippe Soriano. 2016. "Genetic Insights into the Mechanisms of Fgf Signaling." *Genes & Development* 30 (7). Cold Spring Harbor Laboratory Press:751–71. <https://doi.org/10.1101/gad.277137.115>.
- Buckingham, Margaret, and Didier Montarras. 2008. "Skeletal Muscle Stem Cells." *Current Opinion in Genetics & Development* 18 (4). Elsevier Current Trends:330–36. <https://doi.org/10.1016/J.GDE.2008.06.005>.
- Butti, Ramesh, Sumit Das, Vinoth Prasanna Gunasekaran, Amit Singh Yadav, Dhiraj Kumar, and Gopal C Kundu. 2018. "Receptor Tyrosine Kinases (RTKs) in Breast Cancer: Signaling, Therapeutic Implications and Challenges." *Molecular Cancer* 17 (1). BioMed Central:34. <https://doi.org/10.1186/s12943-018-0797-x>.
- Casaleto, Jessica B., and Andrea I. McClatchey. 2012. "Spatial Regulation of Receptor Tyrosine Kinases in Development and Cancer." *Nature Reviews Cancer* 12 (6). Nature Publishing Group:387–400. <https://doi.org/10.1038/nrc3277>.
- Chae, Young Kwang, Keerthi Ranganath, Peter S Hammerman, Christos Vaklavas, Nisha Mohindra, Aparna Kalyan, Maria Matsangou, et al. 2017. "Inhibition of the Fibroblast Growth Factor Receptor (FGFR) Pathway: The Current Landscape and Barriers to Clinical Application." *Oncotarget* 8 (9). Impact Journals, LLC:16052–74. <https://doi.org/10.18632/oncotarget.14109>.
- Cloughesy, Timothy F., Aaron Y. Mochizuki, Joey R. Orpilla, Willy Hugo, Alexander H. Lee, Tom B. Davidson, Anthony C. Wang, et al. 2019. "Neoadjuvant Anti-PD-1 Immunotherapy Promotes a Survival Benefit with Intratumoral and Systemic Immune Responses in Recurrent Glioblastoma." *Nature Medicine* 25 (3). NIH Public Access:477. <https://doi.org/10.1038/S41591-018-0337-7>.
- Cohen, Adam L., Sheri L. Holmen, and Howard Colman. 2013. "IDH1 and IDH2 Mutations in Gliomas." *Current Neurology and Neuroscience Reports* 13 (5). Current Science Inc.:345. <https://doi.org/10.1007/s11910-013-0345-4>.
- Corn, P. G., F. Wang, W. L. McKeenan, and N. Navone. 2013. "Targeting Fibroblast Growth Factor Pathways in Prostate Cancer." *Clinical Cancer Research* 19 (21). American Association for Cancer Research:5856–66. <https://doi.org/10.1158/1078-0432.CCR-13-1550>.
- Costa Andrade, Valéria Cristina da, Orlando Parise, Cora Pereira Hors, Poliana Cristina de Melo Martins, Alexandre Pacheco Silva, and Bernardo Garicochea. 2007. "The Fibroblast Growth Factor Receptor 4 (FGFR4) Arg388 Allele Correlates with Survival in Head and Neck Squamous Cell Carcinoma." *Experimental and Molecular Pathology* 82 (1). Academic Press:53–57. <https://doi.org/10.1016/J.YEXMP.2006.05.003>.
- Craene, Bram De, and Geert Berx. 2013. "Regulatory Networks Defining EMT during Cancer Initiation and Progression." *Nature Reviews Cancer* 13 (2). Nature Publishing Group:97–110. <https://doi.org/10.1038/nrc3447>.
- Croze, L. E. S., K. T. Etheridge, C. Chen, B. Belyea, L. J. Talbot, R. C. Bentley, and C. M. Linardic. 2012. "FGFR4 Blockade Exerts Distinct Antitumorigenic Effects in

- Human Embryonal versus Alveolar Rhabdomyosarcoma." *Clinical Cancer Research* 18 (14):3780–90. <https://doi.org/10.1158/1078-0432.CCR-10-3063>.
- Cross, M J, and L Claesson-Welsh. 2001. "FGF and VEGF Function in Angiogenesis: Signalling Pathways, Biological Responses and Therapeutic Inhibition." *Trends in Pharmacological Sciences* 22 (4). Elsevier:201–7. [https://doi.org/10.1016/s0165-6147\(00\)01676-x](https://doi.org/10.1016/s0165-6147(00)01676-x).
- Custer, R P, G C Bosma, and M J Bosma. 1985. "Severe Combined Immunodeficiency (SCID) in the Mouse. Pathology, Reconstitution, Neoplasms." *The American Journal of Pathology* 120 (3). American Society for Investigative Pathology:464–77. <http://www.ncbi.nlm.nih.gov/pubmed/2412448>.
- Dagenais, Gilles R, Darryl P Leong, Sumathy Rangarajan, Fernando Lanás, Patricio Lopez-Jaramillo, Rajeev Gupta, Rafael Diaz, et al. 2019. "Variations in Common Diseases, Hospital Admissions, and Deaths in Middle-Aged Adults in 21 Countries from Five Continents (PURE): A Prospective Cohort Study." *Lancet (London, England)* 0 (0). Elsevier. [https://doi.org/10.1016/S0140-6736\(19\)32007-0](https://doi.org/10.1016/S0140-6736(19)32007-0).
- Deb, T B, L Su, L Wong, E Bonvini, A Wells, M David, and G R Johnson. 2001. "Epidermal Growth Factor (EGF) Receptor Kinase-Independent Signaling by EGF." *The Journal of Biological Chemistry* 276 (18). American Society for Biochemistry and Molecular Biology:15554–60. <https://doi.org/10.1074/jbc.M100928200>.
- DeVita, V., T. Lawrence, and Steven A Rosenberg. n.d. "Hallmarks of Cancer: An Organizing Principle for Cancer Medicine - DeVita, Hellman, and Rosenberg's Cancer: Principles & Practice of Oncology (Cancer: Principles & Practice (DeVita)(Single Vol.)) 10 Ed." Accessed December 8, 2019. <https://doctorlib.info/oncology/cancer-principles-practice-oncology/2.html>.
- Dine, Jennifer, RuthAnn Gordon, Yelena Shames, Mary Kate Kasler, and Margaret Barton-Burke. 2017. "Immune Checkpoint Inhibitors: An Innovation in Immunotherapy for the Treatment and Management of Patients with Cancer." *Asia-Pacific Journal of Oncology Nursing* 4 (2). Wolters Kluwer -- Medknow Publications:127. https://doi.org/10.4103/APJON.APJON_4_17.
- Dole, M, G Nuñez, A K Merchant, J Maybaum, C K Rode, C A Bloch, and V P Castle. 1994. "Bcl-2 Inhibits Chemotherapy-Induced Apoptosis in Neuroblastoma." *Cancer Research* 54 (12). American Association for Cancer Research:3253–59. <http://www.ncbi.nlm.nih.gov/pubmed/8205548>.
- Dongre, Anushka, and Robert A. Weinberg. 2019. "New Insights into the Mechanisms of Epithelial–mesenchymal Transition and Implications for Cancer." *Nature Reviews Molecular Cell Biology* 20 (2). Nature Publishing Group:69–84. <https://doi.org/10.1038/s41580-018-0080-4>.
- Dougan, Michael, and Glenn Dranoff. 2009. "Immune Therapy for Cancer." *Annual Review of Immunology* 27 (1). Annual Reviews :83–117. <https://doi.org/10.1146/annurev.immunol.021908.132544>.
- Eswarakumar, V.P., I. Lax, and J. Schlessinger. 2005. "Cellular Signaling by Fibroblast Growth Factor Receptors." *Cytokine & Growth Factor Reviews* 16 (2). Pergamon:139–49. <https://doi.org/10.1016/J.CYTOGFR.2005.01.001>.
- Falvella, Felicia S., Elisa Frullanti, Antonella Galvan, Monica Spinola, Sara Noci,

- Loris De Cecco, Mario Nosotti, et al. 2009. "FGFR4 Gly388Arg Polymorphism May Affect the Clinical Stage of Patients with Lung Cancer by Modulating the Transcriptional Profile of Normal Lung." *International Journal of Cancer* 124 (12). John Wiley & Sons, Ltd:2880–85. <https://doi.org/10.1002/ijc.24302>.
- "Figure 1: [Structures of MTT and Colored Formazan Product.]" 2016, July. Eli Lilly & Company and the National Center for Advancing Translational Sciences. <https://www.ncbi.nlm.nih.gov/books/NBK144065/figure/mttassays.F1/>.
- French, Dorothy M., Benjamin C. Lin, Manping Wang, Camellia Adams, Theresa Shek, Kathy Hötzel, Brad Bolon, et al. 2012. "Targeting FGFR4 Inhibits Hepatocellular Carcinoma in Preclinical Mouse Models." Edited by Maria G. Castro. *PLoS ONE* 7 (5). Public Library of Science:e36713. <https://doi.org/10.1371/journal.pone.0036713>.
- Fulda, Simone. 2010. "Evasion of Apoptosis as a Cellular Stress Response in Cancer." *International Journal of Cell Biology* 2010 (February). Hindawi:370835. <https://doi.org/10.1155/2010/370835>.
- Garrett, Michelle D., and Ian Collins. 2011. "Anticancer Therapy with Checkpoint Inhibitors: What, Where and When?" *Trends in Pharmacological Sciences* 32 (5). Elsevier Current Trends:308–16. <https://doi.org/10.1016/J.TIPS.2011.02.014>.
- Gauglhofer, Christine, Jakob Paur, Waltraud C. Schrottmaier, Bettina Winkelhofer, Daniela Huber, Isabelle Naegelen, Christine Pirker, et al. 2014. "Fibroblast Growth Factor Receptor 4: A Putative Key Driver for the Aggressive Phenotype of Hepatocellular Carcinoma." *Carcinogenesis* 35 (10):2331–38. <https://doi.org/10.1093/carcin/bgu151>.
- Ge, Hongfei, Jun Zhang, Yan Gong, Jamila Gupte, Jay Ye, Jennifer Weiszmann, Kim Samayoa, et al. 2014. "Fibroblast Growth Factor Receptor 4 (FGFR4) Deficiency Improves Insulin Resistance and Glucose Metabolism under Diet-Induced Obesity Conditions." *The Journal of Biological Chemistry* 289 (44). American Society for Biochemistry and Molecular Biology:30470–80. <https://doi.org/10.1074/jbc.M114.592022>.
- Giannelli, Gianluigi, Petra Koudelkova, Francesco Dituri, and Wolfgang Mikulits. 2016. "Role of Epithelial to Mesenchymal Transition in Hepatocellular Carcinoma." *Journal of Hepatology* 65 (4). Elsevier:798–808. <https://doi.org/10.1016/J.JHEP.2016.05.007>.
- Gnatenko, D. A., E. P. Kopantsev, and E. D. Sverdlov. 2017. "The Role of the Signaling Pathway FGF/FGFR in Pancreatic Cancer." *Biochemistry (Moscow), Supplement Series B: Biomedical Chemistry* 11 (2). Pleiades Publishing:101–10. <https://doi.org/10.1134/S1990750817020032>.
- Gonzalez, David M, and Damian Medici. 2014. "Signaling Mechanisms of the Epithelial-Mesenchymal Transition." *Science Signaling* 7 (344). NIH Public Access:re8. <https://doi.org/10.1126/scisignal.2005189>.
- Goodenberger, McKinsey L., and Robert B. Jenkins. 2012. "Genetics of Adult Glioma." *Cancer Genetics* 205 (12). Elsevier:613–21. <https://doi.org/10.1016/J.CANCERGEN.2012.10.009>.
- Grabner, Alexander, Karla Schramm, Neerupma Silswal, Matt Hendrix, Christopher Yanucil, Brian Czaya, Saurav Singh, et al. 2017. "FGF23/FGFR4-Mediated Left Ventricular Hypertrophy Is Reversible." *Scientific Reports* 7 (1). Nature

- Publishing Group:1993. <https://doi.org/10.1038/s41598-017-02068-6>.
- Gschwind, Andreas, Oliver M. Fischer, and Axel Ullrich. 2004. "The Discovery of Receptor Tyrosine Kinases: Targets for Cancer Therapy." *Nature Reviews Cancer* 4 (5). Nature Publishing Group:361–70. <https://doi.org/10.1038/nrc1360>.
- Hagel, M., C. Miduturu, M. Sheets, N. Rubin, W. Weng, N. Stransky, N. Bifulco, et al. 2015. "First Selective Small Molecule Inhibitor of FGFR4 for the Treatment of Hepatocellular Carcinomas with an Activated FGFR4 Signaling Pathway." *Cancer Discovery* 5 (4). American Association for Cancer Research:424–37. <https://doi.org/10.1158/2159-8290.CD-14-1029>.
- Hanahan, D, and R A Weinberg. 2000. "The Hallmarks of Cancer." *Cell* 100 (1). Elsevier:57–70. [https://doi.org/10.1016/s0092-8674\(00\)81683-9](https://doi.org/10.1016/s0092-8674(00)81683-9).
- Hanahan, Douglas, and Robert A. Weinberg. 2011. "Hallmarks of Cancer: The Next Generation." *Cell* 144 (5). Cell Press:646–74. <https://doi.org/10.1016/J.CELL.2011.02.013>.
- Hardham, Adrienne R. 2012. "Confocal Microscopy in Plant–Pathogen Interactions." In , 295–309. https://doi.org/10.1007/978-1-61779-501-5_18.
- Harris, Philip A., J.E. Campbell, C. Cano, and K.W. Duncan. 2018. "Inhibitors of the Fibroblast Growth Factor Receptor." In *Cancer II*, edited by Michael J. Waring. Springer. [https://books.google.at/books?id=NkKFDwAAQBAJ&pg=PA176&dq=Overexpression+of+FGFR4+in+prostate,+colon,+liver+cancer+and+rhabdomyosarcoma&hl=de&sa=X&ved=0ahUKEwjYgm1zavmAhXTw8QBHZ_LCJcQ6AEIKTAA#v=onepage&q=Overexpression of FGFR4 in prostate%20c.](https://books.google.at/books?id=NkKFDwAAQBAJ&pg=PA176&dq=Overexpression+of+FGFR4+in+prostate,+colon,+liver+cancer+and+rhabdomyosarcoma&hl=de&sa=X&ved=0ahUKEwjYgm1zavmAhXTw8QBHZ_LCJcQ6AEIKTAA#v=onepage&q=Overexpression%20of%20FGFR4%20in%20prostate%20cancer)
- Haugsten, Ellen Margrethe, Vigdis Sørensen, Michaela Kunova Bosakova, Gustavo Antonio de Souza, Pavel Krejci, Antoni Wiedlocha, and Jørgen Wesche. 2016. "Proximity Labeling Reveals Molecular Determinants of FGFR4 Endosomal Transport." *Journal of Proteome Research* 15 (10). American Chemical Society:3841–55. <https://doi.org/10.1021/acs.jproteome.6b00652>.
- Heinzle, Christine, Zeynep Erdem, Jakob Paur, Bettina Grasl-Kraupp, Klaus Holzmann, Michael Grusch, Walter Berger, and Brigitte Marian. 2014. "Is Fibroblast Growth Factor Receptor 4 a Suitable Target of Cancer Therapy?" *Current Pharmaceutical Design* 20 (17):2881–98. <http://www.ncbi.nlm.nih.gov/pubmed/23944363>.
- Heston, W E. 1965. "Genetic Factors in the Etiology of Cancer." *Cancer Research* 25 (8). American Association for Cancer Research:1320–26. <http://www.ncbi.nlm.nih.gov/pubmed/5320519>.
- Hirose, Y, M S Berger, and R O Pieper. 2001. "p53 Effects Both the Duration of G2/M Arrest and the Fate of Temozolomide-Treated Human Glioblastoma Cells." *Cancer Research* 61 (5). American Association for Cancer Research:1957–63. <http://www.ncbi.nlm.nih.gov/pubmed/11280752>.
- Holland, E C. 2000. "Glioblastoma Multiforme: The Terminator." *Proceedings of the National Academy of Sciences of the United States of America* 97 (12). National Academy of Sciences:6242–44. <https://doi.org/10.1073/pnas.97.12.6242>.
- Holzmann, Klaus, Thomas Grunt, Christine Heinzle, Sandra Sampl, Heinrich Steinhoff, Nicole Reichmann, Miriam Kleiter, Marlene Hauck, and Brigitte Marian.

2012. "Alternative Splicing of Fibroblast Growth Factor Receptor IgIII Loops in Cancer." *Journal of Nucleic Acids* 2012 (December). Hindawi:950508. <https://doi.org/10.1155/2012/950508>.
- Houillier, C., X. Wang, G. Kaloshi, K. Mokhtari, R. Guillemin, J. Laffaire, S. Paris, et al. 2010. "IDH1 or IDH2 Mutations Predict Longer Survival and Response to Temozolomide in Low-Grade Gliomas." *Neurology* 75 (17):1560–66. <https://doi.org/10.1212/WNL.0b013e3181f96282>.
- Huang, X., C. Yang, Y. Luo, C. Jin, F. Wang, and W. L. McKeenan. 2007. "FGFR4 Prevents Hyperlipidemia and Insulin Resistance but Underlies High-Fat Diet Induced Fatty Liver." *Diabetes* 56 (10):2501–10. <https://doi.org/10.2337/db07-0648>.
- Ichimura, Koichi, Danita M. Pearson, Sylvia Kocialkowski, L. Magnus B. cklund, Raymond Chan, David T.W. Jones, and V. Peter Collins. 2009. "IDH1 Mutations Are Present in the Majority of Common Adult Gliomas but Rare in Primary Glioblastomas." *Neuro-Oncology* 11 (4):341–47. <https://doi.org/10.1215/15228517-2009-025>.
- Inagaki, Takeshi, Mihwa Choi, Antonio Moschetta, Li Peng, Carolyn L. Cummins, Jeffrey G. McDonald, Guizhen Luo, et al. 2005. "Fibroblast Growth Factor 15 Functions as an Enterohepatic Signal to Regulate Bile Acid Homeostasis." *Cell Metabolism* 2 (4). Cell Press:217–25. <https://doi.org/10.1016/J.CMET.2005.09.001>.
- Itoh, Nobuyuki, Hiroya Ohta, and Morichika Konishi. 2015. "Endocrine FGFs: Evolution, Physiology, Pathophysiology, and Pharmacotherapy." *Frontiers in Endocrinology* 6. Frontiers Media SA:154. <https://doi.org/10.3389/fendo.2015.00154>.
- Johnson, Douglas B., Matthew J. Rioth, and Leora Horn. 2014. "Immune Checkpoint Inhibitors in NSCLC." *Current Treatment Options in Oncology* 15 (4). Springer US:658–69. <https://doi.org/10.1007/s11864-014-0305-5>.
- Kalinina, Juliya, Kaushik Dutta, Dariush Ilghari, Andrew Beenken, Regina Goetz, Anna V Eliseenkova, David Cowburn, and Moosa Mohammadi. 2012. "The Alternatively Spliced Acid Box Region Plays a Key Role in FGF Receptor Autoinhibition." *Structure (London, England : 1993)* 20 (1). NIH Public Access:77–88. <https://doi.org/10.1016/j.str.2011.10.022>.
- Kalluri, Raghu, and Robert A Weinberg. 2009. "The Basics of Epithelial-Mesenchymal Transition." *The Journal of Clinical Investigation* 119 (6). American Society for Clinical Investigation:1420–28. <https://doi.org/10.1172/JCI39104>.
- Kessenbrock, Kai, Vicki Plaks, and Zena Werb. 2010. "Matrix Metalloproteinases: Regulators of the Tumor Microenvironment." *Cell* 141 (1). NIH Public Access:52–67. <https://doi.org/10.1016/j.cell.2010.03.015>.
- Kim, Do Hyung, Tiaosi Xing, Zhibin Yang, Ronald Dudek, Qun Lu, and Yan-Hua Chen. 2017. "Epithelial Mesenchymal Transition in Embryonic Development, Tissue Repair and Cancer: A Comprehensive Overview." *Journal of Clinical Medicine* 7 (1). Multidisciplinary Digital Publishing Institute (MDPI). <https://doi.org/10.3390/jcm7010001>.
- Kirschbaum, Katja, Martin Kriebel, Eva Ursula Kranz, Oliver Pötz, and Hansjürgen Volkmer. 2009. "Analysis of Non-Canonical Fibroblast Growth Factor Receptor 1

- (FGFR1) Interaction Reveals Regulatory and Activating Domains of Neurofascin." *The Journal of Biological Chemistry* 284 (42). American Society for Biochemistry and Molecular Biology:28533–42. <https://doi.org/10.1074/jbc.M109.004440>.
- Korhonen, J, J Partanen, and K Alitalo. 2002. "Expression of FGFR-4 mRNA in Developing Mouse Tissues." *International Journal of Developmental Biology* 36 (2). UPV/EHU Press:323–29. <https://doi.org/10.1387/IJDB.1326315>.
- Kostrzewa, Markus, and Ulrich Müller. 1998. "Genomic Structure and Complete Sequence of the Human FGFR4 Gene." *Mammalian Genome* 9 (2). Springer-Verlag:131–35. <https://doi.org/10.1007/s003359900703>.
- Kovacic, Jason C, Nadia Mercader, Miguel Torres, Manfred Boehm, and Valentin Fuster. 2012. "Epithelial-to-Mesenchymal and Endothelial-to-Mesenchymal Transition: From Cardiovascular Development to Disease." *Circulation* 125 (14):1795–1808. <https://doi.org/10.1161/CIRCULATIONAHA.111.040352>.
- Krex, D., B. Klink, C. Hartmann, A. von Deimling, T. Pietsch, M. Simon, M. Sabel, et al. 2007. "Long-Term Survival with Glioblastoma Multiforme." *Brain* 130 (10). Narnia:2596–2606. <https://doi.org/10.1093/brain/awm204>.
- Lan, Aiping, Yongfen Qi, and Jie Du. 2014. "Akt2 Mediates TGF- β 1-Induced Epithelial to Mesenchymal Transition by Deactivating GSK3 β /Snail Signaling Pathway in Renal Tubular Epithelial Cells." *Cellular Physiology and Biochemistry* 34 (2):368–82. <https://doi.org/10.1159/000363006>.
- Lang, Liwei, and Yong Teng. 2019. "Fibroblast Growth Factor Receptor 4 Targeting in Cancer: New Insights into Mechanisms and Therapeutic Strategies." *Cells* 8 (1). Multidisciplinary Digital Publishing Institute (MDPI). <https://doi.org/10.3390/cells8010031>.
- Lemmon, Mark A., and Joseph Schlessinger. 2010. "Cell Signaling by Receptor Tyrosine Kinases." *Cell* 141 (7). Cell Press:1117–34. <https://doi.org/10.1016/J.CELL.2010.06.011>.
- Levine, Beth, Sangita Sinha, and Guido Kroemer. 2008. "Bcl-2 Family Members: Dual Regulators of Apoptosis and Autophagy." *Autophagy* 4 (5). NIH Public Access:600–606. <http://www.ncbi.nlm.nih.gov/pubmed/18497563>.
- Levitzki, Alexander, and Aviv Gazit. n.d. "Tyrosine Kinase Inhibition: An Approach to Drug Development." *Science*. American Association for the Advancement of Science. Accessed December 11, 2019. <https://doi.org/10.2307/2886333>.
- Li, Hailong, Jiye Li, Gang Cheng, Jianning Zhang, and Xuezhen Li. 2016. "IDH Mutation and MGMT Promoter Methylation Are Associated with the Pseudoprogression and Improved Prognosis of Glioblastoma Multiforme Patients Who Have Undergone Concurrent and Adjuvant Temozolomide-Based Chemoradiotherapy." *Clinical Neurology and Neurosurgery* 151 (December). Elsevier:31–36. <https://doi.org/10.1016/J.CLINEURO.2016.10.004>.
- Li, Samuel Q, Adam T Cheuk, Jack F Shern, Young K Song, Laura Hurd, Hongling Liao, Jun S Wei, and Javed Khan. 2013. "Targeting Wild-Type and Mutationally Activated FGFR4 in Rhabdomyosarcoma with the Inhibitor Ponatinib (AP24534)." *PloS One* 8 (10). Public Library of Science:e76551. <https://doi.org/10.1371/journal.pone.0076551>.
- Liu, R., J. Li, K. Xie, T. Zhang, Y. Lei, Y. Chen, L. Zhang, et al. 2013. "FGFR4

- Promotes Stroma-Induced Epithelial-to-Mesenchymal Transition in Colorectal Cancer." *Cancer Research* 73 (19). American Association for Cancer Research:5926–35. <https://doi.org/10.1158/0008-5472.CAN-12-4718>.
- Lodish, Harvey, Arnold Berk, S Lawrence Zipursky, Paul Matsudaira, David Baltimore, and James Darnell. 2000. "Proto-Oncogenes and Tumor-Suppressor Genes." W. H. Freeman. <https://www.ncbi.nlm.nih.gov/books/NBK21662/>.
- Louis, David N., M.L. Suvá, P.C. Burger, and et.al. 2016. "WHO Classification of Tumors of the Central Nervous System." In *WHO Classification of Tumors of the Central Nervous System*, edited by David N. Louis, Hiroko Ohgaki, Otmar D. Wiestler, and et.al, 4th Editio, 28–56. Lyon: International Agency for Research on Cancer (IARC).
- Louis, David N., Hiroko Ohgaki, Otmar D. Wiestler, Webster K. Cavenee, David W. Ellison, Dominique Figarella-Branger, Arie Perry, Guido Reifenberger, and Andreas von Deimling. 2016. "WHO Classification of Tumours of the Central Nervous System." In *WHO Classification of Tumours of the Central Nervous System*, edited by David N. Louis, Hiroko Ohgaki, Otmar Wiestler, and W. Cavenee, 4th Editio, 12–13. Lyon: International Agency for Research on Cancer (IARC).
- Low, Kee Chung, and Vinay Tergaonkar. 2013. "Telomerase: Central Regulator of All of the Hallmarks of Cancer." *Trends in Biochemical Sciences* 38 (9). Elsevier:426–34. <https://doi.org/10.1016/j.tibs.2013.07.001>.
- Marics, Irène, Françoise Padilla, Jean-François Guillemot, Martin Scaal, and Christophe Marcelle. 2002. "FGFR4 Signaling Is a Necessary Step in Limb Muscle Differentiation." *Development* 129 (19).
- Mawrin, Christian, Elmar Kirches, Sabine Diete, Falk R. Wiedemann, Thomas Schneider, Raimund Firsching, Siegfried Kropf, et al. 2006. "Analysis of a Single Nucleotide Polymorphism in Codon 388 of the FGFR4 Gene in Malignant Gliomas." *Cancer Letters* 239 (2). Elsevier:239–45. <https://doi.org/10.1016/J.CANLET.2005.08.013>.
- McGranahan, Tresa, Kate Elizabeth Therkelsen, Sarah Ahmad, and Seema Nagpal. 2019. "Current State of Immunotherapy for Treatment of Glioblastoma." *Current Treatment Options in Oncology* 20 (3). Springer:24. <https://doi.org/10.1007/s11864-019-0619-4>.
- Mellinghoff, Ingo K., Maria Y. Wang, Igor Vivanco, Daphne A. Haas-Kogan, Shaojun Zhu, Ederlyn Q. Dia, Kan V. Lu, et al. 2005. "Molecular Determinants of the Response of Glioblastomas to EGFR Kinase Inhibitors." *New England Journal of Medicine* 353 (19). Massachusetts Medical Society :2012–24. <https://doi.org/10.1056/NEJMoa051918>.
- Mhaidat, Nm., XD Zhang, J. Allen, and KA Avery-Kiejda. 2007. "Temozolomide Induces Senescence but Not Apoptosis in Human Melanoma Cells." *British Journal of Cancer*, 1225–33. https://www.researchgate.net/publication/5878606_Temozolomide_induces_senescence_but_not_apoptosis_in_human_melanoma_cells.
- Miranda, Ana, María Blanco-Prieto, João Sousa, Alberto Pais, and Carla Vitorino. 2017. "Breaching Barriers in Glioblastoma. Part I: Molecular Pathways and Novel Treatment Approaches." *International Journal of Pharmaceutics* 531 (1).

- Elsevier:372–88. <https://doi.org/10.1016/J.IJPHARM.2017.07.056>.
- Mohammadi, M, G McMahon, L Sun, C Tang, P Hirth, B K Yeh, S R Hubbard, and J Schlessinger. 1997. "Structures of the Tyrosine Kinase Domain of Fibroblast Growth Factor Receptor in Complex with Inhibitors." *Science (New York, N.Y.)* 276 (5314). American Association for the Advancement of Science:955–60. <https://doi.org/10.1126/science.276.5314.955>.
- Monsonogo-Ornan, E, R Adar, E Rom, and A Yayon. 2002. "FGF Receptors Ubiquitylation: Dependence on Tyrosine Kinase Activity and Role in Downregulation." *FEBS Letters* 528 (1–3). No longer published by Elsevier:83–89. [https://doi.org/10.1016/S0014-5793\(02\)03255-6](https://doi.org/10.1016/S0014-5793(02)03255-6).
- Movassagh, Mehregan, and Roger S.-Y. Foo. 2008. "Simplified Apoptotic Cascades." *Heart Failure Reviews* 13 (2). Springer US:111–19. <https://doi.org/10.1007/s10741-007-9070-x>.
- Murakami, M., A. Elfenbein, and M. Simons. 2008. "Non-Canonical Fibroblast Growth Factor Signalling in Angiogenesis." *Cardiovascular Research* 78 (2):223–31. <https://doi.org/10.1093/cvr/cvm086>.
- My Cancer Genome. n.d. "Receptor Tyrosine Kinase/growth Factor Signaling." Accessed December 8, 2019. <https://www.mycancergenome.org/content/pathways/receptor-tyrosine-kinase-growth-factor-signaling/>.
- "New Global Cancer Data: GLOBOCAN 2018 | UICC." n.d. Accessed September 17, 2019. <https://www.uicc.org/news/new-global-cancer-data-globocan-2018>.
- Ohgaki, H., and P. Kleihues. 2013. "The Definition of Primary and Secondary Glioblastoma." *Clinical Cancer Research* 19 (4):764–72. <https://doi.org/10.1158/1078-0432.CCR-12-3002>.
- Opaliński, Łukasz, Aleksandra Sokołowska-Wędzina, Martyna Szczepara, Małgorzata Zakrzewska, and Jacek Otlewski. 2017. "Antibody-Induced Dimerization of FGFR1 Promotes Receptor Endocytosis Independently of Its Kinase Activity." *Scientific Reports* 7 (1). Nature Publishing Group:7121. <https://doi.org/10.1038/s41598-017-07479-z>.
- Ornitz, David M., and Nobuyuki Itoh. 2015. "The Fibroblast Growth Factor Signaling Pathway." *Wiley Interdisciplinary Reviews: Developmental Biology* 4 (3). John Wiley & Sons, Ltd (10.1111):215–66. <https://doi.org/10.1002/wdev.176>.
- Ornitz, David M, and Nobuyuki Itoh. 2001. "Fibroblast Growth Factors." *Genome Biology* 2 (3). BioMed Central:reviews3005.1. <https://doi.org/10.1186/gb-2001-2-3-reviews3005>.
- Ostrom, Quinn T, Haley Gittleman, Gabrielle Truitt, Alexander Boscia, Carol Kruchko, and Jill S Barnholtz-Sloan. 2018. "CBTRUS Statistical Report: Primary Brain and Other Central Nervous System Tumors Diagnosed in the United States in 2011–2015." *Neuro-Oncology* 20 (suppl_4). Narnia:iv1-iv86. <https://doi.org/10.1093/neuonc/noy131>.
- Park, Jin H, Yingting Liu, Mark A Lemmon, and Ravi Radhakrishnan. 2012. "Erlotinib Binds Both Inactive and Active Conformations of the EGFR Tyrosine Kinase Domain." *The Biochemical Journal* 448 (3). Portland Press Ltd:417–23. <https://doi.org/10.1042/BJ20121513>.
- Paur, Jakob, Lisa Nika, Christiane Maier, Alexander Moscu-Gregor, Julia Kostka,

- Daniela Huber, Thomas Mohr, et al. 2015. "Fibroblast Growth Factor Receptor 3 Isoforms: Novel Therapeutic Targets for Hepatocellular Carcinoma?" *Hepatology* 62 (6). John Wiley & Sons, Ltd:1767–78. <https://doi.org/10.1002/hep.28023>.
- Peláez-García, Alberto, Rodrigo Barderas, Sofía Torres, Pablo Hernández-Varas, Joaquín Teixidó, Félix Bonilla, Antonio Garcia de Herreros, and J Ignacio Casal. 2013. "FGFR4 Role in Epithelial-Mesenchymal Transition and Its Therapeutic Value in Colorectal Cancer." *PloS One* 8 (5). Public Library of Science:e63695. <https://doi.org/10.1371/journal.pone.0063695>.
- Petitjean, A, M I W Achatz, A L Borresen-Dale, P Hainaut, and M Olivier. 2007. "TP53 Mutations in Human Cancers: Functional Selection and Impact on Cancer Prognosis and Outcomes." *Oncogene* 26 (15). Nature Publishing Group:2157–65. <https://doi.org/10.1038/sj.onc.1210302>.
- "Polymerase Chain Reaction (PCR) and Its Principle – The Science Info." n.d. Accessed August 29, 2019. <https://thescienceinfo.com/polymerase-chain-reaction-pcr-and-its-principle/>.
- Popescu, Alisa Madalina, Oana Alexandru, Corina Brindusa, Stefana Oana Purcaru, Daniela Elise Tache, Ligia Gabriela Tataranu, Citto Taisescu, and Anica Dricu. 2015. "Targeting the VEGF and PDGF Signaling Pathway in Glioblastoma Treatment." *International Journal of Clinical and Experimental Pathology* 8 (7). e-Century Publishing Corporation:7825–37. <http://www.ncbi.nlm.nih.gov/pubmed/26339347>.
- Potenta, S, E Zeisberg, and R Kalluri. 2008. "The Role of Endothelial-to-Mesenchymal Transition in Cancer Progression." *British Journal of Cancer* 99 (9). Nature Publishing Group:1375–79. <https://doi.org/10.1038/sj.bjc.6604662>.
- Powers, C J, S w McLeskey, and A Wellenstein. 2000. "Fibroblast Growth Factors, Their Receptors and Signaling." *Endocrine- Related Cancer* 7 (3):165–97. <https://erc.bioscientifica.com/view/journals/erc/7/3/11021964.xml>.
- Presta, Marco, Patrizia Dell'Era, Stefania Mitola, Emanuela Moroni, Roberto Ronca, and Marco Rusnati. 2005. "Fibroblast Growth Factor/fibroblast Growth Factor Receptor System in Angiogenesis." *Cytokine & Growth Factor Reviews* 16 (2). Pergamon:159–78. <https://doi.org/10.1016/J.CYTOGFR.2005.01.004>.
- Rachna, C. n.d. "Difference Between Benign (Non-Cancerous) and Malignant (Cancerous) Tumors (with Comparison Chart) - Bio Differences." Accessed November 2, 2019. <https://biodifferences.com/difference-between-benign-non-cancerous-and-malignant-cancerous-tumors.html>.
- Raineri, Silvia, and Jane Mellor. 2018. "IDH1: Linking Metabolism and Epigenetics." *Frontiers in Genetics* 9. Frontiers Media SA:493. <https://doi.org/10.3389/fgene.2018.00493>.
- Raja, Aroosha, Inkeun Park, Farhan Haq, and Sung-Min Ahn. 2019. "FGF19–FGFR4 Signaling in Hepatocellular Carcinoma." *Cells* 8 (6):536. <https://doi.org/10.3390/cells8060536>.
- Ransohoff, Richard M., and Britta Engelhardt. 2012. "The Anatomical and Cellular Basis of Immune Surveillance in the Central Nervous System." *Nature Reviews Immunology* 2012 12:9 12 (9). Nature Publishing Group:623–35. <https://doi.org/10.1038/nri3265>.
- Reardon, D. A., G. Freeman, C. Wu, E. A. Chiocca, K. W. Wucherpfennig, P. Y. Wen,

- E. F. Fritsch, W. T. Curry, J. H. Sampson, and G. Dranoff. 2014. "Immunotherapy Advances for Glioblastoma." *Neuro-Oncology* 16 (11). Narnia:1441–58. <https://doi.org/10.1093/neuonc/nou212>.
- Regad, Tarik. 2015. "Targeting RTK Signaling Pathways in Cancer." *Cancers* 7 (3). Multidisciplinary Digital Publishing Institute (MDPI):1758–84. <https://doi.org/10.3390/cancers7030860>.
- Regeenes, Romario, Pamuditha N Silva, Huntley H Chang, Edith J Arany, Andrey I Shukalyuk, Julie Audet, Dawn M Kilkenny, and Jonathan V Rocheleau. 2018. "Fibroblast Growth Factor Receptor 5 (FGFR5) Is a Co-Receptor for FGFR1 That Is up-Regulated in Beta-Cells by Cytokine-Induced Inflammation." *The Journal of Biological Chemistry* 293 (44). American Society for Biochemistry and Molecular Biology:17218–28. <https://doi.org/10.1074/jbc.RA118.003036>.
- Reilly, John F., Eiichi Mizukoshi, and Pamela A. Maher. 2004. "Ligand Dependent and Independent Internalization and Nuclear Translocation of Fibroblast Growth Factor (FGF) Receptor 1." *DNA and Cell Biology* 23 (9):538–48. <https://doi.org/10.1089/dna.2004.23.538>.
- Reitman, Zachary J., and Hai Yan. 2010. "Is[1] Z. J. Reitman and H. Yan, 'Isocitrate Dehydrogenase 1 and 2 Mutations in Cancer: Alterations at a Crossroads of Cellular Metabolism,' JNCI J. Natl. Cancer Inst., Vol. 102, No. 13, P. 932, 2010. ocitrate Dehydrogenase 1 and 2 Mutations in Cancer: Alte." *JNCI Journal of the National Cancer Institute* 102 (13). Oxford University Press:932. <https://doi.org/10.1093/JNCI/DJQ187>.
- Rivest, Serge. 2009. "Regulation of Innate Immune Responses in the Brain." *Nature Reviews Immunology* 9 (6):429–39. <https://doi.org/10.1038/nri2565>.
- Robbins, Elizabeth, Mignon L. Loh, and Katherine K. Matthay. 2012. "Congenital Malignant Disorders." *Avery's Diseases of the Newborn*, January. W.B. Saunders, 1143–63. <https://doi.org/10.1016/B978-1-4377-0134-0.10080-0>.
- Roy, David M., Logan A. Walsh, and Timothy A. Chan. 2014. "Driver Mutations of Cancer Epigenomes." *Protein & Cell* 5 (4). Higher Education Press:265–96. <https://doi.org/10.1007/s13238-014-0031-6>.
- Saffell, J L, E J Williams, I J Mason, F S Walsh, and P Doherty. 1997. "Expression of a Dominant Negative FGF Receptor Inhibits Axonal Growth and FGF Receptor Phosphorylation Stimulated by CAMs." *Neuron* 18 (2). Elsevier:231–42. [https://doi.org/10.1016/s0896-6273\(00\)80264-0](https://doi.org/10.1016/s0896-6273(00)80264-0).
- Saunders, N. n.d. "Benign vs. Malignant Tumors: Understanding the Difference." Accessed November 2, 2019. <http://cancerliving.today/benign-vs-malignant-tumors/>.
- Schalper, Kurt A., Maria E. Rodriguez-Ruiz, Ricardo Diez-Valle, Alvaro López-Janeiro, Angelo Porciuncula, Miguel A. Idoate, Susana Inogés, et al. 2019. "Neoadjuvant Nivolumab Modifies the Tumor Immune Microenvironment in Resectable Glioblastoma." *Nature Medicine* 25 (3). Nature Publishing Group:470–76. <https://doi.org/10.1038/s41591-018-0339-5>.
- Schelch, Karin, Christina Wagner, Sonja Hager, Christine Pirker, Katharina Siess, Elisabeth Lang, Ruby Lin, et al. 2018. "FGF2 and EGF Induce Epithelial–mesenchymal Transition in Malignant Pleural Mesothelioma Cells via a MAPKinase/MMP1 Signal." *Carcinogenesis* 39 (4). Narnia:534–45.

- <https://doi.org/10.1093/carcin/bgy018>.
- Schlessinger, J., and A. Ullrich. 1992. "Growth Factor Signaling by Receptor Tyrosine Kinases." *Neuron* 9 (3):383–91. [https://doi.org/10.1016/0896-6273\(92\)90177-F](https://doi.org/10.1016/0896-6273(92)90177-F).
- Sever, Richard, and Joan S Brugge. 2015. "Signal Transduction in Cancer." *Cold Spring Harbor Perspectives in Medicine* 5 (4). Cold Spring Harbor Laboratory Press. <https://doi.org/10.1101/cshperspect.a006098>.
- Shah, Riyaz NH, J Claire Ibbitt, Kari Alitalo, and Helen C Hurst. 2002. "FGFR4 Overexpression in Pancreatic Cancer Is Mediated by an Intronic Enhancer Activated by HNF1 α ." *Oncogene* 21 (54). Nature Publishing Group:8251–61. <https://doi.org/10.1038/sj.onc.1206020>.
- Shi, Si, Xingyu Li, Bo You, Ying Shan, Xiaolei Cao, and Yiwen You. 2015a. "High Expression of FGFR4 Enhances Tumor Growth and Metastasis in Nasopharyngeal Carcinoma." *Journal of Cancer* 6 (12):1245–54. <https://doi.org/10.7150/jca.12825>.
- . 2015b. "High Expression of FGFR4 Enhances Tumor Growth and Metastasis in Nasopharyngeal Carcinoma." *Journal of Cancer* 6 (12). Ivyspring International Publisher:1245–54. <https://doi.org/10.7150/jca.12825>.
- Singh, D., J. M. Chan, P. Zoppoli, F. Niola, R. Sullivan, A. Castano, E. M. Liu, et al. 2012. "Transforming Fusions of FGFR and TACC Genes in Human Glioblastoma." *Science* 337 (6099):1231–35. <https://doi.org/10.1126/science.1220834>.
- Sleeman, Matthew, Jonathan Fraser, Megan McDonald, Shining Yuan, Damian White, Prudence Grandison, Krishnanand Kumble, James D. Watson, and J.Greg Murison. 2001. "Identification of a New Fibroblast Growth Factor Receptor, FGFR5." *Gene* 271 (2). Elsevier:171–82. [https://doi.org/10.1016/S0378-1119\(01\)00518-2](https://doi.org/10.1016/S0378-1119(01)00518-2).
- Smith, Stephanie. 2017. "Tumors of the Central Nervous System." In *Nursing Care of the Pediatric Neurosurgery Patient*, 195–254. Cham: Springer International Publishing. https://doi.org/10.1007/978-3-319-49319-0_7.
- Snuderl, Matija, Ladan Fazlollahi, Long P. Le, Mai Nitta, Boryana H. Zhelyazkova, Christian J. Davidson, Sara Akhavanfard, et al. 2011. "Mosaic Amplification of Multiple Receptor Tyrosine Kinase Genes in Glioblastoma." *Cancer Cell* 20 (6). Cell Press:810–17. <https://doi.org/10.1016/J.CCR.2011.11.005>.
- SongTao, Qi, Yu Lei, Gui Si, Ding YanQing, Han HuiXia, Zhang XueLin, Wu LanXiao, and Yao Fei. 2012. "IDH Mutations Predict Longer Survival and Response to Temozolomide in Secondary Glioblastoma." *Cancer Science* 103 (2). John Wiley & Sons, Ltd (10.1111):269–73. <https://doi.org/10.1111/j.1349-7006.2011.02134.x>.
- SOUTHAM, C M. 1963. "THE COMPLEX ETIOLOGY OF CANCER." *Cancer Research* 23 (8 Part 1). American Association for Cancer Research:1105–15. <http://www.ncbi.nlm.nih.gov/pubmed/14070364>.
- Spangle, Jennifer M, and Thomas M Roberts. 2017. "Epigenetic Regulation of RTK Signaling." *Journal of Molecular Medicine (Berlin, Germany)* 95 (8). NIH Public Access:791–98. <https://doi.org/10.1007/s00109-017-1546-0>.
- Spinola, Monica, Vera Leoni, Carmen Pignatiello, Barbara Conti, Fernando Ravagnani, Ugo Pastorino, and Tommaso A Dragani. 2005. "Functional FGFR4

- Gly388Arg Polymorphism Predicts Prognosis in Lung Adenocarcinoma Patients." *Journal of Clinical Oncology : Official Journal of the American Society of Clinical Oncology* 23 (29). American Society of Clinical Oncology:7307–11. <https://doi.org/10.1200/JCO.2005.17.350>.
- Sporn, Michael B., and Anita B. Roberts. 1985. "Autocrine Growth Factors and Cancer." *Nature* 313 (6005):745–47. <https://doi.org/10.1038/313745a0>.
- Stenmark, Kurt R., Maria Frid, and Frédéric Perros. 2016. "Endothelial-to-Mesenchymal Transition." *Circulation* 133 (18):1734–37. <https://doi.org/10.1161/CIRCULATIONAHA.116.022479>.
- Stratton, Michael R., Peter J. Campbell, and P. Andrew Futreal. 2009. "The Cancer Genome." *Nature* 458 (7239). Nature Publishing Group:719–24. <https://doi.org/10.1038/nature07943>.
- Streit, S, D S Mestel, M Schmidt, A Ullrich, and C Berking. 2006. "FGFR4 Arg388 Allele Correlates with Tumour Thickness and FGFR4 Protein Expression with Survival of Melanoma Patients." *British Journal of Cancer* 94 (12). Nature Publishing Group:1879–86. <https://doi.org/10.1038/sj.bjc.6603181>.
- Streit, Sylvia, Johannes Bange, Alexander Fichtner, Stephan Ihrler, Wolfgang Issing, and Axel Ullrich. 2004. "Involvement of the FGFR4 Arg388 Allele in Head and Neck Squamous Cell Carcinoma." *International Journal of Cancer* 111 (2). John Wiley & Sons, Ltd:213–17. <https://doi.org/10.1002/ijc.20204>.
- Stupp, Roger, Warren P. Mason, Martin J. van den Bent, Michael Weller, Barbara Fisher, Martin J.B. Taphoorn, Karl Belanger, et al. 2005. "Radiotherapy plus Concomitant and Adjuvant Temozolomide for Glioblastoma." *New England Journal of Medicine* 352 (10). Massachusetts Medical Society :987–96. <https://doi.org/10.1056/NEJMoa043330>.
- Sugiyama, N., M. Varjosalo, P. Meller, J. Lohi, M. Hyytiäinen, S. Kilpinen, O. Kallioniemi, et al. 2010. "Fibroblast Growth Factor Receptor 4 Regulates Tumor Invasion by Coupling Fibroblast Growth Factor Signaling to Extracellular Matrix Degradation." *Cancer Research* 70 (20):7851–61. <https://doi.org/10.1158/0008-5472.CAN-10-1223>.
- Sugiyama, Nami, Markku Varjosalo, Pipsa Meller, Jouko Lohi, Kui Ming Chan, Zhongjun Zhou, Kari Alitalo, Jussi Taipale, Jorma Keski-Oja, and Kaisa Lehti. 2010. "FGF Receptor-4 (FGFR4) Polymorphism Acts as an Activity Switch of a Membrane Type 1 Matrix Metalloproteinase-FGFR4 Complex." *Proceedings of the National Academy of Sciences of the United States of America* 107 (36). National Academy of Sciences:15786–91. <https://doi.org/10.1073/pnas.0914459107>.
- Sunayama, Jun, Ken-Ichiro Matsuda, Atsushi Sato, Ken Tachibana, Kaori Suzuki, Yoshitaka Narita, Soichiro Shibui, et al. 2010. "Crosstalk Between the PI3K/mTOR and MEK/ERK Pathways Involved in the Maintenance of Self-Renewal and Tumorigenicity of Glioblastoma Stem-Like Cells." *STEM CELLS* 28 (11). John Wiley & Sons, Ltd:1930–39. <https://doi.org/10.1002/stem.521>.
- Szopa, Wojciech, Thomas A. Burley, Gabriela Kramer-Marek, and Wojciech Kaspera. 2017. "Diagnostic and Therapeutic Biomarkers in Glioblastoma: Current Status and Future Perspectives." *BioMed Research International*. <https://doi.org/10.1155/2017/8013575>.

- Talmadge, J. E., and I. J. Fidler. 2010. "AACR Centennial Series: The Biology of Cancer Metastasis: Historical Perspective." *Cancer Research* 70 (14):5649–69. <https://doi.org/10.1158/0008-5472.CAN-10-1040>.
- Taylor, James G, Adam T Cheuk, Patricia S Tsang, Joon-Yong Chung, Young K Song, Krupa Desai, Yanlin Yu, et al. 2009. "Identification of FGFR4-Activating Mutations in Human Rhabdomyosarcomas That Promote Metastasis in Xenotransplanted Models." *The Journal of Clinical Investigation* 119 (11). American Society for Clinical Investigation:3395–3407. <https://doi.org/10.1172/JCI39703>.
- THE HUMAN PROTEIN ATLAS. n.d. "FGFR4." <https://www.proteinatlas.org/ENSG00000160867-FGFR4/tissue>.
- Thomas, Alissa A., Marc S. Ernstoff, and Camilo E. Fadul. 2012. "Immunotherapy for the Treatment of Glioblastoma." *The Cancer Journal* 18 (1):59–68. <https://doi.org/10.1097/PPO.0b013e3182431a73>.
- Tomasetti, Cristian, Lu Li, and Bert Vogelstein. 2017. "Stem Cell Divisions, Somatic Mutations, Cancer Etiology, and Cancer Prevention." *Science (New York, N.Y.)* 355 (6331). American Association for the Advancement of Science:1330–34. <https://doi.org/10.1126/science.aaf9011>.
- Trichopoulou, A., P. Lagiou, and D. Trichopoulos. 2003. "CANCER | Epidemiology." *Encyclopedia of Food Sciences and Nutrition*, January. Academic Press, 795–99. <https://doi.org/10.1016/B0-12-227055-X/00154-1>.
- Tucker, Julie A., Tobias Klein, Jason Breed, Alexander L. Breeze, Ross Overman, Chris Phillips, and Richard A. Norman. 2014. "Structural Insights into FGFR Kinase Isoform Selectivity: Diverse Binding Modes of AZD4547 and Ponatinib in Complex with FGFR1 and FGFR4." *Structure* 22 (12). Cell Press:1764–74. <https://doi.org/10.1016/J.STR.2014.09.019>.
- Turkington, R C, D B Longley, W L Allen, L Stevenson, K McLaughlin, P D Dunne, J K Blayney, M Salto-Tellez, S Van Schaeybroeck, and P G Johnston. 2014. "Fibroblast Growth Factor Receptor 4 (FGFR4): A Targetable Regulator of Drug Resistance in Colorectal Cancer." *Cell Death & Disease* 5 (2). Nature Publishing Group:e1046–e1046. <https://doi.org/10.1038/cddis.2014.10>.
- Uddin, S. n.d. "Neurologic Manifestations of Glioblastoma Multiforme: Background, Pathophysiology, Epidemiology." Accessed December 8, 2019. <https://emedicine.medscape.com/article/1156220-overview>.
- "Vimentin - an Overview | ScienceDirect Topics." n.d. Accessed December 6, 2019. <https://www.sciencedirect.com/topics/medicine-and-dentistry/vimentin>.
- Wang, Jianghua, Wendong Yu, Yi Cai, Chengxi Ren, and Michael M Ittmann. 2008. "Altered Fibroblast Growth Factor Receptor 4 Stability Promotes Prostate Cancer Progression." *Neoplasia (New York, N.Y.)* 10 (8). Neoplasia Press:847–56. <https://doi.org/10.1593/neo.08450>.
- WebMd. n.d. "Benign Tumors: Types, Causes, and Treatments." Accessed November 11, 2019. <https://www.webmd.com/a-to-z-guides/benign-tumors-causes-treatments#1>.
- "Western Blotting - an Overview | ScienceDirect Topics." n.d. Accessed December 9, 2019. <https://www.sciencedirect.com/topics/medicine-and-dentistry/western-blotting>.

- Wimmer, Eva, Stephan Ihrler, Olivier Gires, Sylvia Streit, Wolfgang Issing, and Christoph Bergmann. 2019. "Fibroblast Growth Factor Receptor 4 Single Nucleotide Polymorphism Gly388Arg in Head and Neck Carcinomas." *World Journal of Clinical Oncology* 10 (3):136–48. <https://doi.org/10.5306/wjco.v10.i3.136>.
- "Worldwide Cancer Statistics | Cancer Research UK." n.d. Accessed December 10, 2019. <https://www.cancerresearchuk.org/health-professional/cancer-statistics/worldwide-cancer#heading-One>.
- Wu, Ai-Luen, Sally Coulter, Christopher Liddle, Anne Wong, Jeffrey Eastham-Anderson, Dorothy M. French, Andrew S. Peterson, and Junichiro Sonoda. 2011. "FGF19 Regulates Cell Proliferation, Glucose and Bile Acid Metabolism via FGFR4-Dependent and Independent Pathways." Edited by Carlo Gaetano. *PLoS ONE* 6 (3). Public Library of Science:e17868. <https://doi.org/10.1371/journal.pone.0017868>.
- Wu, An-hua, Yun-jie Wang, Xue Zhang, and Walter C. Low. 2003. "Expression of Immune-Related Molecules in Glioblastoma Multiform Cells." *Chinese Journal of Cancer Research* 15 (2). Springer:112–15. <https://doi.org/10.1007/BF02974912>.
- Wu, Xinle, Hongfei Ge, Bryan Lemon, Steven Vonderfecht, Jennifer Weiszmann, Randy Hecht, Jamila Gupte, et al. 2010. "FGF19-Induced Hepatocyte Proliferation Is Mediated through FGFR4 Activation." *The Journal of Biological Chemistry* 285 (8). American Society for Biochemistry and Molecular Biology:5165–70. <https://doi.org/10.1074/jbc.M109.068783>.
- Wu, Xinle, and Yang Li. 2009. "Role of FGF19 Induced FGFR4 Activation in the Regulation of Glucose Homeostasis." *Aging (Albany NY)* 1 (12). Impact Journals, LLC:1023. <https://doi.org/10.18632/AGING.100108>.
- Wyatt, Christina M., and Tilman B. Drüeke. 2016. "Fibroblast Growth Factor Receptor 4: The Missing Link between Chronic Kidney Disease and FGF23-Induced Left Ventricular Hypertrophy?" *Kidney International* 89 (1). Elsevier:7–9. <https://doi.org/10.1016/J.KINT.2015.11.012>.
- Xia, Weiya, Yongkun Wei, Yi Du, Jinsong Liu, Bin Chang, Yung-Luen Yu, Long-Fei Huo, Stephanie Miller, and Mien-Chie Hung. 2009. "Nuclear Expression of Epidermal Growth Factor Receptor Is a Novel Prognostic Value in Patients with Ovarian Cancer." *Molecular Carcinogenesis* 48 (7). John Wiley & Sons, Ltd:610–17. <https://doi.org/10.1002/mc.20504>.
- Xian, Wa, Kathryn L. Schwertfeger, and Jeffrey M. Rosen. 2007. "Distinct Roles of Fibroblast Growth Factor Receptor 1 and 2 in Regulating Cell Survival and Epithelial-Mesenchymal Transition." *Molecular Endocrinology* 21 (4). Narnia:987–1000. <https://doi.org/10.1210/me.2006-0518>.
- Xu, Bin, Na Tong, Shu Q Chen, Li X Hua, Zeng J Wang, Zheng D Zhang, and Ming Chen. 2011. "FGFR4 Gly388Arg Polymorphism Contributes to Prostate Cancer Development and Progression: A Meta-Analysis of 2618 Cases and 2305 Controls." *BMC Cancer* 11 (1). BioMed Central:84. <https://doi.org/10.1186/1471-2407-11-84>.
- Xu, Wei, Yan Li, Xueli Wang, Bo Chen, Yan Wang, Shifeng Liu, Jijun Xu, Weihong Zhao, and Jianqing Wu. 2010. "FGFR4 Transmembrane Domain Polymorphism and Cancer Risk: A Meta-Analysis Including 8555 Subjects." *European Journal*

- of *Cancer* 46 (18). Pergamon:3332–38.
<https://doi.org/10.1016/J.EJCA.2010.06.017>.
- Yamada, Shoko M., Shokei Yamada, Yasuto Hayashi, Hiroshi Takahashi, Akira Teramoto, and Koshi Matsumoto. 2002. "Fibroblast Growth Factor Receptor (FGFR) 4 Correlated with the Malignancy of Human Astrocytomas." *Neurological Research* 24 (3). Taylor & Francis:244–48.
<https://doi.org/10.1179/016164102101199864>.
- Yun, Ye-Rang, Jong Eun Won, Eunyi Jeon, Sujin Lee, Wonmo Kang, Hyejin Jo, Jun-Hyeog Jang, Ueon Sang Shin, and Hae-Won Kim. 2010. "Fibroblast Growth Factors: Biology, Function, and Application for Tissue Regeneration." *Journal of Tissue Engineering* 2010 (November). SAGE Publications:218142.
<https://doi.org/10.4061/2010/218142>.
- Zaid, T. M., T.-L. Yeung, M. S. Thompson, C. S. Leung, T. Harding, N.-N. Co, R. S. Schmandt, et al. 2013. "Identification of FGFR4 as a Potential Therapeutic Target for Advanced-Stage, High-Grade Serous Ovarian Cancer." *Clinical Cancer Research* 19 (4). American Association for Cancer Research:809–20.
<https://doi.org/10.1158/1078-0432.CCR-12-2736>.
- Zeisberg, E. M., S. Potenta, L. Xie, M. Zeisberg, and R. Kalluri. 2007. "Discovery of Endothelial to Mesenchymal Transition as a Source for Carcinoma-Associated Fibroblasts." *Cancer Research* 67 (21). American Association for Cancer Research:10123–28. <https://doi.org/10.1158/0008-5472.CAN-07-3127>.
- Zhao, Huakan, Fenglin Lv, Guizhao Liang, Xiaobin Huang, Gang Wu, Wenfa Zhang, Le Yu, Lei Shi, and Yong Teng. 2016. "FGF19 Promotes Epithelial-Mesenchymal Transition in Hepatocellular Carcinoma Cells by Modulating the GSK3 β / β -Catenin Signaling Cascade via FGFR4 Activation." *Oncotarget* 7 (12). Impact Journals, LLC:13575–86. <https://doi.org/10.18632/oncotarget.6185>.
- Zhao, Po, Giuseppina Caretti, Stephanie Mitchell, Wallace L McKeehan, Adele L Boskey, Lauren M Pachman, Vittorio Sartorelli, and Eric P Hoffman. 2006. "Fgfr4 Is Required for Effective Muscle Regeneration in Vivo. Delineation of a MyoD-Tead2-Fgfr4 Transcriptional Pathway." *The Journal of Biological Chemistry* 281 (1). American Society for Biochemistry and Molecular Biology:429–38.
<https://doi.org/10.1074/jbc.M507440200>.
- Zhao, Po, and Eric P. Hoffman. 2004. "Embryonic Myogenesis Pathways in Muscle Regeneration." *Developmental Dynamics* 229 (2). John Wiley & Sons, Ltd:380–92. <https://doi.org/10.1002/dvdy.10457>.
- Zhou, Wen-Ya, Hong Zheng, Xiao-Ling Du, and Ji-Long Yang. 2016. "Characterization of FGFR Signaling Pathway as Therapeutic Targets for Sarcoma Patients." *Cancer Biology & Medicine* 13 (2). Chinese Anti-Cancer Association:260–68. <https://doi.org/10.20892/j.issn.2095-3941.2015.0102>.
- Zwick, Esther, Johannes Bange, and Axel Ullrich. 2002. "Receptor Tyrosine Kinases as Targets for Anticancer Drugs." *Trends in Molecular Medicine* 8 (1). Elsevier Current Trends:17–23. [https://doi.org/10.1016/S1471-4914\(01\)02217-1](https://doi.org/10.1016/S1471-4914(01)02217-1).

12 List of Tables

<i>Table 1 Used cell lines in this study</i>	31
<i>Table 2 Used cell concentrations</i>	32
<i>Table 3 2*HBS buffer</i>	35
<i>Table 4 Used drugs</i>	38
<i>Table 5. 10* PBS solution</i>	40
<i>Table 6. Crystal violet solution</i>	40
<i>Table 7 NB+ Medium recipe</i>	41
<i>Table 8 Lysis buffer recipe</i>	45
<i>Table 9 Buffers for membrane enriched fractions</i>	46
<i>Table 10 Acrylamide gels recipe</i>	47
<i>Table 11 Buffers and solutions for Western blotting</i>	49
<i>Table 12. Luminol</i>	51
<i>Table 13 Used Antibodies</i>	52
<i>Table 14 Reverse transcription master mix</i>	54
<i>Table 15. PCR program (qPCR)</i>	56
<i>Table 16. Mixture for 1 TaqMan PCR reaction</i>	57
<i>Table 17. PCR program (TaqMan PCR)</i>	57
<i>Table 18 RFLP PCR Mastermix</i>	58
<i>Table 19 RFLP PCR program</i>	59
<i>Table 20 Restriction digest Master mix</i>	59
<i>Table 21. IC50 table of different RTKIs in SIWA M1 models</i>	89

13 List of Figures

<i>Figure 1 Cancer incidence and mortality rates worldwide adapted from</i>	1
<i>Figure 2. The hallmarks of cancer</i>	6
<i>Figure 3. WHO classification of tumors of the central nervous system 2016</i>	7
<i>Figure 4. MRI of glioblastoma multiforme (GBM)</i>	8
<i>Figure 5. Receptor tyrosine kinases signaling pathways and therapeutic intervention methods</i>	13
<i>Figure 6. Subfamilies of fibroblast growth factors, their cofactors and receptors</i>	14
<i>Figure 7. Splice variants of FGFRs</i>	16
<i>Figure 8. Tissue distribution of different FGFR splice variants</i>	17
<i>Figure 9. FGFR signaling</i>	18
<i>Figure 10. Structure of FGFR</i>	20
<i>Figure 11. Non- canonical FGFR signaling</i>	21
<i>Figure 12. FGFR4- Position of single nucleotide polymorphism (SNP) in transmembrane domain</i>	25
<i>Figure 13. Epithelial to mesenchymal transition (EMT)</i>	27
<i>Figure 14. FGF19 modulates EMT via FGFR4- GSK3β signaling</i>	28
<i>Figure 15. Role of FGFR4 signaling during epithelial to mesenchymal transition</i>	29
<i>Figure 16. Puromycin</i>	33
<i>Figure 17 Vector map of FGFR4-KD-GFP variant</i>	34
<i>Figure 18. Formazan formation by NADH dependent oxidoreductase</i>	37
<i>Figure 19. Confocal laser scanning microscopy</i>	44
<i>Figure 20 Western blotting</i>	49
<i>Figure 21 Polymerase chain reaction (PCR)</i>	53
<i>Figure 22. RFLP PCR products and MSPI restriction sites in FGFR4-388Gly and FGFR4-388Arg variants</i>	60
<i>Figure 23 siRNA technique</i>	61
<i>Figure 24 Exemplary FACS results</i>	62
<i>Figure 25 SCID mouse</i>	63
<i>Figure 26 FGFR4 expression in glioma</i>	64
<i>Figure 27. RFLP-PCR of FGFR4 over-expressing glioma cells</i>	65
<i>Figure 28. FGFR4-expressing SIWA M1 cell lines</i>	66
<i>Figure 29. FGFR4-expressing BTL1376 cell models</i>	67
<i>Figure 30. Confocal microphotographs of SIWA M1 cell models</i>	68
<i>Figure 31. Confocal microphotographs of BTL1376 cell models</i>	69
<i>Figure 32. Western blot of total protein, cytoplasmic and nuclear extracts from SIWA M1 and BTL1376</i>	70
<i>Figure 33. Membrane fractions of SIWA M1</i>	70
<i>Figure 34. qPCR results indicating FGFR4 and GFP expression levels</i>	71
<i>Figure 35 Flow cytometry analysis of SIWA M1 cell models</i>	72
<i>Figure 36 Flow cytometry analysis of BTL1376 cell models</i>	73
<i>Figure 37 Analysis of FITC positive cells measured by FACS analysis</i>	73
<i>Figure 38. Western blots showing overexpression of FGFR4 in the KD variant</i>	74
<i>Figure 39. KLB expression levels in BTL1376</i>	75
<i>Figure 40. KLB expression upon knock-down of FGFR4 in U373 FGFR4-Gly and SIWA M1</i>	76
<i>Figure 41. Western blot showing FGFR4 expression and downstream signaling in SIWA M1 and BTL1376</i>	77
<i>Figure 42. Western blot after knock-down of FGFR4 followed by stimulation with FGF2</i>	78

<i>Figure 43 Colony formation assays upon FGFR4 inactivation..</i>	<i>79</i>
<i>Figure 44. Stimulation assay BTL1376 with FGF2 and FGF23..</i>	<i>80</i>
<i>Figure 45. Sphere formation assay BTL1376..</i>	<i>82</i>
<i>Figure 46. Sphere formation assay SIWA M1.</i>	<i>83</i>
<i>Figure 47. Sphere formation assay SIWA M1 with stimulation via FGF23..</i>	<i>84</i>
<i>Figure 48. In vivo tumor formation of SIWA M1 cell models.....</i>	<i>86</i>
<i>Figure 49. Cell viability assays of SIWA M1..</i>	<i>87</i>
<i>Figure 50. Graphical IC50 presentation of the indicated RTKIs in SIWA M1 cell models.....</i>	<i>88</i>
<i>Figure 51. Sensitivity of BTL1376 towards RTKIs..</i>	<i>90</i>
<i>Figure 52. Downstream signaling in FGFR4 modified SIWA M1 cell models upon ponatinib treatment.....</i>	<i>91</i>
<i>Figure 53. Migration / invasion assay in SIWA M1 FGFR4 altered cell models.</i>	<i>92</i>
<i>Figure 54. Migration / invasion assay in BTL1376 FGFR4 altered cell models.</i>	<i>93</i>
<i>Figure 55. Wound healing analysis of SIWA M1.</i>	<i>94</i>
<i>Figure 56. mRNA expression levels of EMT markers in SIWA M1 models.....</i>	<i>95</i>
<i>Figure 57. Expression of EMT markers in BTL1376.....</i>	<i>96</i>
<i>Figure 58. EMT marker expression after knock-down of FGFR4 in SIWA M1.</i>	<i>97</i>
<i>Figure 59. Western blot analysis of vimentin expression in SIWA M1 upon knock-down of FGFR4.....</i>	<i>98</i>